Journal of Statistical Physics, Vol. 96, Nos. 3/4, 1999

Antiferromagnetic Potts Models on the Square Lattice: A High-Precision Monte Carlo Study

Sabino José Ferreira[1] **and Alan D. Sokal**[2]

Received December 3, 1998; revised April 8, 1999

We study the antiferromagnetic q-state Potts model on the square lattice for $q=3$ and $q=4$, using the Wang–Swendsen–Kotecký (WSK) Monte Carlo algorithm and a powerful finite-size-scaling extrapolation method. For $q=3$ we obtain good control up to correlation length $\xi \sim 5000$; the data are consistent with $\xi(\beta) = Ae^{2\beta}\beta^p(1+a_1e^{-\beta}+\cdots)$ as $\beta\to\infty$, with $p\approx 1$. The staggered susceptibility behaves as $\chi_{\text{stagg}} \sim \xi^{5/3}$. For $q=4$ the model is disordered ($\xi \lesssim 2$) even at zero temperature. In appendices we prove a correlation inequality for Potts antiferromagnets on a bipartite lattice, and we prove ergodicity of the WSK algorithm at zero temperature for Potts antiferromagnets on a bipartite lattice.

KEY WORDS: Potts model; antiferromagnet; square lattice; phase transition, zero-temperature critical point; Monte Carlo; cluster algorithm; Swendsen–Wang algorithm, Wang–Swendsen–Kotecký algorithm; finite-size scaling.

1. INTRODUCTION

The Potts model[1–3] plays an important role in the general theory of critical phenomena, especially in two dimensions,[4–6] and has applications to various condensed-matter systems.[2] Ferromagnetic Potts models have been extensively studied over the last two decades, and much is known about their phase diagrams[2, 3] and critical exponents.[5–7] But for antiferromagnetic Potts models, many basic questions remain open: Is there a phase transition at finite temperature, and if so, of what order? What is the nature of the low-temperature phase(s)? If there is a critical point, what are

[1] Departamento de Estatística—ICEx, Universidade Federal de Minas Gerais, Belo Horizonte, MG 30161-970 Brazil; e-mail sabino@est.ufmg.br.

[2] Department of Physics, New York University, New York, New York 10003; e-mail: sokal@nyu.edu.

0022-4715/99/0800-0461$16.00/0

the critical exponents and the universality classes? Can these exponents be understood (for two-dimensional models) in terms of conformal field theory?

One thing is known rigorously:[8, 9] for q large enough (how large depends on the lattice in question), the antiferromagnetic q-state Potts model has a unique infinite-volume Gibbs measure and exponential decay of correlations at all temperatures, *including zero temperature*: the system is disordered as a result of the large ground-state entropy. However, for smaller values of q, phase transitions can and do occur. Moreover, for these antiferromagnetic models the nature of the phase transition is highly lattice-dependent, in sharp contrast to the universality typically enjoyed by ferromagnets. Thus, one expects that for each lattice $\mathscr{L}$ there will be a value $q_c(\mathscr{L})$ such that

(a) For $q > q_c(\mathscr{L})$ the model has exponential decay of correlations uniformly at all temperatures, including zero temperature.

(b) For $q = q_c(\mathscr{L})$ the model has a critical point at zero temperature.

(c) For $q < q_c(\mathscr{L})$ any behavior is possible. Often (though not always) the model has a phase transition at nonzero temperature, which may be of either first or second order.

The problem, for each lattice, is to find $q_c(\mathscr{L})$ and to determine the precise behavior for each $q \leqslant q_c(\mathscr{L})$.

In this paper we report the results of a large-scale Monte Carlo study of the 3-state and 4-state antiferromagnetic Potts models on the (two-dimensional) *square lattice*, using the Wang–Swendsen–Kotecký (WSK)[10–12] cluster algorithm.[3] We use a powerful finite-size-scaling (FSS) extrapolation method[14–22] to estimate the infinite-volume correlation length ξ and staggered susceptibility χ_{stagg}. Using lattices up to 1536×1536, we can attain an accuracy of a few percent on ξ and χ_{stagg} at correlation lengths ξ as large as 5000. This allows us to conjecture the exact form of the critical behavior for the 3-state model.

The q-state Potts model is defined by the reduced Hamiltonian

$$\mathscr{H} = -J \sum_{\langle xy \rangle} \delta_{\sigma_x, \sigma_y} \tag{1.1}$$

where the sum runs over all nearest-neighbor pairs of lattice sites, and each spin takes values $\sigma_x \in \{1, 2, ..., q\}$. The antiferromagnetic case corresponds to $J = -\beta < 0$. Henceforth we restrict attention to the model (1.1) on the square lattice.

[3] A preliminary version of this work has appeared previously.[13]

Baxter[4, 23] has determined the exact free energy (among other quantities) for the square-lattice Potts model on two special curves in the (J, q)-plane:

$$e^J = 1 \pm \sqrt{q} \tag{1.2}$$

$$e^J = -1 \pm \sqrt{4-q} \tag{1.3}$$

Curve (1.2_+) is known to correspond to the ferromagnetic critical point, and Baxter[23] conjectured that curve (1.3_+) corresponds to the antiferromagnetic critical point. For $q=2$ this gives the known exact value;[24] for $q=3$ it predicts a zero-temperature critical point ($J_c = -\infty$), in accordance with previous belief;[25, 26][4] and for $q>3$ it predicts that the putative critical point lies in the unphysical region ($e^{J_c}<0$), so that the entire physical region $-\infty \leqslant J \leqslant 0$ lies in the disordered phase. In other words, Baxter[23] predicts that $q_c(\text{square lattice}) = 3$, a prediction that we will verify numerically in this paper.

Some properties of the zero-temperature critical point for $q=3$ are known (nonrigorously) as a consequence of the mapping of this model onto a height model, whose long-wavelength behavior is that of a massless Gaussian.[30–34] In particular, the critical exponents associated to the staggered and uniform magnetizations are predicted[30, 32] to be $\eta_{\text{stagg}} = 1/3$ and $\eta_u = 4/3$, respectively.[5] However, the approach to the critical point is much less well understood. In what way, for example, do ξ and χ_{stagg} diverge as $\beta \to \infty$?

Nightingale and Schick,[35] using a phenomenological-renormalization method based on infinite strips of width 2–8, claimed that the correlation length diverges as $\xi \sim \exp(c\beta^{\approx 1.3})$. Wang, Swendsen, and Kotecký,[10, 11] using Monte Carlo, claimed to confirm this latter behavior. But this behavior seems *a priori* implausible to us: the fundamental variable in the Potts model is $t = e^J$, so an ordinary power-law critical point $\xi \sim (t - t_c)^{-\nu}$ with $t_c = 0$ would correspond to $\xi \sim e^{\nu\beta}$. Moreover, we suspect that this model can be exactly solved (at least in the sense of determining the exact asymptotic behavior as $\beta \to \infty$), in which case ν would most likely be a rational number. We are unable to imagine any mechanism leading to $\xi \sim \exp(c\beta^\kappa)$ with $\kappa \neq 1$.

[4] Note also that the $q=3$ model is exactly soluble at zero temperature in an arbitrary magnetic field;[26–29] this might increase one's suspicions that the zero-temperature zero-field case is critical.

[5] These predictions have recently been verified numerically to high precision.[34]

In this paper we shall present numerical evidence that strongly suggests the asymptotic behavior

$$\xi(\beta) = Ae^{2\beta}\beta^p[1 + a_1 e^{-\beta} + a_2 e^{-2\beta} + \cdots] \tag{1.4}$$

with $p \approx 1$. The critical exponent $\nu = 2$ found here corresponds to an operator with scaling dimension $X = 2 - 1/\nu = 3/2$, which is one of the possibilities proposed by Saleur [36, p. 248]—though not the one he considered most likely! The multiplicative logarithmic correction $\beta^p \sim (\log t)^p$ is harder to understand theoretically. Indeed, our data can arguably be reconciled with $p = 0$ at the price of including additive corrections to scaling based on fractional powers of $e^{-\beta}$:

$$\xi(\beta) = Ae^{2\beta}[1 + a_1 e^{-\lambda_1\beta} + a_2 e^{-\lambda_2\beta} + \cdots] \tag{1.5}$$

with $\lambda_1 \approx 0.5$. But this Ansatz too has its theoretical difficulties; see Section 7.1 for discussion of all these issues. We hope, in any case, that the numerical results presented here will serve as useful clues toward the exact solution of this model. The works of Saleur[37, 36] and Henley[38] provide some tantalizing ideas in this direction.

As for the staggered susceptibility, the predicted critical exponent $\eta = 1/3$[30, 32] leads via the scaling law $\gamma = (2 - \eta)\nu$ to the behavior $\chi_{\text{stagg}} \sim \xi^{5/3}$. Our numerical results are consistent with this prediction, unmodified by any further powers of β.

The plan of this paper is as follows: In Section 2 we set the notation and recall briefly our finite size-scaling extrapolation method and the Wang–Swendsen–Kotecký (WSK) Monte Carlo algorithm. In Section 3 we report our raw data. In Section 4 we analyze our static data for the 3-state model, using the finite-size-scaling extrapolation method. In Section 5 we analyze the dynamic critical behavior of the WSK algorithm for the 3-state model. In Section 6 we analyze the data for the 4-state model. In Section 7 we summarize our conclusions and discuss prospects for future work. In Appendix A we prove a correlation inequality for antiferromagnetic Potts models on a bipartite lattice. In Appendix B we prove the ergodicity of the WSK algorithm at zero temperature for antiferromagnetic Potts models on a bipartite lattice.

2. PRELIMINARIES

2.1. Definitions and Notation

The q-state Potts model is defined by the reduced Hamiltonian

$$\mathscr{H} = -J \sum_{\langle xy \rangle} \delta_{\sigma_x, \sigma_y} \tag{2.1}$$

where the sum runs over all nearest-neighbor pairs of lattice sites, and each spin takes values $\sigma_x \in \{1, 2, ..., q\}$. The antiferromagnetic case corresponds to $J = -\beta < 0$. It is useful to represent the q possible values of the spin σ_x by unit vectors $\mathbf{e}^{(1)}, ..., \mathbf{e}^{(q)} \in \mathbb{R}^{q-1}$ pointing from the center to the vertices of a hypertetrahedron; these vectors satisfy

$$\mathbf{e}^{(i)} \cdot \mathbf{e}^{(j)} = \frac{q\delta_{ij} - 1}{q-1} = \begin{cases} 1 & \text{if} \quad i = j \\ -\dfrac{1}{q-1} & \text{if} \quad i \neq j \end{cases} \tag{2.2}$$

We denote this "vectorial" spin by $\boldsymbol{\sigma}_x \equiv \mathbf{e}^{(\sigma_x)}$.

The two-point correlation function $G(x, y)$ is defined by

$$\begin{aligned} G(x, y) &\equiv \langle \boldsymbol{\sigma}_x \cdot \boldsymbol{\sigma}_y \rangle \\ &= \left\langle \frac{q\delta_{\sigma_x, \sigma_y} - 1}{q-1} \right\rangle \end{aligned} \tag{2.3}$$

Henceforth we exploit translation invariance and write $G(x, y) = G(x - y)$. We also define the Fourier-transformed correlation function at wavevector ("momentum") p:

$$\tilde{G}(p) = \sum_x e^{ip \cdot x} G(x) \tag{2.4}$$

On the square lattice, the relevant staggering wavevector for antiferromagnetic Potts models is

$$p_{\text{stagg}} \equiv (\pi, \pi) \tag{2.5}$$

in the sense that $\tilde{G}(p)$ is maximum at $p = (\pi, \pi)$: this follows from the correlation inequality proven in Appendix A. On a finite $L \times L$ lattice with periodic boundary conditions, we also define the four smallest nonzero wavevectors,

$$p_{\text{min}, \pm 1} \equiv (\pm 2\pi/L, 0) \tag{2.6a}$$

$$p_{\text{min}, \pm 2} \equiv (0, \pm 2\pi/L) \tag{2.6b}$$

We wish to study the following quantities:

(a) The energy[6]

$$E = \langle \delta_{\sigma_0, \sigma_{\mathbf{e}}} \rangle \tag{2.7}$$

where **e** stands for any nearest neighbor of the origin.

(b) The staggered susceptibility

$$\chi_{\text{stagg}} = \tilde{G}(p_{\text{stagg}}) \tag{2.8}$$

Note that on a finite lattice this is well-defined only if the lattice size L is *even*.

(c) The second-moment correlation length, which is defined in finite volume by

$$\xi_L = \frac{[(\chi_{\text{stagg}}/F_{\text{stagg}}) - 1]^{1/2}}{2 \sin(\pi/L)} \tag{2.9}$$

where

$$F_{\text{stagg}} \equiv \tilde{G}(p_{\text{stagg}} + p_{\text{min}, \pm 1}) = \tilde{G}(p_{\text{stagg}} + p_{\text{min}, \pm 2}) \tag{2.10}$$

is the correlation function at the wavevectors closest to p_{stagg}.[7] Again L must be even.

All these quantities can be expressed as expectations involving the following observables:

$$\mathscr{M}^2_{\text{stagg}} = \left(\sum_x e^{ip_{\text{stagg}} \cdot x} \boldsymbol{\sigma}_x \right)^2 \tag{2.11a}$$

$$\mathscr{F}_{\text{stagg}} = \frac{1}{2} \left[\left| \sum_x e^{i(p_{\text{stagg}} + p_{\text{min}, +1}) \cdot x} \boldsymbol{\sigma}_x \right|^2 + \left| \sum_x e^{i(p_{\text{stagg}} + p_{\text{min}, +2}) \cdot x} \boldsymbol{\sigma}_x \right|^2 \right] \tag{2.11b}$$

$$\mathscr{E} = \sum_{\langle xy \rangle} \delta_{\sigma_x, \sigma_y} \tag{2.11c}$$

[6] Here E is the mean energy per *link* in the antiferromagnetic model; we have chosen this normalization in order to have $0 \leqslant E \leqslant 1$, with $E = 0$ for an antiferromagnetic ground state and $E = 1$ for a ferromagnetic ground state. The mean energy per *site* is of course $2E$.

[7] See, e.g., [39, Eqs. (4.11)–(4.13)] for the definition of the second-moment correlation length in a ferromagnetic model, along with its motivation. Here we make the obvious transcription to an antiferromagnetic model that orders at momentum $p_{\text{stagg}} = (\pi, \pi)$.

Thus, we have

$$\chi_{\text{stagg}} = \frac{1}{V} \langle \mathscr{M}^2_{\text{stagg}} \rangle \tag{2.12a}$$

$$F_{\text{stagg}} = \frac{1}{V} \langle \mathscr{F}_{\text{stagg}} \rangle \tag{2.12b}$$

$$E = \frac{1}{2V} \langle \mathscr{E} \rangle \tag{2.12c}$$

where $V = L^2$ is the number of lattice sites.

In addition to studying the (static) behavior of the antiferromagnetic Potts model, we are also interested in studying the dynamic critical behavior of the Wang–Swendsen–Kotecký (WSK) Monte Carlo algorithm. So let A be an observable (i.e., a function of the spin configuration $\{\sigma\}$). We define the unnormalized autocorrelation function

$$C_{AA}(t) = \langle A_s A_{s+t} \rangle - \langle A \rangle^2 \tag{2.13}$$

where expectations are taken *in equilibrium*, and the corresponding normalized autocorrelation function

$$\rho_{AA}(t) = C_{AA}(t)/C_{AA}(0) \tag{2.14}$$

We furthermore define the integrated autocorrelation time

$$\tau_{\text{int},A} = \frac{1}{2} \sum_{t=-\infty}^{\infty} \rho_{AA}(t) \tag{2.15a}$$

$$= \frac{1}{2} + \sum_{t=1}^{\infty} \rho_{AA}(t) \tag{2.15b}$$

[The factor of $\frac{1}{2}$ is purely a matter of convention; it is inserted so that $\tau_{\text{int},A} \approx \tau$ if $\rho_{AA}(t) \approx e^{-|t|/\tau}$ with $\tau \gg 1$.] Finally, we define the exponential autocorrelation times

$$\tau_{\text{exp},A} = \limsup_{t \to \infty} \frac{|t|}{-\log |\rho_{AA}(t)|} \tag{2.16}$$

and

$$\tau_{\text{exp}} = \sup_A \tau_{\text{exp},A} \tag{2.17}$$

Note that $\tau_{\exp} = \tau_{\exp,\,A}$ whenever the observable A is not orthogonal to the slowest mode of the system.

The integrated autocorrelation time controls the statistical error in Monte Carlo measurements of $\langle A \rangle$. More precisely, the sample mean

$$\bar{A} \equiv \frac{1}{n} \sum_{t=1}^{n} A_t \tag{2.18}$$

has variance

$$\operatorname{var}(\bar{A}) = \frac{1}{n^2} \sum_{r,\,s=1}^{n} C_{AA}(r-s) \tag{2.19a}$$

$$= \frac{1}{n} \sum_{t=-(n-1)}^{n-1} \left(1 - \frac{|t|}{n}\right) C_{AA}(t) \tag{2.19b}$$

$$\approx \frac{1}{n} (2\tau_{\text{int},\,A})\, C_{AA}(0) \qquad \text{for} \quad n \gg \tau \tag{2.19c}$$

Thus, the variance of $\bar{A}$ is a factor $2\tau_{\text{int},\,A}$ larger than it would be if the $\{A_t\}$ were statistically independent. Stated differently, the number of "effectively independent samples" in a run of length n is roughly $n/2\tau_{\text{int},\,A}$. The autocorrelation time $\tau_{\text{int},\,A}$ (for interesting observables A) is therefore a "figure of (de)merit" of a Monte Carlo algorithm.

The integrated autocorrelation time $\tau_{\text{int},\,A}$ can be estimated by standard procedures of statistical time-series analysis.[40, 41] These procedures also give statistically valid *error bars* on $\langle A \rangle$ and $\tau_{\text{int},\,A}$. For more details, see [42, Appendix C] or [43, Section 3]. In this paper we have used a self-consistent truncation window of width $c\tau_{\text{int},\,A}$, where $c = 6$; this choice is reasonable whenever the autocorrelation function $\rho_{AA}(t)$ decays roughly exponentially, as it does here (see Section 5.2 below).

In setting the error bars on ξ [defined in (2.9)] we have used the triangle inequality; such error bars are overly conservative, but we were too lazy to measure the cross-correlations between $\mathscr{M}^2_{\text{stagg}}$ and $\mathscr{F}_{\text{stagg}}$. (This was a mistake, and in future work we *will* measure these cross-correlations.)

2.2. Finite-Size-Scaling Extrapolation Method

In the theory of critical phenomena we are usually interested in infinite-volume systems, but Monte Carlo simulations are perforce carried out on finite lattices. One traditional approach has been to run on lattice

sizes $L \gtrsim 6\xi$, which are large enough so that the finite-size corrections are negligible. In the past few years, however, methods have become available for extrapolating finite-size data to $L = \infty$, based on finite-size-scaling (FSS) theory; these methods allow one to work, for a given lattice size L, at correlation lengths ξ much larger than were previously attainable. In this subsection we review an extremely powerful and general method of this kind, due originally to Lüscher, Weisz, and Wolff [14] and more recently elaborated by our group.[20–22] This extrapolation method plays a crucial role in the present work, as it allows us to reach correlation lengths ξ of order 5000, whereas in the traditional approach we would have been limited to $\xi \lesssim 250$.

Consider, for simplicity, a model controlled by a renormalization-group fixed point having *one* relevant operator. (The parameter β may be multidimensional, but only one direction in β-space should be relevant in the RG sense. In other words, the continuum limit should be unique modulo length rescalings.) Let us work on a periodic lattice of linear size L. Let $\xi(\beta, L)$ be a suitably defined finite-volume correlation length, such as the second-moment correlation length defined by (2.9); and let $\mathcal{O}$ be any long-distance observable (e.g., the correlation length or the susceptibility). Then finite-size-scaling theory[44–46] predicts that

$$\frac{\mathcal{O}(\beta, L)}{\mathcal{O}(\beta, \infty)} = f_{\mathcal{O}}\big(\xi(\beta, \infty)/L\big) + O(\xi^{-\omega}, L^{-\omega}) \tag{2.20}$$

where $f_{\mathcal{O}}$ is a universal (though usually unknown) function and ω is a correction-to-scaling exponent.[8] It follows that if s is any fixed scale factor (usually we take $s = 2$), then

$$\frac{\mathcal{O}(\beta, sL)}{\mathcal{O}(\beta, L)} = F_{\mathcal{O}}\big(\xi(\beta, L)/L; s\big) + O(\xi^{-\omega}, L^{-\omega}) \tag{2.21}$$

where $F_{\mathcal{O}}$ can easily be expressed in terms of $f_{\mathcal{O}}$ and f_ξ. (Henceforth we shall suppress the argument s if it is clear from the context.) In other words, if we make a plot of $\mathcal{O}(\beta, sL)/\mathcal{O}(\beta, L)$ versus $\xi(\beta, L)/L$, then all the points should lie on a single curve, modulo corrections of order $\xi^{-\omega}$ and $L^{-\omega}$.

[8] This form of finite-size scaling assumes hyperscaling, and thus is expected to hold only below the upper critical dimension of the model. See, e.g., [46, Chapter I, Section 2.7]. Note also that when we say $f_{\mathcal{O}}$ is "universal," we mean only that it is the same for all models in a given universality class. Of course $f_{\mathcal{O}}$ varies from one universality class to another.

Our method proceeds as follows:[9] Make Monte Carlo runs at numerous pairs (β, L) and (β, sL). Plot $\mathcal{O}(\beta, sL)/\mathcal{O}(\beta, L)$ versus $\xi(\beta, L)/L$, using those points satisfying both $\xi(\beta, L) \geqslant$ some value $\xi_{\min}$ and $L \geqslant$ some value $L_{\min}$. If all these points fall with good accuracy on a single curve —thus verifying the Ansatz (2.21) for $\xi \geqslant \xi_{\min}$, $L \geqslant L_{\min}$—choose a smooth fitting function $F_{\mathcal{O}}$. Then, using the functions F_ξ and $F_{\mathcal{O}}$, extrapolate the pair $(\xi, \mathcal{O})$ successively from $L \to sL \to s^2L \to \cdots \to \infty$.

We have chosen to use functions $F_{\mathcal{O}}$ of the form[10]

$$F_{\mathcal{O}}(x) = 1 + a_1 e^{-1/x} + a_2 e^{-2/x} + \cdots + a_n e^{-n/x} \tag{2.22}$$

[9] Our method[20–22] is essentially identical to that of Lüscher, Weisz, and Wolff.[14] The principal difference is that Lüscher *et al.* choose carefully their runs (β, L) so as to produce only a few distinct values of $x \equiv \xi(\beta, L)/L$, while we attempt to cover an entire interval of x. Which approach is preferable depends on one's aims and on the available CPU time. Also, the motivations are somewhat different: the primary aim of Lüscher *et al.*[14] is to compare the asymptotic behavior of the finite-size-scaling functions $F_{\mathcal{O}}(x)$ at large x to the perturbative predictions; they did not discuss the possibility of obtaining extrapolations to $L = \infty$ at each fixed β, although this is of course implicit in their method. The method of Kim[15–19] is also very closely related, but he compares lattice size L to ∞ rather than to sL; this is a (slight) disadvantage. Our method also has many features in common with that used by Flyvbjerg and Larsen[47,48] to extrapolate their $1/N$-expansion finite-lattice data. It should be emphasized that all these methods are completely general; although they were historically first applied to asymptotically free theories,[14] they are in no way limited to this case. Note also that all these methods share the property of working only with observable quantities (ξ, $\mathcal{O}$, and L) and not with bare quantities (β). Therefore, they rely only on "scaling" and not on "asymptotic scaling;" and they differ from other FSS-based methods such as phenomenological renormalization.[49]

[10] In performing this fit, one may use any basis one pleases in the space spanned by the functions $\{e^{-k/x}\}_{1 \leqslant k \leqslant n}$; the final result (in exact arithmetic) is of course the same. However, in finite-precision arithmetic the calculation may become numerically unstable if the condition number of the least-squares matrix gets too large. In particular, this disaster occurs if we use as a basis the monomials t^k (where $t = e^{-1/x}$). The trouble is that these monomials are "almost collinear" in the relevant Hilbert space $L^2(\mu)$ defined by $\mu(t) = \sum_i w_i \, \delta(t - t_i)$, where t_i are the values of $t \equiv e^{-L/\xi(\beta, L)}$ arising in the data pairs and $w_i = 1/[\text{error on } \mathcal{O}(2L)/\mathcal{O}(L)]^2$ are the corresponding weights. To avoid this disaster, we should seek to use a basis that is closer to orthogonal in $L^2(\mu)$. Of course, exactly orthogonalizing in $L^2(\mu)$ is equivalent to diagonalizing the least-squares matrix, which is unfeasible; but we can do well enough by using polynomials with zero constant term that are orthogonal with respect to the simple measure $w(t) = t^a(t_{\max} - t)^b$ on $[0, t_{\max}]$, where a and b are some chosen numbers > -1. These polynomials are Jacobi polynomials $f_k(t) = tP_{k-1}^{(b, a+2)}(2t/t_{\max} - 1)$ for $1 \leqslant k \leqslant n$ [50, pp. 321–328]. The idea here is that the measure $w(t) = t^a(t_{\max} - t)^b$ should roughly approximate the measure $\mu(t)$. We have here used $a = 0$, $b = -3/4$; but the performance is very insensitive to the choices of a and b. This cleverness in the choice of basis *vastly* improves the numerical stability of the result, by reducing the condition number of the matrix arising in the fit. Typical condition numbers using Jacobi polynomials are ~ 20 for $n = 3$ and ~ 100 for $n = 9$.

(Other forms of fitting functions can be used instead.) This form is partially motivated by theory, which tells us that in some cases $F_{\mathcal{O}}(x) \to 1$ exponentially fast as $x \to 0$. Typically a fit of order $3 \leqslant n \leqslant 13$ is sufficient; the required order depends on the range of x values covered by the data and on the shape of the curve. Empirically, we increase n until the χ^2 of the fit becomes essentially constant. The resulting χ^2 value provides a check on the systematic errors arising from corrections to scaling and/or from the inadequacies of the form (2.22).

The *statistical* error on the extrapolated value of $\mathcal{O}_\infty(\beta) \equiv \mathcal{O}(\beta, \infty)$ comes from three sources:

(i) Error on $\mathcal{O}(\beta, L)$, which gets multiplicatively propagated to $\mathcal{O}_\infty$.

(ii) Error on $\xi(\beta, L)$, which affects the argument $x \equiv \xi(\beta, L)/L$ of the scaling functions F_ξ and $F_{\mathcal{O}}$.

(iii) Statistical error in our estimate of the coefficients $a_1, ..., a_n$ in F_ξ and $F_{\mathcal{O}}$.

The errors of type (i) and (ii) depend on the statistics available at the single point (β, L), while the error of type (iii) depends on the statistics in the whole set of runs. Errors (i) + (ii) [resp. (i) + (ii) + (iii)] can be quantified by performing an auxiliary Monte Carlo experiment in which the input data at (β, L) [resp. the whole set of input data] are varied randomly within their error bars and then extrapolated (we call this the method of "fake data sets").[11]

The discrepancies between the extrapolated values from different lattice sizes at the same β—to the extent that these exceed the estimated statistical errors—can serve as a rough estimate of the remaining systematic errors. More precisely, let $\mathcal{O}_i$ $(i = 1, ..., m)$ be the extrapolated values at some given β, and let $C = (C_{ij})_{i,j=1}^m$ be the estimated covariance matrix for their statistical errors.[12] [Errors of type (iii) induce off-diagonal terms in C.] Then we form the weighted average

$$\bar{\mathcal{O}} = \left(\sum_{i,j=1}^{m} (C^{-1})_{ij} \mathcal{O}_j \right) \Big/ \left(\sum_{i,j=1}^{m} (C^{-1})_{ij} \right), \tag{2.23}$$

[11] In principle, ξ and $\mathcal{O}$ should be generated from a *joint* Gaussian with the correct covariance. We ignored this subtlety and simply generated *independent* fluctuations on ξ and $\mathcal{O}$.

[12] This covariance matrix is computed from the auxiliary Monte Carlo experiment mentioned in the preceding paragraph. Since this C is only a statistical estimate, the values of $\bar{\mathcal{O}}$, $\bar{\sigma}$ and $\mathcal{R}$ will vary *slightly* from one analysis run to the next.

the error bar on the weighted average

$$\bar{\sigma} = \left(\sum_{i,\, j=1}^{m} (C^{-1})_{ij} \right)^{-1/2}, \tag{2.24}$$

and the residual sum-of-squares

$$\mathscr{R} = \sum_{i,\, j=1}^{m} (\mathcal{O}_i - \bar{\mathcal{O}})(C^{-1})_{ij} (\mathcal{O}_j - \bar{\mathcal{O}}). \tag{2.25}$$

Under the assumptions that

(a) the fluctuations among the $\mathcal{O}_1, ..., \mathcal{O}_m$ are purely statistical [i.e., there are *no* systematic errors in the extrapolation], and

(b) the statistical error bars are correct,

$\mathscr{R}$ should be distributed as a χ^2 random variable with $m-1$ degrees of freedom. Moreover, the sum of $\mathscr{R}$ over all the values of β should be distributed as a χ^2 random variable with $\sum (m-1)$ degrees of freedom.[13] In this way, we can search for values of β for which the extrapolations from different lattice sizes are mutually inconsistent; and we can test the overall self-consistency of the extrapolations.

A figure of (de)merit of the method is the relative variance on the extrapolated value $\mathcal{O}_\infty(\beta)$, multiplied by the computer time needed to obtain it.[14] We expect this *relative variance-time product* [for errors (i) + (ii) only] to scale as

$$\mathrm{RVTP}(\beta, L) \approx \xi_\infty(\beta)^{d + z_{\mathrm{int},\,\mathcal{O}}} G_{\mathcal{O}}(\xi_\infty(\beta)/L) \tag{2.26}$$

where d is the spatial dimension and $z_{\mathrm{int},\,\mathcal{O}}$ is the dynamic critical exponent of the Monte Carlo algorithm being used; here $G_{\mathcal{O}}$ is a combination of several static and dynamic finite-size-scaling functions, and depends both on the observable $\mathcal{O}$ and on the algorithm but not on the scale factor s. As ξ_∞/L tends to zero, we expect $G_{\mathcal{O}}$ to diverge as $(\xi_\infty/L)^{-d}$ (since it is wasteful to use a lattice $L \gg \xi_\infty$). As ξ_∞/L tends to infinity, we expect

[13] This latter statement is not quite correct, as it ignores the correlations between the various $\mathcal{O}_i$ at *different* β, which are induced by errors of type (iii). [Correlations between different $\mathcal{O}_i$ at the *same* β, which are also induced by errors of type (iii), *are* included in (2.23)–(2.25).]

[14] At fixed (β, L), this variance-time product tends to a constant as the CPU time tends to infinity. However, if the CPU time used is too small, then the variance-time product can be significantly larger than its asymptotic value, due to nonlinear cross terms between error sources (i) and (ii).

$G_{\mathcal{O}} \sim (\xi_\infty/L)^p$ for some power p (see ref. 22 for details). Note that *the power p can be either positive or negative*. If $p > 0$, there is an optimum value of ξ_∞/L; this determines the best lattice size at which to perform runs for a given β. If $p < 0$, it is most efficient to use the *smallest* lattice size for which the corrections to scaling are negligible compared to the statistical errors. [Of course, this analysis neglects errors of type (iii). The optimization becomes much more complicated if errors of type (iii) are included, as it is then necessary to optimize the set of runs as a whole.]

The reader is referred to refs. 21 and 22 for a fuller treatment of this extrapolation method, in particular the finite-size-scaling theory and the analysis of the propagation of statistical errors.

Let us make one final comment about the physics contained in the scaling function $F_\xi(x)$. At the critical point β_c, the correlation length $\xi(\beta_c, L)$ is proportional to L: one thus has

$$\lim_{L \to \infty} \frac{\xi(\beta_c, L)}{L} = \text{some value } x^* \tag{2.27}$$

and

$$\lim_{L \to \infty} \frac{\xi(\beta_c, sL)}{\xi(\beta_c, L)} = s \tag{2.28}$$

Therefore, x^* is determined by the relation

$$F_\xi(x^*; s) = s \tag{2.29}$$

The constant x^* is characteristic of the massless field theory corresponding to the given critical point, on a continuum torus with aspect ratio 1; for two-dimensional models it should in principle be calculable via conformal field theory. Likewise, for any observable $\mathcal{O}$ which behaves in the critical region like $\mathcal{O} \sim \xi^{\gamma_{\mathcal{O}}/\nu}$, one has

$$F_{\mathcal{O}}(x^*; s) = s^{\gamma_{\mathcal{O}}/\nu} \tag{2.30}$$

2.3. Wang–Swendsen–Kotecký (WSK) Algorithm

About a decade ago, Wang, Swendsen, and Kotecký (WSK)[10, 11] proposed an elegant and extraordinarily efficient Monte Carlo algorithm for simulating the antiferromagnetic q-state Potts model on an arbitrary finite graph G. The elementary update of their algorithm goes as follows: Choose at random two distinct "colors" $i, j \in \{1,..., q\}$; freeze all the spins

σ_x currently taking values $k \neq i, j$, and allow the remaining spins to take value either i or j. The induced model is thus an antiferromagnetic *Ising* model (in zero magnetic field)[15] on a subgraph of G; this model can be updated by any legitimate Monte Carlo algorithm, such as the Swendsen–Wang algorithm[51] or Wolff's single-cluster variant[52] (we use the former). It is easy to see that this algorithm leaves invariant the Gibbs measure of the underlying Potts model.

At zero temperature ($\beta = \infty$) the antiferromagnetic Potts model reduces to the equal-weight distribution on q-colorings of G, and the WSK algorithm becomes: independently for each connected cluster of i–j spins, either leave that cluster as is or else flip it (interchanging i and j).

The WSK algorithm is trivially seen to be ergodic at any nonzero temperature. However, the ergodicity at zero temperature is a very subtle problem, which has thus far been only partially resolved, Lubin and Sokal[12] showed that for $q = 3$ the WSK algorithm is *non-ergodic* at zero temperature on periodic square lattices of size $3m \times 3n$ where m and n are relatively prime. On the other hand, in Appendix B we shall prove that the WSK algorithm is *ergodic* for all q whenever the graph G is bipartite; in particular, this happens on periodic square lattices of size $m \times n$ whenever m and n are both *even*. For other cases the ergodicity is an open problem.

It should be noted that the problem of ergodicity at zero temperature is not merely a theoretical one, even if all our simulations are performed at nonzero temperature. If the algorithm is non-ergodic at $\beta = \infty$, then the autocorrelation time must diverge as $\beta \to \infty$, *even on a fixed finite lattice*.[16] This behavior, if it occurs, could be a severe impediment to high-precision Monte Carlo study of the model. So it is fortunate that our model here lies precisely in the situation for which ergodicity has been proven: the periodic square lattice with L even.

3. SUMMARY OF OUR RUNS

We simulated the square-lattice Potts antiferromagnets for $q = 3$ and $q = 4$, using the WSK algorithm with standard (multi-cluster) Swendsen–Wang updates of the induced Ising model.

[15] The key point here is that the interaction energies $i-k$ and $j-k$ are equal. This guarantees that the induced Ising model has zero magnetic field.

[16] More precisely, it is the *exponential* autocorrelation time τ_{exp} (corresponding to the slowest mode in the system) which must diverge. The integrated autocorrelation time $\tau_{\text{int},A}$ for any given observable A need not diverge; that depends on the choice of A. Moreover, even if it does diverge, the divergence could be very weak, if A has "weak overlap" with the slowest mode. On the other hand, the divergence of τ_{exp} already calls into question the convergence to equilibrium, by raising the specter of "metastability."

For $q=3$ we ran on $L\times L$ periodic lattices with $L=32$, 64, 128, 256, 512, 1024, 1536 at 149 different pairs (β, L) in the range $2.0\leqslant\beta\leqslant 6.0$ (corresponding to $5\lesssim\xi_\infty\lesssim 20000$). Our data cover rather densely the range $0.09\lesssim x\equiv\xi(\beta, L)/L\lesssim 0.63$. Each data point comprises between 2×10^5 and 2.2×10^7 iterations of the WSK algorithm, which corresponds to anywhere from 40000τ to $5\times 10^6\tau$. We discarded the first 10000 iterations of each run, which ought to be more than enough for equilibration ($>2000\tau$!); we also made spot checks for evidence of initialization bias after the discard interval, and found none. Most of the runs used a random initial configuration ("hot start"). In some cases with $L=32$, 64 we made multiple independent runs, some of which used an antiferromagnetically ordered initial configuration ("cold start"); statistical tests showed complete agreement between the runs. The data from independent runs were merged statistically in the usual way. The raw data for $q=3$ can be found in Table 1.

The CPU time for our program is $4.4L^2$ μs/sweep on an IBM RS-6000/370, and the total CPU time was about 2.5 years on this same machine. (This is an "equivalent" figure: in fact our runs were performed on a variety of mostly slower machines in both New York and Belo Horizonte, so the actual total CPU time was more than this.)

For $q=4$ it sufficed to make a small number of runs for $L=32$, 64; the total CPU time was less than 3 days on an IBM RS-6000/370. The raw data can be found in Table 2.

4. DATA ANALYSIS: $q=3$, STATIC QUANTITIES

In this section we analyze the static data for $q=3$. Concerning the correlation length ξ and the staggered susceptibility χ_{stagg}, we first extrapolate these quantities to infinite volume (Section 4.1) and then analyze the behavior as $\beta\to\infty$ of the extrapolated data (Section 4.2). We conclude by taking a brief look at the energy E (Section 4.3).

4.1. Extrapolation to Infinite Volume

We shall extrapolate ξ and χ_{stagg} to infinite volume using the method of Section 2.2 with scale factor $s=2$. This method is specified by three parameters: the cut points $\xi_{\min}$ and $L_{\min}$, and the interpolation order n. We shall therefore vary these parameters systematically and study the systematic errors attributable to them.

4.1.1. Correlation Length. In Table 3 we report the quality of the fit—chi-squared (χ^2), number of degrees of freedom (DF), χ^2/DF, and

Table 1. Our Monte Carlo Data for the 3-State Potts Antiferromagnet[a]

L	β	Total	Discard	ξ	χ_{stagg}	E	$\tau_{\text{int},\mathcal{M}^2_{\text{stagg}}}$	$\tau_{\text{int},\mathcal{E}}$
32	2.00	200000	10000	5.572 (0.032)	49.02 (0.22)	0.07027100 (0.00005919)	2.53 (0.05)	3.16 (0.06)
32	2.25	200000	10000	8.222 (0.036)	89.75 (0.38)	0.04771217 (0.00005094)	3.39 (0.07)	3.35 (0.07)
32	2.50	6000000	60000	11.594 (0.008)	145.77 (0.09)	0.03207236 (0.00000761)	4.17 (0.02)	3.49 (0.01)
32	2.70	6000000	60000	14.116 (0.009)	186.45 (0.09)	0.02354641 (0.00000625)	4.31 (0.02)	3.36 (0.01)
32	3.00	6000000	60000	16.834 (0.009)	227.51 (0.08)	0.01529180 (0.00000460)	4.19 (0.02)	3.06 (0.01)
32	3.20	6000000	60000	17.956 (0.009)	243.94 (0.07)	0.01171553 (0.00000381)	4.14 (0.02)	2.91 (0.01)
32	3.50	22000000	220000	19.015 (0.005)	259.29 (0.03)	0.00804395 (0.00000155)	4.12 (0.01)	2.76 (0.01)
32	4.00	6000000	60000	19.812 (0.009)	271.55 (0.06)	0.00449722 (0.00000209)	4.22 (0.02)	2.63 (0.00)
32	4.50	6000000	60000	20.130 (0.009)	276.87 (0.06)	0.00259774 (0.00000153)	4.34 (0.02)	2.56 (0.00)
32	5.00	6000000	60000	20.263 (0.009)	279.45 (0.06)	0.00153121 (0.00000116)	4.41 (0.02)	2.55 (0.00)
64	2.00	200000	10000	5.579 (0.074)	49.43 (0.20)	0.07048701 (0.00002977)	1.75 (0.03)	3.21 (0.07)
64	2.25	200000	10000	8.534 (0.064)	97.32 (0.42)	0.04814820 (0.00002498)	2.07 (0.03)	3.27 (0.07)
64	2.50	2000000	20000	13.181 (0.021)	196.58 (0.27)	0.03288755 (0.00000638)	2.96 (0.02)	3.31 (0.02)
64	2.60	200000	10000	15.628 (0.073)	256.47 (1.15)	0.02829046 (0.00001911)	3.58 (0.08)	3.32 (0.07)
64	2.70	2000000	20000	18.349 (0.024)	327.45 (0.42)	0.02432931 (0.00000549)	3.86 (0.03)	3.37 (0.02)
64	2.80	200000	10000	21.167 (0.083)	403.52 (1.53)	0.02098848 (0.00001660)	4.15 (0.10)	3.50 (0.07)
64	2.90	200000	10000	23.956 (0.090)	477.13 (1.65)	0.01814113 (0.00001506)	4.49 (0.11)	3.35 (0.07)
64	3.00	2000000	20000	26.715 (0.029)	549.54 (0.51)	0.01572752 (0.00000419)	4.46 (0.04)	3.23 (0.02)
64	3.10	200000	10000	29.067 (0.098)	609.52 (1.61)	0.01371684 (0.00001249)	4.49 (0.11)	3.21 (0.07)
64	3.20	2000000	20000	31.188 (0.031)	661.13 (0.48)	0.01197822 (0.00000345)	4.44 (0.04)	3.04 (0.02)
64	3.30	200000	10000	32.883 (0.098)	702.93 (1.46)	0.01050532 (0.00001010)	4.31 (0.10)	2.94 (0.06)
64	3.40	200000	10000	34.326 (0.101)	736.49 (1.40)	0.00924902 (0.00000937)	4.26 (0.10)	2.92 (0.06)
64	3.50	2000000	20000	35.517 (0.031)	764.61 (0.42)	0.00816692 (0.00000265)	4.36 (0.03)	2.83 (0.01)
64	3.60	200000	10000	36.605 (0.102)	789.12 (1.29)	0.00722325 (0.00000786)	4.21 (0.10)	2.77 (0.05)
64	3.70	200000	10000	37.183 (0.102)	804.16 (1.26)	0.00641653 (0.00000739)	4.38 (0.11)	2.79 (0.05)
64	3.80	200000	10000	38.082 (0.102)	822.54 (1.21)	0.00571353 (0.00000668)	4.24 (0.10)	2.63 (0.05)
64	3.90	200000	10000	38.398 (0.101)	832.77 (1.19)	0.00508284 (0.00000638)	4.31 (0.10)	2.70 (0.05)
64	4.00	2000000	20000	38.786 (0.031)	842.08 (0.36)	0.00453673 (0.00000183)	4.21 (0.03)	2.65 (0.01)
64	4.50	2000000	20000	39.891 (0.032)	871.56 (0.34)	0.00261704 (0.00000134)	4.32 (0.03)	2.57 (0.01)
64	5.00	2000000	20000	40.325 (0.032)	884.30 (0.34)	0.00153744 (0.00000100)	4.43 (0.04)	2.54 (0.01)
128	2.00	200000	10000	5.442 (0.244)	49.37 (0.20)	0.07048002 (0.00001449)	1.52 (0.02)	3.05 (0.06)
128	2.25	200000	10000	8.817 (0.174)	98.61 (0.41)	0.04817305 (0.00001255)	1.70 (0.03)	3.30 (0.07)
128	2.50	200000	10000	13.335 (0.136)	201.66 (0.84)	0.03295390 (0.00001007)	1.81 (0.03)	3.20 (0.07)
128	2.60	200000	10000	15.967 (0.131)	271.66 (1.18)	0.02837582 (0.00000939)	2.10 (0.04)	3.25 (0.07)
128	2.70	200000	10000	19.267 (0.127)	368.40 (1.59)	0.02450218 (0.00000868)	2.27 (0.04)	3.26 (0.07)
128	2.80	200000	10000	23.237 (0.129)	500.07 (2.20)	0.02118313 (0.00000790)	2.63 (0.05)	3.20 (0.07)
128	2.90	200000	10000	27.867 (0.138)	672.92 (3.01)	0.01836736 (0.00000724)	3.11 (0.06)	3.14 (0.06)
128	2.95	200000	10000	30.271 (0.143)	767.77 (3.43)	0.01711320 (0.00000701)	3.41 (0.07)	3.20 (0.07)
128	3.00	200000	10000	33.203 (0.151)	886.35 (3.92)	0.01595897 (0.00000679)	3.79 (0.08)	3.25 (0.07)
128	3.10	200000	10000	38.836 (0.162)	1121.29 (4.57)	0.01389865 (0.00000626)	4.04 (0.09)	3.21 (0.07)
128	3.20	200000	10000	44.917 (0.176)	1382.17 (5.10)	0.01213496 (0.00000569)	4.40 (0.11)	3.13 (0.06)
128	3.30	200000	10000	50.858 (0.187)	1630.23 (5.32)	0.01064182 (0.00000528)	4.58 (0.11)	3.12 (0.06)
128	3.40	200000	10000	55.937 (0.195)	1845.96 (5.34)	0.00935202 (0.00000477)	4.68 (0.12)	2.95 (0.06)
128	3.45	200000	10000	58.310 (0.196)	1935.27 (5.23)	0.00877467 (0.00000460)	4.66 (0.11)	2.95 (0.06)
128	3.50	1000000	10000	60.607 (0.087)	2029.01 (2.21)	0.00824378 (0.00000193)	4.48 (0.05)	2.93 (0.03)

[a] "Total" is the total number of WSK iterations performed. "Discard" is the number of iterations discarded for equilibration. Error bars (one standard deviation) are shown in parentheses.

Table 1. (*Continued*)

L	β	Total	Discard	ξ	χ_{stagg}	E	$\tau_{\text{int},\mathcal{M}^2_{\text{stagg}}}$	$\tau_{\text{int},\mathcal{E}}$
128	3.60	200000	10000	64.455 (0.202)	2178.61 (4.87)	0.00728348 (0.00000400)	4.54 (0.11)	2.82 (0.05)
128	3.70	200000	10000	67.788 (0.203)	2304.67 (4.61)	0.00646723 (0.00000375)	4.41 (0.11)	2.80 (0.05)
128	3.80	200000	10000	70.305 (0.207)	2403.28 (4.43)	0.00574268 (0.00000342)	4.47 (0.11)	2.73 (0.05)
128	3.90	200000	10000	72.160 (0.207)	2474.84 (4.24)	0.00511211 (0.00000320)	4.40 (0.11)	2.72 (0.05)
128	3.95	200000	10000	73.286 (0.201)	2513.98 (4.10)	0.00482635 (0.00000313)	4.29 (0.10)	2.72 (0.05)
128	4.00	200000	10000	73.922 (0.207)	2542.02 (4.14)	0.00455744 (0.00000300)	4.48 (0.11)	2.71 (0.05)
128	4.10	200000	10000	75.419 (0.204)	2594.69 (3.94)	0.00406992 (0.00000280)	4.32 (0.10)	2.69 (0.05)
128	4.20	200000	10000	76.508 (0.205)	2636.64 (3.92)	0.00363639 (0.00000262)	4.52 (0.11)	2.64 (0.05)
128	4.30	1000000	10000	77.427 (0.090)	2670.89 (1.64)	0.00325960 (0.00000107)	4.29 (0.04)	2.62 (0.02)
128	4.40	1000000	10000	78.050 (0.089)	2697.29 (1.61)	0.00291971 (0.00000101)	4.27 (0.04)	2.61 (0.02)
128	4.50	1000000	10000	78.772 (0.090)	2723.43 (1.59)	0.00262197 (0.00000095)	4.32 (0.04)	2.59 (0.02)
128	4.60	1000000	10000	79.136 (0.090)	2742.07 (1.59)	0.00235324 (0.00000090)	4.37 (0.05)	2.59 (0.02)
128	4.70	1000000	10000	79.505 (0.091)	2756.45 (1.58)	0.00211402 (0.00000084)	4.41 (0.05)	2.56 (0.02)
128	4.80	1000000	10000	79.952 (0.090)	2771.60 (1.56)	0.00190149 (0.00000080)	4.40 (0.05)	2.56 (0.02)
128	4.90	1000000	10000	80.091 (0.091)	2781.79 (1.56)	0.00171139 (0.00000075)	4.42 (0.05)	2.56 (0.02)
128	5.00	1000000	10000	80.174 (0.091)	2788.86 (1.56)	0.00154123 (0.00000071)	4.42 (0.05)	2.53 (0.02)
128	5.10	1000000	10000	80.443 (0.090)	2797.74 (1.54)	0.00138704 (0.00000067)	4.37 (0.05)	2.52 (0.02)
128	5.20	1000000	10000	80.612 (0.091)	2805.76 (1.54)	0.00125012 (0.00000064)	4.40 (0.05)	2.55 (0.02)
256	2.50	200000	10000	13.104 (0.422)	201.34 (0.81)	0.03295828 (0.00000517)	1.57 (0.02)	3.34 (0.07)
256	2.60	200000	10000	16.185 (0.356)	273.13 (1.08)	0.02839657 (0.00000461)	1.56 (0.02)	3.18 (0.07)
256	2.70	200000	10000	19.126 (0.325)	369.05 (1.51)	0.02450313 (0.00000423)	1.69 (0.03)	3.15 (0.06)
256	2.80	200000	10000	23.045 (0.293)	502.20 (2.08)	0.02119791 (0.00000393)	1.76 (0.03)	3.16 (0.06)
256	2.90	200000	10000	28.119 (0.269)	693.32 (2.93)	0.01837763 (0.00000362)	1.90 (0.03)	3.16 (0.06)
256	3.00	200000	10000	34.305 (0.258)	954.62 (4.09)	0.01599052 (0.00000333)	2.09 (0.04)	3.13 (0.06)
256	3.10	200000	10000	41.701 (0.260)	1313.21 (5.88)	0.01394816 (0.00000305)	2.48 (0.04)	3.10 (0.06)
256	3.20	200000	10000	50.453 (0.269)	1803.02 (8.21)	0.01219458 (0.00000281)	2.96 (0.06)	3.05 (0.06)
256	3.30	200000	10000	60.839 (0.286)	2439.41 (10.78)	0.01069957 (0.00000263)	3.35 (0.07)	3.08 (0.06)
256	3.40	200000	10000	72.254 (0.316)	3198.35 (13.71)	0.00940398 (0.00000238)	3.99 (0.09)	2.94 (0.06)
256	3.50	1000000	10000	84.685 (0.150)	4036.07 (6.91)	0.00829150 (0.00000096)	4.38 (0.05)	2.92 (0.03)
256	3.60	200000	10000	96.720 (0.365)	4854.04 (16.67)	0.00732740 (0.00000203)	4.48 (0.11)	2.85 (0.06)
256	3.70	200000	10000	107.817 (0.380)	5595.86 (16.87)	0.00648727 (0.00000188)	4.59 (0.11)	2.82 (0.05)
256	3.80	200000	10000	117.698 (0.392)	6228.98 (16.33)	0.00576244 (0.00000175)	4.50 (0.11)	2.81 (0.05)
256	3.90	200000	10000	125.908 (0.414)	6756.45 (16.21)	0.00512698 (0.00000163)	4.77 (0.12)	2.78 (0.05)
256	4.00	200000	10000	132.919 (0.413)	7173.99 (15.25)	0.00456912 (0.00000151)	4.62 (0.11)	2.72 (0.05)
256	4.10	200000	10000	138.468 (0.409)	7524.03 (14.19)	0.00407866 (0.00000140)	4.40 (0.11)	2.64 (0.05)
256	4.20	200000	10000	143.448 (0.409)	7812.70 (13.50)	0.00364854 (0.00000133)	4.30 (0.10)	2.70 (0.05)
256	4.30	200000	10000	146.776 (0.404)	8024.93 (12.99)	0.00326371 (0.00000124)	4.29 (0.10)	2.66 (0.05)
256	4.40	200000	10000	150.305 (0.412)	8207.19 (12.71)	0.00292610 (0.00000116)	4.36 (0.10)	2.58 (0.05)
256	4.50	1000000	10000	152.769 (0.180)	8361.37 (5.39)	0.00262364 (0.00000048)	4.33 (0.04)	2.62 (0.02)
256	4.60	1000000	10000	154.560 (0.181)	8472.30 (5.32)	0.00235575 (0.00000045)	4.39 (0.05)	2.56 (0.02)
256	4.65	1000000	10000	154.914 (0.181)	8512.61 (5.26)	0.00223281 (0.00000043)	4.36 (0.05)	2.57 (0.02)
256	4.70	1000000	10000	155.773 (0.179)	8560.34 (5.21)	0.00211659 (0.00000042)	4.35 (0.05)	2.57 (0.02)
256	4.80	1000000	10000	157.217 (0.179)	8645.33 (5.05)	0.00190282 (0.00000040)	4.25 (0.04)	2.54 (0.02)
256	4.90	1000000	10000	157.807 (0.179)	8696.27 (5.02)	0.00171308 (0.00000038)	4.27 (0.04)	2.53 (0.02)
256	5.00	1000000	10000	158.676 (0.180)	8750.44 (5.01)	0.00154114 (0.00000036)	4.35 (0.05)	2.54 (0.02)
256	5.10	1000000	10000	159.453 (0.182)	8796.18 (5.02)	0.00138804 (0.00000034)	4.43 (0.05)	2.57 (0.02)
256	5.20	1000000	10000	160.061 (0.182)	8833.00 (4.98)	0.00125104 (0.00000032)	4.42 (0.05)	2.56 (0.02)
256	5.30	1000000	10000	160.395 (0.182)	8864.52 (4.96)	0.00112784 (0.00000030)	4.43 (0.05)	2.53 (0.02)
256	5.40	1000000	10000	160.835 (0.182)	8892.90 (4.93)	0.00101687 (0.00000029)	4.40 (0.05)	2.52 (0.02)
512	2.80	500000	10000	23.428 (0.577)	505.57 (1.25)	0.02119445 (0.00000123)	1.54 (0.01)	3.22 (0.04)
512	2.90	500000	10000	27.679 (0.508)	690.13 (1.74)	0.01838339 (0.00000113)	1.61 (0.01)	3.17 (0.04)
512	3.00	500000	10000	33.500 (0.442)	949.08 (2.41)	0.01598973 (0.00000104)	1.64 (0.02)	3.14 (0.04)

Table 1. (*Continued*)

L	β	Total	Discard	ξ	χ_{stagg}	E	$\tau_{\text{int},\mathscr{M}^2_{\text{stagg}}}$	$\tau_{\text{int},\mathscr{E}}$
512	3.10	200000	10000	41.719 (0.619)	1325.44 (5.48)	0.01394838 (0.00000152)	1.73 (0.03)	3.07 (0.06)
512	3.20	200000	10000	50.521 (0.559)	1830.24 (7.59)	0.01220209 (0.00000139)	1.81 (0.03)	2.99 (0.06)
512	3.30	500000	10000	61.816 (0.330)	2552.67 (6.83)	0.01070391 (0.00000080)	2.03 (0.02)	3.00 (0.04)
512	3.40	500000	10000	75.572 (0.320)	3563.37 (9.72)	0.00941670 (0.00000075)	2.29 (0.02)	2.99 (0.04)
512	3.50	500000	10000	92.478 (0.330)	4976.76 (14.11)	0.00830439 (0.00000068)	2.76 (0.03)	2.90 (0.04)
512	3.60	500000	10000	112.345 (0.350)	6836.58 (19.37)	0.00734161 (0.00000063)	3.26 (0.04)	2.82 (0.03)
512	3.65	500000	10000	123.233 (0.366)	7933.08 (22.46)	0.00690976 (0.00000061)	3.60 (0.05)	2.85 (0.03)
512	3.70	500000	10000	135.191 (0.382)	9165.68 (25.34)	0.00650506 (0.00000058)	3.87 (0.05)	2.81 (0.03)
512	3.80	500000	10000	159.602 (0.412)	11762.98 (30.00)	0.00577529 (0.00000054)	4.29 (0.06)	2.74 (0.03)
512	3.90	500000	10000	184.606 (0.444)	14484.50 (32.72)	0.00513675 (0.00000050)	4.52 (0.07)	2.73 (0.03)
512	4.00	1000000	10000	208.293 (0.333)	16999.84 (23.79)	0.00457741 (0.00000033)	4.66 (0.05)	2.69 (0.02)
512	4.10	500000	10000	228.543 (0.493)	19137.93 (33.65)	0.00408612 (0.00000044)	4.76 (0.07)	2.70 (0.03)
512	4.15	200000	10000	238.737 (0.802)	20119.40 (53.26)	0.00386233 (0.00000068)	4.76 (0.12)	2.62 (0.05)
512	4.20	500000	10000	247.620 (0.501)	21047.86 (32.20)	0.00365104 (0.00000041)	4.70 (0.07)	2.70 (0.03)
512	4.30	1000000	10000	262.509 (0.359)	22500.19 (21.64)	0.00326851 (0.00000027)	4.62 (0.05)	2.63 (0.02)
512	4.40	1000000	10000	274.947 (0.359)	23690.60 (20.38)	0.00292813 (0.00000025)	4.51 (0.05)	2.62 (0.02)
512	4.50	1000000	10000	284.440 (0.363)	24612.46 (19.59)	0.00262622 (0.00000024)	4.52 (0.05)	2.58 (0.02)
512	4.60	1000000	10000	292.529 (0.362)	25377.99 (18.57)	0.00235787 (0.00000022)	4.40 (0.05)	2.56 (0.02)
512	4.65	1000000	10000	296.361 (0.362)	25722.12 (18.29)	0.00223424 (0.00000022)	4.42 (0.05)	2.59 (0.02)
512	4.70	1000000	10000	298.694 (0.360)	25963.60 (17.91)	0.00211828 (0.00000021)	4.36 (0.05)	2.56 (0.02)
512	4.80	1000000	10000	303.862 (0.362)	26460.25 (17.54)	0.00190436 (0.00000020)	4.40 (0.05)	2.58 (0.02)
512	4.90	1000000	10000	308.228 (0.363)	26871.14 (17.09)	0.00171327 (0.00000019)	4.36 (0.05)	2.56 (0.02)
512	5.00	1000000	10000	311.295 (0.359)	27167.08 (16.42)	0.00154191 (0.00000018)	4.24 (0.04)	2.55 (0.02)
512	5.10	1000000	10000	313.277 (0.362)	27407.74 (16.52)	0.00138888 (0.00000017)	4.39 (0.05)	2.58 (0.02)
512	5.20	1000000	10000	316.141 (0.361)	27635.16 (16.17)	0.00125163 (0.00000016)	4.37 (0.05)	2.53 (0.02)
512	5.30	1000000	10000	317.469 (0.362)	27803.43 (16.16)	0.00112815 (0.00000015)	4.44 (0.05)	2.56 (0.02)
512	5.40	1000000	10000	318.518 (0.364)	27951.61 (16.08)	0.00101697 (0.00000014)	4.45 (0.05)	2.53 (0.02)
512	5.50	1000000	10000	320.114 (0.364)	28082.10 (15.88)	0.00091721 (0.00000014)	4.44 (0.05)	2.53 (0.02)
512	5.60	600000	10000	320.704 (0.470)	28166.84 (20.43)	0.00082793 (0.00000017)	4.42 (0.06)	2.49 (0.03)
512	5.70	1000000	10000	321.343 (0.363)	28247.64 (15.64)	0.00074740 (0.00000012)	4.39 (0.05)	2.51 (0.02)
1024	3.50	200000	10000	93.782 (1.169)	5025.28 (21.00)	0.00830634 (0.00000055)	1.79 (0.03)	2.92 (0.06)
1024	4.00	200000	10000	253.855 (1.161)	26336.19 (115.46)	0.00458170 (0.00000038)	3.53 (0.08)	2.76 (0.05)
1024	4.20	200000	10000	351.988 (1.424)	43182.70 (167.96)	0.00365419 (0.00000033)	4.66 (0.11)	2.64 (0.05)
1024	4.50	200000	10000	481.901 (1.582)	64990.58 (167.30)	0.00262718 (0.00000027)	4.72 (0.12)	2.58 (0.05)
1024	4.70	200000	10000	543.182 (1.645)	74421.27 (152.23)	0.00211861 (0.00000024)	4.66 (0.11)	2.57 (0.05)
1024	4.80	435000	10000	564.506 (1.102)	77670.79 (95.63)	0.00190502 (0.00000015)	4.45 (0.07)	2.56 (0.03)
1024	4.90	350000	10000	581.321 (1.233)	80085.31 (103.34)	0.00171359 (0.00000016)	4.49 (0.08)	2.57 (0.04)
1024	5.00	200000	10000	597.074 (1.646)	82401.80 (128.63)	0.00154236 (0.00000020)	4.25 (0.10)	2.47 (0.04)
1024	5.10	500000	10000	604.335 (1.023)	83709.00 (79.97)	0.00138923 (0.00000012)	4.39 (0.07)	2.52 (0.03)
1024	5.20	315000	10000	614.282 (1.298)	85148.87 (97.33)	0.00125153 (0.00000014)	4.33 (0.08)	2.55 (0.04)
1024	5.30	300000	10000	619.635 (1.346)	86150.77 (99.78)	0.00112806 (0.00000014)	4.46 (0.09)	2.44 (0.04)
1024	5.40	500000	10000	624.864 (1.029)	86978.99 (75.68)	0.00101735 (0.00000010)	4.45 (0.07)	2.55 (0.03)
1024	5.50	500000	10000	630.919 (1.022)	87719.01 (72.87)	0.00091759 (0.00000010)	4.32 (0.06)	2.51 (0.03)
1024	5.60	500000	10000	634.020 (1.030)	88261.17 (72.93)	0.00082786 (0.00000009)	4.40 (0.07)	2.53 (0.03)
1024	5.70	350000	10000	636.439 (1.243)	88750.82 (86.74)	0.00074709 (0.00000010)	4.39 (0.08)	2.53 (0.04)
1024	5.80	500000	10000	639.532 (1.034)	89200.43 (71.47)	0.00067443 (0.00000008)	4.39 (0.07)	2.53 (0.03)
1024	5.80	400000	10000	640.955 (1.148)	89486.27 (79.44)	0.00060909 (0.00000009)	4.36 (0.07)	2.54 (0.03)
1536	5.40	200000	10000	921.169 (2.484)	167548.48 (247.24)	0.00101730 (0.00000011)	4.47 (0.11)	2.47 (0.04)
1536	5.50	300000	10000	929.501 (2.010)	169381.15 (196.44)	0.00091779 (0.00000008)	4.45 (0.09)	2.56 (0.04)
1536	5.60	500000	10000	939.605 (1.537)	171375.42 (146.36)	0.00082793 (0.00000006)	4.33 (0.06)	2.51 (0.03)
1536	5.70	500000	10000	945.918 (1.553)	172479.44 (147.38)	0.00074711 (0.00000006)	4.48 (0.07)	2.51 (0.03)
1536	6.00	200000	10000	963.094 (2.481)	175739.34 (225.37)	0.00055010 (0.00000008)	4.39 (0.11)	2.46 (0.04)

Table 2. Our Monte Carlo Data for the 4-State Potts Antiferromagnet[a]

L	β	Total	Discard	ξ	χ_{stagg}	E	$\tau_{\text{int},\mathcal{M}^2_{\text{stagg}}}$	$\tau_{\text{int},\mathcal{E}}$
32	0.50	1000000	10000	0.408 (0.088)	1.64 (0.00)	0.33333424 (0.00004069)	2.47 (0.02)	2.86 (0.02)
32	1.00	1000000	10000	0.713 (0.051)	2.62 (0.00)	0.20768309 (0.00003587)	2.49 (0.02)	3.12 (0.03)
32	1.50	1000000	10000	0.963 (0.039)	3.86 (0.01)	0.12339135 (0.00002967)	2.54 (0.02)	3.39 (0.03)
32	2.00	1000000	10000	1.284 (0.029)	5.22 (0.01)	0.07216655 (0.00002316)	2.54 (0.02)	3.51 (0.03)
32	2.50	1000000	10000	1.494 (0.026)	6.45 (0.01)	0.04227138 (0.00001777)	2.56 (0.02)	3.55 (0.03)
32	2.60	200000	10000	1.597 (0.055)	6.72 (0.03)	0.03809065 (0.00003844)	2.52 (0.05)	3.57 (0.08)
32	2.70	200000	10000	1.513 (0.060)	6.85 (0.03)	0.03421029 (0.00003588)	2.72 (0.05)	3.49 (0.07)
32	2.80	200000	10000	1.597 (0.056)	7.06 (0.03)	0.03081867 (0.00003480)	2.53 (0.05)	3.63 (0.08)
32	2.90	200000	10000	1.707 (0.053)	7.32 (0.03)	0.02778558 (0.00003256)	2.53 (0.05)	3.51 (0.08)
32	3.00	1000000	10000	1.694 (0.023)	7.48 (0.01)	0.02498434 (0.00001345)	2.59 (0.02)	3.53 (0.03)
32	3.10	200000	10000	1.686 (0.053)	7.62 (0.03)	0.02251044 (0.00002917)	2.56 (0.05)	3.50 (0.07)
32	3.20	200000	10000	1.737 (0.052)	7.76 (0.03)	0.02031029 (0.00002774)	2.54 (0.05)	3.53 (0.08)
32	3.30	200000	10000	1.727 (0.052)	7.90 (0.03)	0.01828279 (0.00002590)	2.60 (0.05)	3.45 (0.07)
32	3.40	200000	10000	1.744 (0.051)	8.03 (0.03)	0.01646475 (0.00002463)	2.54 (0.05)	3.49 (0.07)
32	3.50	1000000	10000	1.832 (0.022)	8.20 (0.02)	0.01488912 (0.00001037)	2.63 (0.02)	3.55 (0.03)
32	3.60	200000	10000	1.791 (0.052)	8.27 (0.04)	0.01341060 (0.00002191)	2.71 (0.05)	3.43 (0.07)
32	3.70	200000	10000	1.855 (0.050)	8.44 (0.04)	0.01207502 (0.00002158)	2.61 (0.05)	3.64 (0.08)
32	3.80	200000	10000	1.870 (0.049)	8.52 (0.04)	0.01094776 (0.00002028)	2.59 (0.05)	3.56 (0.08)
32	3.90	200000	10000	1.864 (0.049)	8.58 (0.04)	0.00985439 (0.00001904)	2.63 (0.05)	3.53 (0.08)
32	4.00	1000000	10000	1.865 (0.022)	8.68 (0.02)	0.00891195 (0.00000792)	2.63 (0.02)	3.53 (0.03)
32	4.10	200000	10000	1.837 (0.050)	8.69 (0.04)	0.00805595 (0.00001717)	2.58 (0.05)	3.53 (0.08)
32	4.20	200000	10000	1.890 (0.049)	8.79 (0.04)	0.00726329 (0.00001631)	2.69 (0.05)	3.51 (0.08)
32	4.30	200000	10000	1.907 (0.048)	8.87 (0.04)	0.00656180 (0.00001557)	2.57 (0.05)	3.54 (0.08)
32	4.40	200000	10000	1.917 (0.048)	8.96 (0.04)	0.00591430 (0.00001478)	2.61 (0.05)	3.54 (0.08)
32	4.50	1000000	10000	1.907 (0.021)	8.99 (0.02)	0.00536798 (0.00000617)	2.62 (0.02)	3.54 (0.03)
32	4.60	200000	10000	1.906 (0.049)	9.05 (0.04)	0.00486859 (0.00001338)	2.72 (0.05)	3.54 (0.08)
32	4.70	200000	10000	1.911 (0.049)	9.06 (0.04)	0.00439399 (0.00001268)	2.62 (0.05)	3.52 (0.08)
32	4.80	200000	10000	1.905 (0.049)	9.11 (0.04)	0.00395714 (0.00001187)	2.61 (0.05)	3.45 (0.07)
32	4.90	200000	10000	1.996 (0.048)	9.20 (0.04)	0.00358136 (0.00001127)	2.78 (0.05)	3.43 (0.07)
32	5.00	1000000	10000	1.960 (0.021)	9.21 (0.02)	0.00323220 (0.00000472)	2.63 (0.02)	3.47 (0.03)
64	2.50	1000000	10000	1.559 (0.093)	6.47 (0.01)	0.04228318 (0.00000895)	2.52 (0.02)	3.60 (0.03)
64	3.00	1000000	10000	1.765 (0.083)	7.47 (0.01)	0.02497250 (0.00000678)	2.51 (0.02)	3.56 (0.03)
64	3.50	1000000	10000	1.729 (0.085)	8.17 (0.01)	0.01488177 (0.00000517)	2.51 (0.02)	3.53 (0.03)
64	4.00	1000000	10000	1.754 (0.084)	8.65 (0.02)	0.00890631 (0.00000397)	2.49 (0.02)	3.53 (0.03)
64	4.50	1000000	10000	1.890 (0.078)	9.00 (0.02)	0.00536320 (0.00000308)	2.52 (0.02)	3.56 (0.03)
64	5.00	1000000	10000	1.894 (0.078)	9.18 (0.02)	0.00323899 (0.00000236)	2.52 (0.02)	3.48 (0.03)

[a] "Total" is the total number of WSK iterations performed. "Discard" is the number of iterations discarded for equilibration. Error bars (one standard deviation) are shown in parentheses.

Table 3. χ^2 for the Fit (2.22) of $\xi(\beta, 2L)/\xi(\beta, L)$ versus $\xi(\beta, L)/L$[a]

$L_{\min}$	$n=3$	$n=4$	$n=5$	$n=6$	$n=7$	$n=8$	$n=9$
32	571.70, 94 6.08, 0.0%	178.98, 93 1.92, 0.0%	138.80, 92 1.51, 0.1%	138.62, 91 1.52, 0.1%	135.95, 90 1.51, 0.1%	134.00, 89 1.51, 0.1%	125.94, 88 1.43, 0.5%
64	263.84, 86 3.07, 0.0%	113.41, 85 1.33, 2.1%	100.21, 84 1.19, 11.0%	100.11, 83 1.21, 9.7%	98.52, 82 1.20, 10.3%	96.49, 81 1.19, 11.5%	92.60, 80 1.16, 15.9%
128	206.52, 68 3.04, 0.0%	87.32, 67 1.30, 4.8%	75.41, 66 1.14, 20.0%	75.21, 65 1.16, 18.1%	72.97, 64 1.14, 20.7%	72.58, 63 1.15, 19.1%	70.02, 62 1.13, 22.6%
256	119.94, 40 3.00, 0.0%	63.84, 39 1.64, 0.7%	58.22, 38 1.53, 1.9%	58.17, 37 1.57, 1.5%	57.01, 36 1.58, 1.4%	55.12, 35 1.57, 1.7%	52.71, 34 1.55, 2.1%

[a] The first line is χ^2 followed by DF (number of degrees of freedom). Second line is χ^2/DF followed by the confidence level. In all cases $\xi_{\min} = 10$.

the corresponding confidence level[17]—for the function $F_\xi \equiv \xi(\beta, 2L)/\xi(\beta, L)$ as a function of the interpolation order n and the cut point $L_{\min}$; here we have used $\xi_{\min} = 10$. (We tried also $\xi_{\min} = 20$ and the results are virtually unchanged.) A reasonable χ^2 is obtained when $n \geqslant 5$ and $L_{\min} \geqslant 64$; a slightly better χ^2/DF is obtained by taking $L_{\min} = 128$. Further increases in n and/or $L_{\min}$ do *not* improve the χ^2/DF.[18] Our preferred fit is therefore $n = 5$, $\xi_{\min} = 10$ and $L_{\min} = 128$: we get

$$F_\xi(x) = 1 + 0.896737e^{-1/x} + 29.243141e^{-2/x} - 253.811947e^{-3/x} + 2092.996892e^{-4/x} - 5334.794958e^{-5/x} \tag{4.1}$$

which is plotted in Fig. 1. This fit is reliable only in the interval where there are data points contributing to it, namely $x \leqslant x_{\max} \approx 0.629781$.

We remind the reader that our raw-data error bars on ξ are *overestimates*, as a result of our use of the triangle inequality; therefore, the χ^2 values reported in Table 3 are *underestimates*, and only their *relative*

[17] "Confidence level" is the probability that χ^2 would exceed the observed value, assuming that the underlying statistical model is correct. An unusually low confidence level (e.g., less than 5%) thus suggests that the underlying statistical model is *incorrect*. Here this may be due to an inadequate interpolation Ansatz (too low n) or to corrections to scaling (too low $\xi_{\min}$ or $L_{\min}$). Another possible cause of unusually low confidence levels will be discussed in Section 4.1.2.

[18] Indeed, for $L_{\min} = 256$ the χ^2/DF is *worse* than for $L_{\min} = 64, 128$; it is, in fact, as bad as for $L_{\min} = 32$! We do not understand the reason for this behavior, which may be simply a statistical fluctuation.

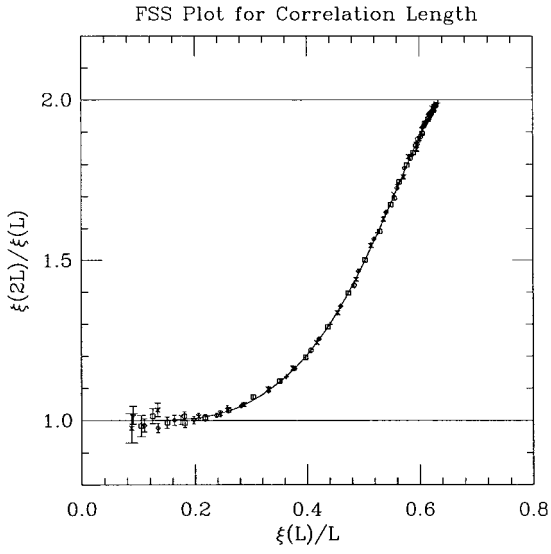

Fig. 1. $\xi(\beta, 2L)/\xi(\beta, L)$ versus $\xi(\beta, L)/L$. Symbols indicate $L = 32$ (+), 64 (×), 128 (□), 256 (◇), 512 (○). Error bars are one standard deviation. Curve is a fifth-order fit in (2.22), with $\xi_{\min} = 10$ and $L_{\min} = 128$.

magnitudes can be considered to be reliable. The absolute quality of the fit is, therefore, not as good as it looks. This will be further discussed below in connection with χ_{stagg} (Section 4.1.2).

We can make a crude estimate of the universal value x^* defined by $F_\xi(x^*) = 2$ [cf. (2.29)]. On the one hand, $F_\xi(x_{\max}) = 1.987350$, so $x^* > x_{\max} \approx 0.629781$. On the other hand, $F'_\xi(x_{\max}) = 3.080022$, so if we extrapolate linearly for $x \geqslant x_{\max}$, we get $x^* = 0.633888$. This is not far from the value $x^* = 0.633983$ obtained by taking (4.1) seriously even for $x > x_{\max}$. So it is a fair guess that $x^* \approx 0.633888$.[19]

In Fig. 2(a) we plot the *deviations* from our preferred fit together with their error bars. The points with $L = 32$ show weak (< 0.01) but apparently statistically significant deviations, of positive sign, in the interval $0.52 \lesssim x \lesssim 0.625$: see the blow-up of this region in Fig. 2(b).[20] It is a reasonable guess that these deviations arise from systematic corrections to scaling. However, a careful test of this hypothesis would require higher statistics and more densely spaced points; in addition, it would be useful to obtain data with

[19] After completion of this work, Salas and Sokal[34] obtained $x^* = 0.63457 \pm 0.00033$ by high-precision simulation of this model *at* $\beta = \infty$.

[20] The $L = 32$ point at $x \approx 0.633$ lies outside the range of x covered by the fit ($x_{\max} \approx 0.630$ when $L_{\min} = 128$), so the negative deviation exhibited by this point may not be meaningful.

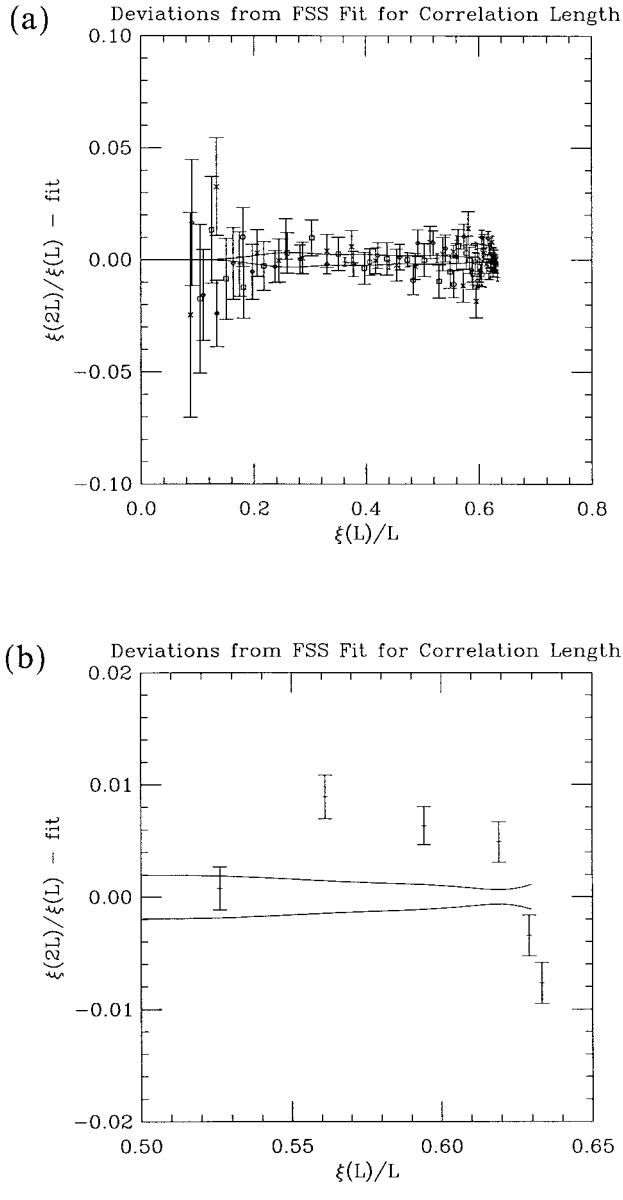

Fig. 2. Deviation of points from fit to F_ξ with $s = 2$, $n = 5$, $\xi_{\min} = 10$ and $L_{\min} = 128$. Symbols indicate $L = 32$ (+), 64 (×), 128 (□), 256 (◇), 512 (○). Error bars are one standard deviation. Curves near zero indicate statistical error bars (± one standard deviation) on the function $F_\xi(x)$. Plot (a) shows all points; plot (b) is a blow-up showing the $L = 32$ points at $x \geqslant 0.50$.

extremely high statistics ($\sim 10^8$ sweeps) on smaller lattices than we have bothered to use here ($L=16$ and even $L=8$), in order to observe a stronger correction-to-scaling "signal." The points with $L \geqslant 64$ do not seem to show any systematic deviations from the fit. Because we observe statistically significant corrections to scaling on only one lattice size, we are unable to make any firm statement about the L-dependence of the correction-to-scaling term (which we expect to be of the form $L^{-\Delta}$, where $\Delta > 0$ is a correction-to-scaling exponent). All we can say is that Δ is not *too* small, since otherwise the correction to scaling would be observable also on the $L=64$ lattice. But we are unable to say whether, for example, $\Delta \approx 1$ or $\Delta \approx 2$. Let us remark that Salas and Sokal[34] have recently predicted, on the basis of the height representation of the zero-temperature model,[30–34] that $\Delta = 2$ (at least when $\beta = \infty$).

We now compute the extrapolated values ξ_∞, using the function F_ξ given by our preferred fit as well as by several alternative fits that use more or less stringent choices of $L_{\min}$. (In all cases we take $n=5$; the results for $n=6$ or $n=7$ differ in almost all cases by <0.4 standard deviations.) The statistical error bars on ξ_∞ are computed by an auxiliary Monte Carlo process using "fake data sets," as described in Section 2.2, and include errors of types (i)+(ii)+(iii). In particular, the correlations between the extrapolated values ξ_∞ from different lattice sizes at the same β (though not those at different β values) are taken account of in this computation. For each β we compute the weighted average (2.23) of the various estimates ξ_∞, along with the statistical error bar (2.24) and the $\mathscr{R}$ value (2.25). These are reported in Table 4. The statistical errors on ξ_∞ are of order 1% (resp. 2%, 3%, 5%) at $\xi_\infty \approx 1000$ (resp. 2000, 5000, 10000). These extrapolated values from different lattice sizes at the same β are found to be consistent within statistical errors: only two of the 42 β values has an $\mathscr{R}$ value too large at the 5% level; and summing all β values we have $\sum \mathscr{R} = 43.45$ (75 DF, level $= 99.9\%$). This unusually low chi-squared is probably due, at least in part, to our overestimation of the raw-data error bars on ξ_L, which leads to an overestimation of the error bars on ξ_∞.

The discrepancies between the extrapolations with $L_{\min} = 64, 128, 256$ are in almost all cases less than half the quoted statistical error.[21] We are thus reasonably confident that we have obtained quantitative control over the systematic errors due to corrections to scaling, and that their effect can be at most to double the quoted statistical errors.

[21] On the other hand, the extrapolations with $L_{\min} = 32$ frequently deviate from our preferred $L_{\min} = 128$ extrapolation by as much as $\approx 1\sigma$. These deviations are probably a correction-to-scaling effect on the borderline of statistical significance.

Table 4. Estimated Infinite-Volume Correlation Lengths ξ_∞ and Staggered Susceptibilities $\chi_{\text{stagg},\infty}$ as a Function of β, from Extrapolations Using Various $L_{\min}$[a]

β	$L_{\min}$	ξ_∞	$\mathscr{R}$ for ξ_∞	$\chi_{\text{stagg},\infty}$	$\mathscr{R}$ for $\chi_{\text{stagg},\infty}$
2.50	32	13.30 (0.03)	0.45 (3 DF, 93.0%)	200.85 (0.31)	2.14 (3 DF, 54.4%)
2.50	64	13.31 (0.04)	0.27 (2 DF, 87.4%)	201.13 (0.39)	0.84 (2 DF, 65.9%)
2.50	*128*	*13.32 (0.13)*	*0.27 (1 DF, 60.2%)*	*201.51 (0.09)*	*0.09 (1 DF, 76.6%)*
2.50	**256**	**13.10 (0.42)**	**0.00 (0 DF, 100.0%)**	**201.34 (0.80)**	**0.00 (0 DF, 100.0%)**
2.60	32	15.99 (0.08)	0.32 (2 DF, 85.3%)	272.17 (0.69)	1.54 (2 DF, 46.3%)
2.60	64	16.00 (0.08)	0.31 (2 DF, 85.8%)	272.22 (0.70)	1.38 (2 DF, 50.3%)
2.60	*128*	*16.00 (0.12)*	*0.31 (1 DF, 57.7%)*	*272.54 (0.79)*	*0.66 (1 DF, 41.7%)*
2.60	**256**	**16.18 (0.36)**	**0.00 (0 DF, 100.0%)**	**273.13 (1.10)**	**0.00 (0 DF, 100.0%)**
2.70	32	19.29 (0.05)	0.43 (3 DF, 93.3%)	369.78 (0.69)	0.73 (3 DF, 86.6%)
2.70	64	19.29 (0.06)	0.27 (2 DF, 87.6%)	369.51 (0.75)	0.13 (2 DF, 93.7%)
2.70	*128*	*19.27 (0.12)*	*0.22 (1 DF, 63.8%)*	*369.28 (1.09)*	*0.05 (1 DF, 83.0%)*
2.70	**256**	**19.13 (0.33)**	**0.00 (0 DF, 100.0%)**	**369.05 (1.51)**	**0.00 (0 DF, 100.0%)**
2.80	32	23.27 (0.09)	0.91 (3 DF, 82.2%)	504.73 (0.92)	1.94 (3 DF, 58.5%)
2.80	64	23.28 (0.09)	1.00 (3 DF, 80.0%)	504.74 (0.91)	1.97 (3 DF, 57.8%)
2.80	*128*	*23.29 (0.12)*	*0.86 (2 DF, 65.2%)*	*504.80 (0.98)*	*1.99 (2 DF, 37.0%)*
2.80	**256**	**23.13 (0.27)**	**0.36 (1 DF, 55.1%)**	**504.68 (1.07)**	**1.95 (1 DF, 16.3%)**
2.90	32	28.11 (0.11)	1.29 (3 DF, 73.2%)	690.90 (1.31)	3.05 (3 DF, 38.4%)
2.90	64	28.13 (0.12)	1.34 (3 DF, 72.0%)	690.94 (1.33)	3.32 (3 DF, 34.4%)
2.90	*128*	*28.14 (0.14)*	*0.94 (2 DF, 62.6%)*	*691.27 (1.40)*	*1.24 (2 DF, 53.9%)*
2.90	**256**	**28.02 (0.24)**	**0.59 (1 DF, 44.2%)**	**691.04 (1.51)**	**0.99 (1 DF, 32.0%)**
2.95	32	30.84 (0.18)	0.00 (0 DF, 100.0%)	804.48 (4.06)	0.00 (0 DF, 100.0%)
2.95	64	30.87 (0.19)	0.00 (0 DF, 100.0%)	804.91 (4.20)	0.00 (0 DF, 100.0%)
2.95	*128*	*30.84 (0.20)*	*0.00 (0 DF, 100.0%)*	*804.34 (4.35)*	*0.00 (0 DF, 100.0%)*
3.00	32	34.19 (0.10)	2.86 (4 DF, 58.1%)	952.35 (1.70)	3.81 (4 DF, 43.2%)
3.00	64	34.23 (0.11)	2.89 (3 DF, 41.0%)	952.09 (1.80)	3.45 (3 DF, 32.8%)
3.00	*128*	*34.16 (0.16)*	*2.72 (2 DF, 25.7%)*	*951.17 (1.93)*	*2.53 (2 DF, 28.3%)*
3.00	**256**	**34.11 (0.23)**	**2.51 (1 DF, 11.3%)**	**950.81 (2.12)**	**2.08 (1 DF, 14.9%)**
3.10	32	41.56 (0.17)	1.39 (3 DF, 70.8%)	1319.45 (3.44)	3.11 (3 DF, 37.5%)
3.10	64	41.59 (0.17)	1.23 (3 DF, 74.6%)	1319.40 (3.43)	3.36 (3 DF, 34.0%)
3.10	*128*	*41.57 (0.18)*	*1.46 (2 DF, 48.1%)*	*1318.96 (3.57)*	*4.82 (2 DF, 9.0%)*
3.10	**256**	**41.77 (0.25)**	**0.01 (1 DF, 92.5%)**	**1322.89 (4.06)**	**0.48 (1 DF, 49.0%)**
3.20	32	50.63 (0.16)	5.25 (4 DF, 26.2%)	1831.78 (4.49)	5.95 (4 DF, 20.3%)
3.20	64	50.81 (0.17)	0.60 (3 DF, 89.7%)	1834.33 (4.75)	1.35 (3 DF, 71.7%)
3.20	*128*	*50.70 (0.22)*	*0.23 (2 DF, 89.2%)*	*1831.27 (5.25)*	*0.16 (2 DF, 92.2%)*
3.20	**256**	**50.72 (0.27)**	**0.17 (1 DF, 68.3%)**	**1831.56 (6.16)**	**0.07 (1 DF, 79.5%)**

[a] Error bars are one standard deviation (statistical errors only). All extrapolations use $n = 5$ for ξ and $n = 6$ for χ_{stagg}. $\mathscr{R}$ indicates the residual sum-of-squares (2.25) for combining estimates from different L at the same β; the number of degrees of freedom (DF) and the confidence level are indicated. Our preferred fit is shown in *italics*; a more conservative good fit is shown in sans-serif; bad fits are shown in roman.

Table 4. (*Continued*)

β	$L_{\min}$	ξ_∞	$\mathscr{R}$ for ξ_∞	$\chi_{\text{stagg},\infty}$	$\mathscr{R}$ for $\chi_{\text{stagg},\infty}$
3.30	32	61.96 (0.22)	0.64 (3 DF, 88.8%)	2556.28 (5.94)	0.91 (3 DF, 82.3%)
3.30	64	62.01 (0.22)	0.95 (3 DF, 81.4%)	2556.71 (5.95)	1.15 (3 DF, 76.5%)
3.30	*128*	*61.98 (0.23)*	*0.60 (2 DF, 74.1%)*	*2556.23 (6.16)*	*0.69 (2 DF, 70.7%)*
3.30	**256**	**61.89 (0.27)**	**0.10 (1 DF, 75.8%)**	**2554.73 (6.52)**	**0.06 (1 DF, 79.9%)**
3.40	32	75.63 (0.26)	0.05 (3 DF, 99.7%)	3574.64 (8.59)	0.29 (3 DF, 96.2%)
3.40	64	75.68 (0.26)	0.04 (3 DF, 99.8%)	3575.04 (8.50)	0.24 (3 DF, 97.0%)
3.40	*128*	*75.64 (0.27)*	*0.01 (2 DF, 99.6%)*	*3573.43 (8.99)*	*0.02 (2 DF, 99.1%)*
3.40	**256**	**75.60 (0.30)**	**0.11 (1 DF, 73.5%)**	**3571.90 (9.54)**	**0.04 (1 DF, 84.6%)**
3.45	32	83.56 (0.76)	0.00 (0 DF, 100.0%)	4220.00 (47.16)	0.00 (0 DF, 100.0%)
3.45	64	83.75 (0.76)	0.00 (0 DF, 100.0%)	4223.68 (47.21)	0.00 (0 DF, 100.0%)
3.45	*128*	*83.64 (0.78)*	*0.00 (0 DF, 100.0%)*	*4215.80 (47.28)*	*0.00 (0 DF, 100.0%)*
3.50	32	92.94 (0.25)	4.88 (5 DF, 43.1%)	5035.19 (9.43)	6.50 (5 DF, 26.0%)
3.50	64	93.05 (0.26)	1.45 (4 DF, 83.5%)	5034.94 (9.86)	1.85 (4 DF, 76.3%)
3.50	*128*	*93.02 (0.29)*	*0.68 (3 DF, 87.9%)*	*5030.37 (10.68)*	*0.37 (3 DF, 94.7%)*
3.50	**256**	**92.90 (0.34)**	**0.63 (2 DF, 72.8%)**	**5025.27 (12.41)**	**0.01 (2 DF, 99.3%)**
3.60	32	113.85 (0.41)	1.82 (3 DF, 61.0%)	7054.43 (22.62)	2.11 (3 DF, 54.9%)
3.60	64	113.96 (0.42)	1.27 (3 DF, 73.7%)	7058.81 (23.51)	1.34 (3 DF, 72.0%)
3.60	*128*	*113.81 (0.46)*	*0.08 (2 DF, 96.0%)*	*7053.38 (25.92)*	*0.02 (2 DF, 98.9%)*
3.60	**256**	**113.70 (0.52)**	**0.01 (1 DF, 91.5%)**	**7048.81 (30.78)**	**0.00 (1 DF, 97.9%)**
3.65	32	125.80 (0.55)	0.00 (0 DF, 100.0%)	8350.93 (30.21)	0.00 (0 DF, 100.0%)
3.65	64	125.92 (0.57)	0.00 (0 DF, 100.0%)	8354.88 (31.24)	0.00 (0 DF, 100.0%)
3.65	*128*	*125.78 (0.63)*	*0.00 (0 DF, 100.0%)*	*8338.35 (34.51)*	*0.00 (0 DF, 100.0%)*
3.65	**256**	**125.66 (0.70)**	**0.00 (0 DF, 100.0%)**	**8341.72 (40.35)**	**0.00 (0 DF, 100.0%)**
3.70	32	139.75 (0.58)	1.07 (3 DF, 78.4%)	9952.36 (34.98)	1.32 (3 DF, 72.5%)
3.70	64	139.91 (0.59)	1.44 (3 DF, 69.7%)	9952.21 (35.13)	1.69 (3 DF, 63.8%)
3.70	*128*	*139.76 (0.67)*	*0.64 (2 DF, 72.5%)*	*9940.95 (38.57)*	*0.82 (2 DF, 66.5%)*
3.70	**256**	**139.51 (0.77)**	**0.05 (1 DF, 82.7%)**	**9927.15 (45.42)**	**0.12 (1 DF, 72.4%)**
3.80	32	171.68 (0.70)	4.96 (3 DF, 17.5%)	14021.81 (49.40)	5.11 (3 DF, 16.4%)
3.80	64	171.85 (0.73)	3.22 (3 DF, 35.9%)	14009.84 (51.53)	3.37 (3 DF, 33.8%)
3.80	*128*	*171.59 (0.79)*	*0.18 (2 DF, 91.5%)*	*13982.10 (54.81)*	*0.27 (2 DF, 67.4%)*
3.80	**256**	**171.23 (0.90)**	**0.00 (1 DF, 97.6%)**	**13953.90 (61.64)**	**0.03 (1 DF, 86.8%)**
3.90	32	211.00 (0.88)	0.98 (3 DF, 80.6%)	19803.32 (77.69)	1.08 (3 DF, 78.3%)
3.90	64	211.19 (0.91)	1.09 (3 DF, 78.0%)	19790.24 (81.81)	1.26 (3 DF, 73.8%)
3.90	*128*	*210.98 (0.99)*	*1.30 (2 DF, 52.3%)*	*19765.50 (87.33)*	*1.48 (2 DF, 47.8%)*
3.90	**256**	**210.74 (1.13)**	**0.34 (1 DF, 55.9%)**	**19737.60 (99.20)**	**0.34 (1 DF, 56.1%)**
3.95	32	237.95 (6.17)	0.00 (0 DF, 100.0%)	24159.76 (969.01)	0.00 (0 DF, 100.0%)
3.95	64	236.37 (5.97)	0.00 (0 DF, 100.0%)	23848.23 (931.88)	0.00 (0 DF, 100.0%)
3.95	*128*	*235.80 (6.14)*	*0.00 (0 DF, 100.0%)*	*23773.60 (954.62)*	*0.00 (0 DF, 100.0%)*
4.00	32	259.76 (0.92)	4.79 (5 DF, 44.2%)	27975.61 (95.23)	5.05 (5 DF, 41.0%)
4.00	64	260.24 (0.96)	1.09 (4 DF, 89.7%)	27993.91 (103.35)	1.27 (4 DF, 86.6%)
4.00	*128*	*259.98 (1.07)*	*0.92 (3 DF, 82.1%)*	*27970.00 (116.37)*	*1.12 (3 DF, 77.2%)*
4.00	**256**	**259.73 (1.30)**	**0.40 (2 DF, 81.7%)**	**27941.80 (143.30)**	**0.58 (2 DF, 74.8%)**

Table 4. (*Continued*)

β	$L_{\min}$	ξ_∞	$\mathscr{R}$ for ξ_∞	$\chi_{\text{stagg},\infty}$	$\mathscr{R}$ for $\chi_{\text{stagg},\infty}$
4.10	32	317.61 (1.78)	0.61 (2 DF, 73.6%)	39274.02 (257.27)	0.61 (2 DF, 73.7%)
4.10	64	318.18 (1.82)	0.28 (2 DF, 87.0%)	39291.96 (262.01)	0.30 (2 DF, 86.0%)
4.10	*128*	*317.70* (*1.97*)	*0.30* (*2* DF, *86.0%*)	*39219.30* (*273.74*)	*0.34* (*2* DF, *84.4%*)
4.10	**256**	**317.47** (**2.39**)	**0.16** (**1** DF, **69.3%**)	**39222.30** (**325.32**)	**0.18** (**1** DF, **67.5%**)
4.15	32	355.81 (3.47)	0.00 (0 DF, 100.0%)	47353.74 (572.90)	0.00 (0 DF, 100.0%)
4.15	64	356.61 (3.49)	0.00 (0 DF, 100.0%)	47389.86 (581.04)	0.00 (0 DF, 100.0%)
4.15	*128*	*356.11* (*3.58*)	*0.00* (*0* DF, *100.0%*)	*47294.50* (*588.26*)	*0.00* (*0* DF, *100.0%*)
4.15	**256**	**355.96** (**3.93**)	**0.00** (**0** DF, **100.0%**)	**47319.30** (**627.61**)	**0.00** (**0** DF, **100.0%**)
4.20	32	394.98 (1.92)	1.43 (3 DF, 69.8%)	56299.87 (272.76)	2.48 (3 DF, 47.9%)
4.20	64	395.38 (1.96)	1.44 (3 DF, 69.7%)	56273.48 (284.20)	2.48 (3 DF, 47.9%)
4.20	*128*	*394.85* (*2.12*)	*1.23* (*3* DF, *74.5%*)	*56161.10* (*300.19*)	*2.26* (*3* DF, *52.1%*)
4.20	**256**	**394.00** (**2.47**)	**1.71** (**2** DF, **42.6%**)	**56045.30** (**332.62**)	**3.02** (**2** DF, **22.1%**)
4.30	32	489.45 (3.01)	1.82 (2 DF, 40.2%)	80567.72 (664.23)	1.82 (2 DF, 40.3%)
4.30	64	489.42 (3.14)	0.99 (2 DF, 61.1%)	80425.79 (687.24)	1.03 (2 DF, 59.7%)
4.30	*128*	*488.45* (*3.56*)	*1.00* (*2* DF, *60.8%*)	*80248.30* (*747.13*)	*1.05* (*2* DF, *59.0%*)
4.30	**256**	**488.41** (**4.61**)	**0.94** (**1** DF, **33.2%**)	**80379.20** (**962.86**)	**1.00** (**1** DF, **31.7%**)
4.40	32	608.66 (4.77)	0.50 (2 DF, 77.9%)	116045.88 (1258.07)	0.50 (2 DF, 77.9%)
4.40	64	607.55 (4.90)	0.68 (2 DF, 71.2%)	115438.34 (1297.88)	0.69 (2 DF, 70.8%)
4.40	*128*	*606.22* (*5.45*)	*0.75* (*2* DF, *68.7%*)	*115121.00* (*1390.11*)	*0.76* (*2* DF, *68.4%*)
4.40	**256**	**607.38** (**7.01**)	**0.13** (**1** DF, **71.4%**)	**115580.00** (**1724.71**)	**0.13** (**1** DF, **71.5%**)
4.50	32	743.91 (4.99)	17.63 (5 DF, 0.3%)	161644.96 (1441.16)	18.91 (5 DF, 0.2%)
4.50	64	741.86 (5.25)	11.36 (4 DF, 2.3%)	160749.98 (1524.23)	12.20 (4 DF, 1.6%)
4.50	*128*	*740.18* (*5.90*)	*8.57* (*3* DF, *3.6%*)	*160184.00* (*1641.99*)	*9.19* (*3* DF, *2.7%*)
4.50	**256**	**737.83** (**7.34**)	**6.81** (**2** DF, **3.3%**)	**159681.00** (**1957.27**)	**7.34** (**2** DF, **2.5%**)
4.60	32	940.15 (9.85)	2.23 (2 DF, 32.8%)	239226.36 (3809.46)	2.27 (2 DF, 32.2%)
4.60	64	932.11 (10.39)	1.00 (2 DF, 60.6%)	235469.71 (3977.98)	1.02 (2 DF, 60.2%)
4.60	*128*	*929.18* (*11.49*)	*1.01* (*2* DF, *60.4%*)	*234461.00* (*4288.18*)	*1.02* (*2* DF, *60.1%*)
4.60	**256**	**929.73** (**14.09**)	**0.93** (**1** DF, **33.6%**)	**235038.00** (**5147.64**)	**0.95** (**1** DF, **33.1%**)
4.65	32	1049.65 (12.82)	2.08 (1 DF, 14.9%)	287837.94 (5463.27)	2.16 (1 DF, 14.1%)
4.65	64	1036.57 (13.29)	3.93 (1 DF, 4.8%)	281335.40 (5552.70)	4.10 (1 DF, 4.3%)
4.65	*128*	*1033.49* (*14.50*)	*4.08* (*1* DF, *4.3%*)	*280163.00* (*5953.38*)	*4.24* (*1* DF, *3.9%*)
4.65	**256**	**1034.53** (**17.16**)	**4.14** (**1** DF, **4.2%**)	**281019.00** (**6811.95**)	**4.32** (**1** DF, **3.8%**)
4.70	32	1149.03 (11.81)	0.39 (3 DF, 94.3%)	334974.41 (5138.61)	0.40 (3 DF, 94.0%)
4.70	64	1140.40 (12.25)	0.16 (3 DF, 98.4%)	330406.55 (5250.77)	0.17 (3 DF, 98.3%)
4.70	*128*	*1137.34* (*13.39*)	*0.20* (*3* DF, *97.7%*)	*329280.00* (*5587.85*)	*0.21* (*3* DF, *97.6%*)
4.70	**256**	**1138.49** (**16.23**)	**0.20** (**2** DF, **90.5%**)	**330203.00** (**6544.22**)	**0.21** (**2** DF, **90.1%**)
4.80	32	1435.78 (15.18)	3.99 (3 DF, 26.3%)	485576.51 (7655.78)	3.86 (3 DF, 27.7%)
4.80	64	1423.46 (16.09)	2.25 (3 DF, 52.2%)	478214.99 (8078.91)	2.09 (3 DF, 55.3%)
4.80	*128*	*1419.96* (*17.36*)	*2.00* (*3* DF, *57.3%*)	*476453.00* (*8528.54*)	*1.87* (*3* DF, *60.0%*)
4.80	**256**	**1418.50** (**20.45**)	**0.45** (**2** DF, **79.9%**)	**476657.00** (**9743.68**)	**0.45** (**2** DF, **80.0%**)
4.90	32	1779.47 (24.92)	3.54 (3 DF, 31.6%)	693347.95 (15088.08)	3.66 (3 DF, 30.1%)
4.90	64	1759.03 (25.37)	3.76 (3 DF, 28.9%)	679244.94 (15148.94)	3.90 (3 DF, 27.2%)
4.90	*128*	*1755.04* (*26.90*)	*3.83* (*3* DF, *28.1%*)	*677221.00* (*15901.70*)	*3.97* (*3* DF, *26.4%*)
4.90	**256**	**1753.30** (**30.59**)	**3.72** (**2** DF, **15.5%**)	**677150.00** (**17675.40**)	**3.86** (**2** DF, **14.5%**)

Table 4. (*Continued*)

β	$L_{\min}$	ξ_∞	$\mathscr{R}$ for ξ_∞	$\chi_{\text{stagg},\infty}$	$\mathscr{R}$ for $\chi_{\text{stagg},\infty}$
5.00	32	2218.69 (44.16)	10.43 (5 DF, 6.4%)	1001133.00 (32465.03)	10.42 (5 DF, 6.4%)
5.00	64	2198.02 (44.85)	4.62 (4 DF, 32.8%)	986315.31 (32381.73)	4.75 (4 DF, 31.4%)
5.00	*128*	*2189.50 (47.16)*	*5.32 (3 DF, 15.0%)*	*980853.00 (33603.90)*	*5.53 (3 DF, 13.7%)*
5.00	**256**	**2202.41 (53.21)**	**2.84 (2 DF, 24.2%)**	**991980.00 (37473.90)**	**2.95 (2 DF, 22.9%)**
5.10	32	2670.51 (51.77)	0.02 (3 DF, 99.9%)	1371476.00 (42469.89)	0.02 (3 DF, 99.9%)
5.10	64	2627.87 (51.80)	0.23 (3 DF, 97.3%)	1332282.00 (42007.23)	0.21 (3 DF, 97.6%)
5.10	*128*	*2618.49 (54.00)*	*0.14 (3 DF, 98.7%)*	*1325547.00 (43166.40)*	*0.14 (3 DF, 98.7%)*
5.10	**256**	**2619.75 (60.40)**	**0.10 (2 DF, 94.9%)**	**1328528.00 (47282.20)**	**0.10 (2 DF, 94.9%)**
5.20	32	3488.77 (96.81)	0.79 (3 DF, 85.2%)	2133709.00 (96738.46)	0.77 (3 DF, 85.6%)
5.20	64	3431.88 (100.37)	0.64 (3 DF, 88.8%)	2070752.00 (98793.74)	0.59 (3 DF, 89.9%)
5.20	*128*	*3416.96 (99.80)*	*0.54 (3 DF, 91.0%)*	*2058294.00 (97987.50)*	*0.52 (3 DF, 91.4%)*
5.20	**256**	**3419.80 (109.80)**	**0.50 (2 DF, 78.0%)**	**2064205.00 (106605.00)**	**0.49 (2 DF, 78.2%)**
5.30	32	4134.51 (138.26)	0.72 (2 DF, 69.9%)	2835978.00 (156936.69)	0.69 (2 DF, 70.7%)
5.30	64	4061.19 (142.43)	0.50 (2 DF, 77.9%)	2747493.00 (159307.94)	0.48 (2 DF, 78.6%)
5.30	*128*	*4038.28 (142.59)*	*0.47 (2 DF, 79.0%)*	*2725035.00 (158160.00)*	*0.45 (2 DF, 79.7%)*
5.30	**256**	**4057.82 (156.95)**	**0.54 (2 DF, 76.4%)**	**2749120.00 (173702.00)**	**0.52 (2 DF, 77.1%)**
5.40	32	5039.09 (148.02)	0.28 (3 DF, 96.4%)	3955726.00 (190762.23)	0.27 (3 DF, 96.6%)
5.40	64	4953.59 (148.53)	0.71 (3 DF, 87.1%)	3831850.00 (188716.09)	0.66 (3 DF, 88.2%)
5.40	*128*	*4928.06 (152.69)*	*0.60 (3 DF, 89.7%)*	*3804126.00 (192397.00)*	*0.57 (3 DF, 90.4%)*
5.40	**256**	**4941.46 (163.20)**	**1.01 (3 DF, 79.8%)**	**3823421.00 (204251.00)**	**0.92 (3 DF, 82.1%)**
5.50	32	6377.29 (217.63)	1.99 (2 DF, 37.0%)	5821262.00 (327977.26)	1.99 (2 DF, 36.9%)
5.50	64	6223.22 (221.23)	2.19 (2 DF, 33.4%)	5574691.00 (326750.54)	2.15 (2 DF, 34.2%)
5.50	*128*	*6203.03 (224.08)*	*1.96 (2 DF, 37.6%)*	*5553237.00 (330812.00)*	*1.92 (2 DF, 38.3%)*
5.50	**256**	**6197.48 (238.44)**	**2.28 (2 DF, 31.9%)**	**5546998.00 (347228.00)**	**2.20 (2 DF, 33.3%)**
5.60	32	7970.66 (301.47)	0.04 (2 DF, 97.8%)	8498373.00 (534485.16)	0.04 (2 DF, 98.0%)
5.60	64	7801.45 (309.62)	0.02 (2 DF, 99.0%)	8180645.00 (538772.90)	0.01 (2 DF, 99.3%)
5.60	*128*	*7760.02 (311.34)*	*0.01 (2 DF, 99.6%)*	*8116724.00 (540193.00)*	*0.01 (2 DF, 99.7%)*
5.60	**256**	**7790.68 (326.89)**	**0.05 (2 DF, 97.4%)**	**8178031.00 (561400.00)**	**0.04 (2 DF, 97.8%)**
5.70	32	9664.89 (456.80)	0.23 (2 DF, 89.2%)	11718104.00 (928104.64)	0.22 (2 DF, 89.9%)
5.70	64	9531.97 (469.77)	0.02 (2 DF, 98.9%)	11427243.00 (940367.35)	0.02 (2 DF, 99.0%)
5.70	*128*	*9460.68 (459.20)*	*0.04 (2 DF, 97.9%)*	*11295711.00 (915422.00)*	*0.04 (2 DF, 98.1%)*
5.70	**256**	**9548.22 (514.52)**	**0.04 (2 DF, 97.8%)**	**11476466.00 (1029147.00)**	**0.04 (2 DF, 98.0%)**
5.80	32	12659.85 (1409.69)	0.00 (0 DF, 100.0%)	18383870.00 (3478048.00)	0.00 (0 DF, 100.0%)
5.80	64	12557.84 (1515.32)	0.00 (0 DF, 100.0%)	18099541.00 (3740026.00)	0.00 (0 DF, 100.0%)
5.80	*128*	*12416.40 (1475.70)*	*0.00 (0 DF, 100.0%)*	*17772288.00 (3613560.00)*	*0.00 (0 DF, 100.0%)*
5.80	**256**	**12649.50 (1593.68)**	**0.00 (0 DF, 100.0%)**	**18354042.00 (3979249.00)**	**0.00 (0 DF, 100.0%)**
5.90	32	14796.02 (2144.26)	0.00 (0 DF, 100.0%)	23832311.00 (6025802.00)	0.00 (0 DF, 100.0%)
5.90	64	14844.78 (2373.04)	0.00 (0 DF, 100.0%)	23910024.00 (6775206.00)	0.00 (0 DF, 100.0%)
5.90	*128*	*14634.30 (2366.26)*	*0.00 (0 DF, 100.0%)*	*23371893.00 (6702087.00)*	*0.00 (0 DF, 100.0%)*
5.90	**256**	**15023.40 (2645.59)**	**0.00 (0 DF, 100.0%)**	**24447729.00 (7839348.00)**	**0.00 (0 DF, 100.0%)**
6.00	32	25502.30 (7489.41)	0.00 (0 DF, 100.0%)	58916945.00 (37012150.00)	0.00 (0 DF, 100.0%)
6.00	64	25937.75 (8904.71)	0.00 (0 DF, 100.0%)	60454213.00 (45821760.00)	0.00 (0 DF, 100.0%)
6.00	*128*	*25480.80 (8389.04)*	*0.00 (0 DF, 100.0%)*	*58758630.00 (41692067.00)*	*0.00 (0 DF, 100.0%)*
6.00	**256**	**26391.60 (∞)**	**0.00 (0 DF, 100.0%)**	**62389831.00 (∞)**	**0.00 (0 DF, 100.0%)**

Table 5. χ^2 for the Fit (2.22) of $\chi_{\text{stagg}}(\beta, 2L)/\chi_{\text{stagg}}(\beta, L)$ versus $\xi(\beta, L)/L$[a]

$L_{\min}$	$n=3$	$n=4$	$n=5$	$n=6$	$n=7$	$n=8$	$n=9$
32	1738.06, 94 18.49, 0.0%	288.25, 93 3.10, 0.0%	277.13, 92 3.01, 0.0%	244.18, 91 2.68, 0.0%	243.54, 90 2.71, 0.0%	236.75, 89 2.66, 0.0%	228.29, 88 2.59, 0.0%
64	932.48, 86 10.84, 0.0%	196.30, 85 2.31, 0.0%	193.24, 84 2.30, 0.0%	178.47, 83 2.15, 0.0%	177.49, 82 2.16, 0.0%	171.16, 81 2.11, 0.0%	164.95, 80 2.06, 0.0%
128	692.28, 68 10.18, 0.0%	142.15, 67 2.12, 0.0%	138.73, 66 2.10, 0.0%	131.45, 65 2.02, 0.0%	128.69, 64 2.01, 0.0%	127.09, 63 2.02, 0.0%	123.49, 62 1.99, 0.0%
256	387.08, 40 9.68, 0.0%	106.87, 39 2.74, 0.0%	106.47, 38 2.80, 0.0%	101.90, 37 2.75, 0.0%	100.23, 36 2.78, 0.0%	95.69, 35 2.73, 0.0%	90.82, 34 2.67, 0.0%

[a] The first line is χ^2 followed by DF (number of degrees of freedom). Second line is χ^2/DF followed by the confidence level. In all cases $\xi_{\min} = 10$.

4.1.2. Staggered Susceptibility. Next we carry out an analogous analysis for the staggered susceptibility χ_{stagg}. Note that for this observable our raw-data error bars are reliable, so the absolute χ^2 values can be taken seriously.

In Table 5 we report the quality of the fit for the function $F_{\chi_{\text{stagg}}} \equiv \chi_{\text{stagg}}(\beta, 2L)/\chi_{\text{stagg}}(\beta, L)$ as a functions of the interpolation order n and the cut point $L_{\min}$; here we have used $\xi_{\min} = 10$. (We tried also $\xi_{\min} = 20$ and the results are virtually unchanged.) The χ^2/DF is smallest when $n \geqslant 6$ and $L_{\min} \geqslant 128$.[22] However, this χ^2/DF is ≈ 2, rather than the ≈ 1 that it ought to be; and as a result, the confidence levels are extremely low (of order 10^{-6}). We do not understand this behavior, but we can make a few observations:

(a) Clearly, the explanation cannot be either an inadequate fitting function or corrections to scaling, because increasing n and/or $L_{\min}$ and/or $\xi_{\min}$ does *not* improve the fit.

(b) One possible explanation might be that our raw-data error bars are underestimated; but we tried various alternative statistical methods, such as breaking up long runs into sub-runs, and all gave compatible error bars. So we do not think that this is the problem.

(c) It is worth noting that nearly all the points with poor χ^2 come from the region of large x, particularly $x \gtrsim 0.59$. Indeed, if we look

[22] The χ^2/DF gets *worse* for $L_{\min} = 256$, just as it does for the correlation length (see footnote 18 above).

separately at the contributions to χ^2 (using the fit with $n=6$, $\xi_{\min}=10$, $L_{\min}=128$) coming from the intervals $x \leqslant 0.53$, $0.53 < x < 0.59$ and $x \geqslant 0.59$, we find that the first interval contains 29 points which together contribute 24.31 to the χ^2 ($\chi^2/\mathrm{DF}=0.84$, level $=71.4\%$), the second interval contains 10 points which together contribute 16.65 to the χ^2 ($\chi^2/\mathrm{DF}=1.67$, level $=8.2\%$), while the third interval contains 32 points which together contribute 90.49 to the χ^2 ($\chi^2/\mathrm{DF}=2.83$, level $=1.7\times10^{-7}$).

(d) This behavior can also be seen in Fig. 3, where we show the deviations from the fit $n=6$, $\xi_{\min}=10$, $L_{\min}=128$ together with their error bars. The points with $L=32$ show weak (<0.02) but statistically significant deviations, of positive sign, in the interval $0.53 \lesssim x \lesssim 0.625$: see the blow-up of this region in Fig. 3(b).[23] However, for $L \geqslant 64$ the corrections to scaling have become completely invisible. On the other hand, for $x > 0.58$ [see the enlarged view in Fig. 3(c)] we see that several points deviate from the fitting curve by 2–4 standard deviations; but there does not seem to be any systematic trend to these deviations, nor do the absolute deviations seem to be larger for smaller L. So, once again, it is unlikely that these deviations are caused by corrections to scaling, or indeed by any process that causes a *systematic* bias.

(e) One *possible* cause of the unusually high χ^2 is the following: We treated the points in the fit—which of course correspond to *pairs* $(\beta, L)/(\beta, 2L)$—as statistically independent; but this is not quite right, as the same raw-data point $(\beta, 2L)$ can contribute to *two* pairs, namely $(\beta, L)/(\beta, 2L)$ and $(\beta, 2L)/(\beta, 4L)$, being in the numerator of the first and in the denominator of the second. As a result, these pairs of pairs are significantly *anti*correlated—one would expect a correlation coefficient of $\approx -1/2$, if all three raw-data points have roughly the same relative error—and they will thus tend to deviate from each other by *more* than would have been predicted from independent fluctuations with the given error bars. Furthermore, when $\xi(\beta, L)/L$ is close to x^*, $\xi(\beta, 2L)/2L$ is in turn not much smaller than $\xi(\beta, L)/L$, so this anticorrelation acts on pairs of points having relatively *nearby* values of x. This could explain why the large contributions to χ^2 come almost exclusively from the region $x \gtrsim 0.59$, and why they are apparently completely random. Unfortunately, it seemed unfeasible for us to invert the large matrices (of order ≈ 70) that would be needed to take proper account of these correlations. Suffice it to say that *if* this is the correct explanation, then the observed large χ^2 is simply spurious, and the fit is in reality good after all! Moreover, in this case the

[23] The $L=32$ point at $x \approx 0.633$ lies outside the range of x covered by the fit ($x_{\max} \approx 0.630$ when $L_{\min}=128$), so the negative deviation exhibited by this point may not be meaningful.

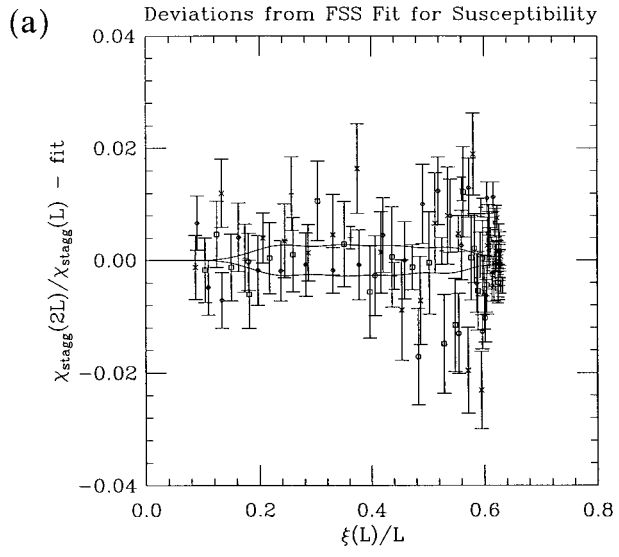

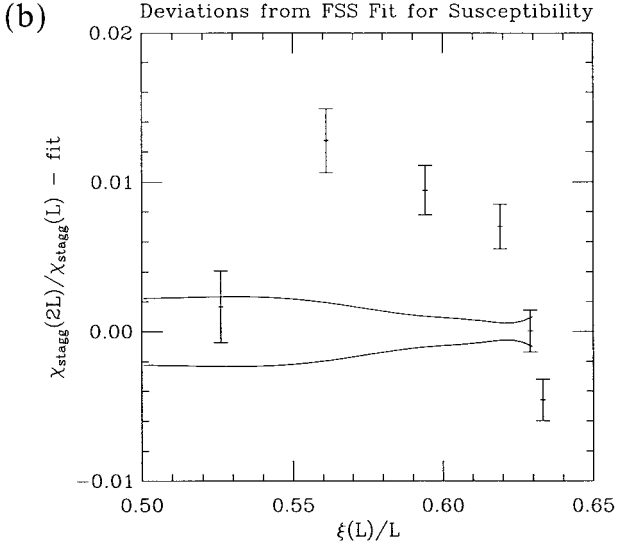

Fig. 3. Deviation of points from fit to $F_{\chi_{\text{stagg}}}$ with $s = 2$, $n = 6$, $\xi_{\min} = 10$ and $L_{\min} = 128$. Symbols indicate $L = 32$ (+), 64 (×), 128 (□), 256 (◇), 512 (○). Error bars are one standard deviation. Curves near zero indicate statistical error bars (± one standard deviation) on the function $F_{\chi_{\text{stagg}}}(x)$. Plot (a) shows all points; plot (b) is a blow-up showing the $L = 32$ points at $x \geqslant 0.50$; plot (c) is a blow-up showing all points with $x \geqslant 0.58$.

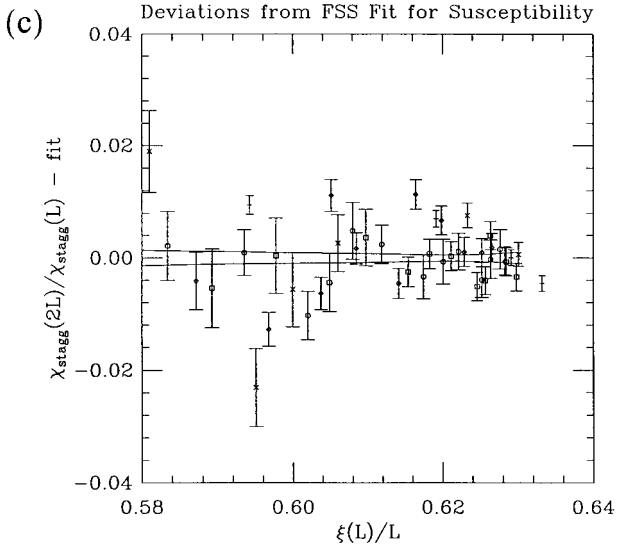

Fig. 3. (*Continued*)

error bars on the extrapolated values ξ_∞ and $\chi_{\text{stagg},\infty}$ will be correct, as the method of "fake data sets" *does* take proper account of the aforementioned correlations.

Modulo these caveats, therefore, we take as our preferred fit the one with $n=6$, $\xi_{\min}=10$ and $L_{\min}=128$: we get

$$F_{\chi_{\text{stagg}}}(x) = 1 + 2.234450e^{-1/x} + 80.120833e^{-2/x} - 966.050470e^{-3/x} + 10728.802555e^{-4/x} - 49077.175871e^{-5/x} + 73776.084137e^{-6/x} \tag{4.2}$$

which is plotted in Fig. 4. This fit is reliable in the interval $x \leqslant x_{\max} \approx 0.629781$. Using the value $x^* \approx 0.633888$ derived from F_ξ, we have

$$F_{\chi_{\text{stagg}}}(x^*) = 3.172742 = 2^{1.66573} \tag{4.3}$$

if we extrapolate (4.2) linearly for $x \geqslant x_{\max}$, or

$$F_{\chi_{\text{stagg}}}(x^*) = 3.172345 = 2^{1.66555} \tag{4.4}$$

if we take (4.2) seriously also for $x > x_{\max}$. Either way, this is in excellent agreement with the prediction[32] $\gamma/\nu = 5/3$ [cf. (2.30)].

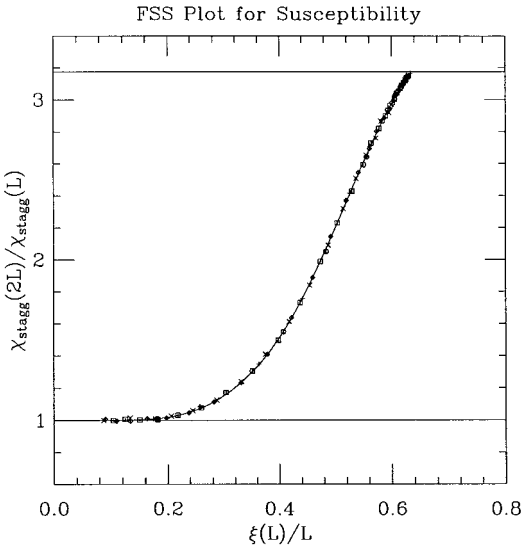

Fig. 4. $\chi_{\text{stagg}}(\beta, 2L)/\chi_{\text{stagg}}(\beta, L)$ versus $\xi(\beta, L)/L$. Symbols indicate $L = 32$ (+), 64 (×), 128 (□), 256 (◇), 512 (○). Error bars are one standard deviation. Curve is a sixth-order fit in (2.22), with $\xi_{\min} = 10$ and $L_{\min} = 128$.

We can now compute the extrapolated values $\chi_{\text{stagg},\infty}$, using the functions F_ξ and $F_{\chi_{\text{stagg}}}$ given by our preferred fit as well as by several alternative fits that use more or less stringent choices of $L_{\min}$. (In all cases we take $n = 5$ for F_ξ and $n = 6$ for $F_{\chi_{\text{stagg}}}$; the results for larger n differ in almost all cases by < 0.6 standard deviations.) The statistical error bars on $\chi_{\text{stagg},\infty}$ are computed as before by an auxiliary Monte Carlo process, and include errors of types (i) + (ii) + (iii). For each β we compute the weighted average (2.23) of the various estimates $\chi_{\text{stagg},\infty}$ along with the statistical error bar (2.24) and the $\mathscr{R}$ value (2.25). These are reported in Table 4. The statistical errors on $\chi_{\text{stagg},\infty}$ are of order 2% (resp. 3%, 5%, 8%) at $\xi_\infty \approx 1000$ (resp. 2000, 5000, 10000), that is, about twice as big as those on ξ_∞. These extrapolated values from different lattice sizes at the same β are found to be consistent within statistical errors: only two of the 42 β values has an $\mathscr{R}$ value too large at the 5% level; and summing all β values we have $\sum \mathscr{R} = 50.41$ (75 DF, level = 98.7%). We don't know why this chi-squared is so small; it may be due in part to our overestimation of the raw-data error bars on ξ_L, which leads to an overestimation of the errors of type (ii) on $\chi_{\text{stagg},\infty}$.

The discrepancies between the extrapolations with $L_{\min} = 64, 128, 256$ are again less than half the quoted statistical error in nearly all cases.[24] We are thus reasonably confident that we have obtained quantitative control over the systematic errors due to corrections to scaling, and that their effect can be at most to double the quoted statistical errors.

4.2. Analysis of Extrapolated Data

In this section we analyze the behavior as $\beta \to \infty$ of the extrapolated data for ξ and χ_{stagg}. In all cases we use the preferred extrapolations, namely the ones with $\xi_{\min} = 10$, $L_{\min} = 128$, and $n = 5$ (resp. 6) for ξ (resp. χ_{stagg}).

4.2.1. Correlation Length. Our data are in clear agreement with the prediction of a critical point at $\beta = \infty$. The correlation length ξ_∞ rises roughly like $e^{2\beta}$, and we initially thought that this was the exact asymptotic behavior. However, at $\beta \gtrsim 3.4$ ($\xi_\infty \gtrsim 75$), ξ_∞ begins to rise *faster* than this (Fig. 5a), and this rise shows no sign of abating at least up to $\beta \approx 5.9$ ($\xi_\infty \approx 15000$). We therefore guessed a multiplicative logarithmic correction, i.e., $\xi_\infty \sim e^{2\beta}\beta^p$ for some power $p > 0$: see Figs. 5b,c for $p = 1/2$ and $p = 1$, respectively.

In order to distinguish between these scenarios, we need to make some assumption on the form of the additive corrections to the leading asymptotic behavior. Unfortunately we do not know how to carry out a low-temperature expansion around the (critical) zero-temperature state; but the simplest hypothesis is that there exists an expansion in powers of $e^{-\beta}$, which corresponds to a minimum energy cost of one unit for an "overturned" spin. That is, we expect

$$\xi_\infty(\beta) = Ae^{2\beta}\beta^p[1 + a_1 e^{-\beta} + a_2 e^{-2\beta} + \cdots] \tag{4.5}$$

If we accept this Ansatz, a value $p \approx 1$ is clearly favored (Fig. 6). A fit to the first two terms of (4.5) with $p = 1$, using the data points with $\beta \geqslant 2.95$ ($e^{-\beta} \lesssim 0.052$), yields $A = 0.01814 \pm 0.00006$ and $Aa_1 = 0.20051 \pm 0.00225$ (hence $a_1 \approx 15$) with $\chi^2 = 13.10$ (35 DF, level $= 99.97\%$).

[24] The extrapolations with $L_{\min} = 32$ frequently deviate from our preferred $L_{\min} = 128$ extrapolation by as much as $\approx 1.2\sigma$. These deviations are, once again, probably a correction-to-scaling effect on the borderline of statistical significance.

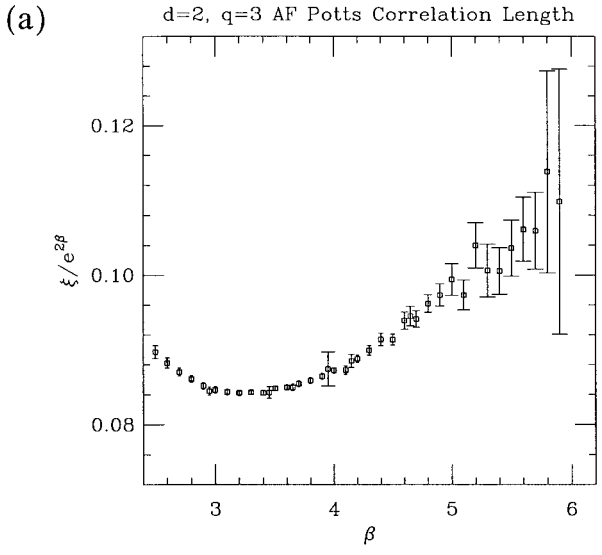

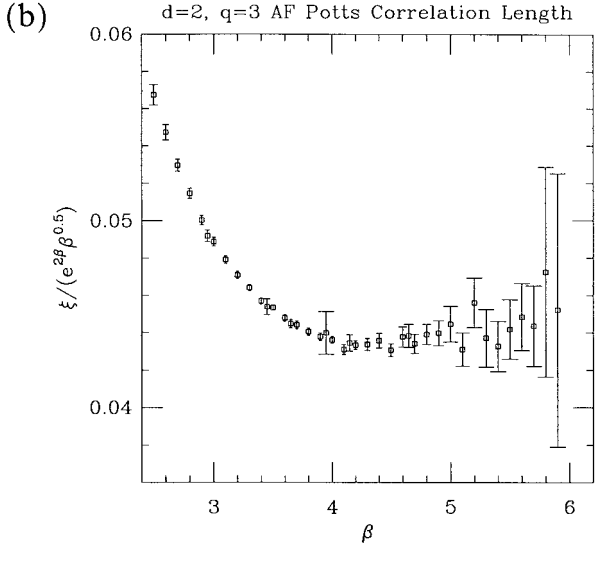

Fig. 5. Infinite-volume correlation length ξ_∞ divided by $e^{2\beta}\beta^p$ for (a) $p=0$, (b) $p=1/2$, (c) $p=1$. Error bars are one standard deviation.

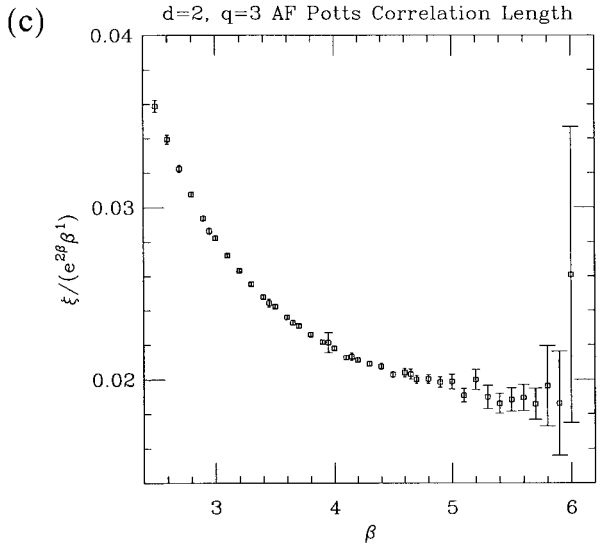

Fig. 5. (*Continued*)

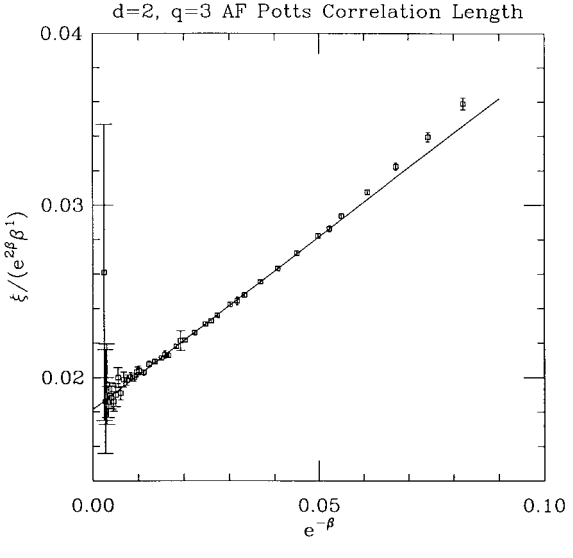

Fig. 6. $\xi_\infty/(e^{2\beta}\beta^p)$ with $p=1$, plotted versus $e^{-\beta}$. Note the nearly linear behavior, in good agreement with (4.5). Straight line is $\xi_\infty/(e^{2\beta}\beta) = 0.01814 + 0.20051e^{-\beta}$, which is the least-squares fit to the data with $\beta \geqslant 2.95$ ($e^{-\beta} \lesssim 0.052$).

On the other hand, Chris Henley (private communication) has suggested to us that the corrections to scaling might contain *fractional* powers of $e^{-\beta}$:

$$\xi_\infty(\beta) = Ae^{2\beta}\beta^p[\,1 + a_1 e^{-\lambda_1\beta} + a_2 e^{-\lambda_2\beta} + \cdots\,] \tag{4.6}$$

with $\lambda_1 < 1$. Since $e^{-\lambda_1\beta} \sim \xi^{-\lambda_1/2}$, such behavior would ordinarily arise from a correction-to-scaling exponent $\Delta = \lambda_1/2$; and our data for the finite-size-scaling functions show no evidence of a correction-to-scaling exponent anywhere near this small (see Section 4.1.1). Let us nevertheless consider the Ansatz (4.6) open-mindedly and see whether it can accommodate $p = 0$. In Fig. 7a,b we plot $\xi_\infty(\beta)/e^{2\beta}$ versus $e^{-\lambda\beta}$ for $\lambda = 1$ and 0.5, respectively. With $\lambda = 1$, the plot shows both strong curvature and a rather high slope near the origin; for $\beta \geqslant 4.50$ ($e^{-\beta} \lesssim 0.011$) the data can be fit well by a straight line with $A \approx 0.110$ and $a_1 \approx -15$. With $\lambda = 0.5$, the curvature and slope are less radical; the data for $\beta \geqslant 4.50$ ($e^{-0.5\beta} \lesssim 0.105$) can be fit well by a straight line with $A \approx 0.122$ and $a_1 \approx -2.4$. However, even this latter plot is nowhere near as convincing as Fig. 6.

Finally, an anonymous referee has suggested to us that the corrections to scaling might be in *powers* of $1/\beta$:

$$\xi_\infty(\beta) = Ae^{2\beta}\beta^p\left[\,1 + \frac{a_1}{\beta} + \frac{a_2}{\beta^2} + \cdots\right] \tag{4.7}$$

(see Section 7.1 for theoretical discussion). In Figs. 8a, b, c we plot $\xi_\infty(\beta)/(e^{2\beta}\beta^p)$ versus $1/\beta$ for $p = 0, 1/2, 1$. Clearly, our data—which lie in the range $0.15 \lesssim 1/\beta \lesssim 0.4$—are so far from asymptotic that no conclusion can be drawn. In particular, the plot for $p = 0$ (resp. $p = 1$) shows such a large negative (resp. positive) slope at the smallest available value of $1/\beta$ that the extrapolated intercept at $1/\beta = 0$ differs by nearly a factor of 2 from the last data point; and the plot for $p = 1/2$ shows a large third derivative (i.e., abrupt change from parabolic to flat) at $1/\beta \approx 0.2$.

Let us note in passing that our data fit much less well the Ansatz $\xi_\infty \sim \exp(c\beta^\kappa)$ used by some previous workers.[35, 10, 11] Indeed, a log–log plot of $\log \xi_\infty$ versus β (Fig. 9) shows significant curvature: the apparent exponent κ varies from ≈ 1.69 at small β to ≈ 1.38 at larger β. (This decrease is consistent with our conjecture that the true asymptotic value of the exponent κ is 1.) Moreover, as noted in the Introduction, we have been unable to imagine any theoretical mechanism leading to $\xi \sim \exp(c\beta^\kappa)$ with $\kappa \neq 1$.

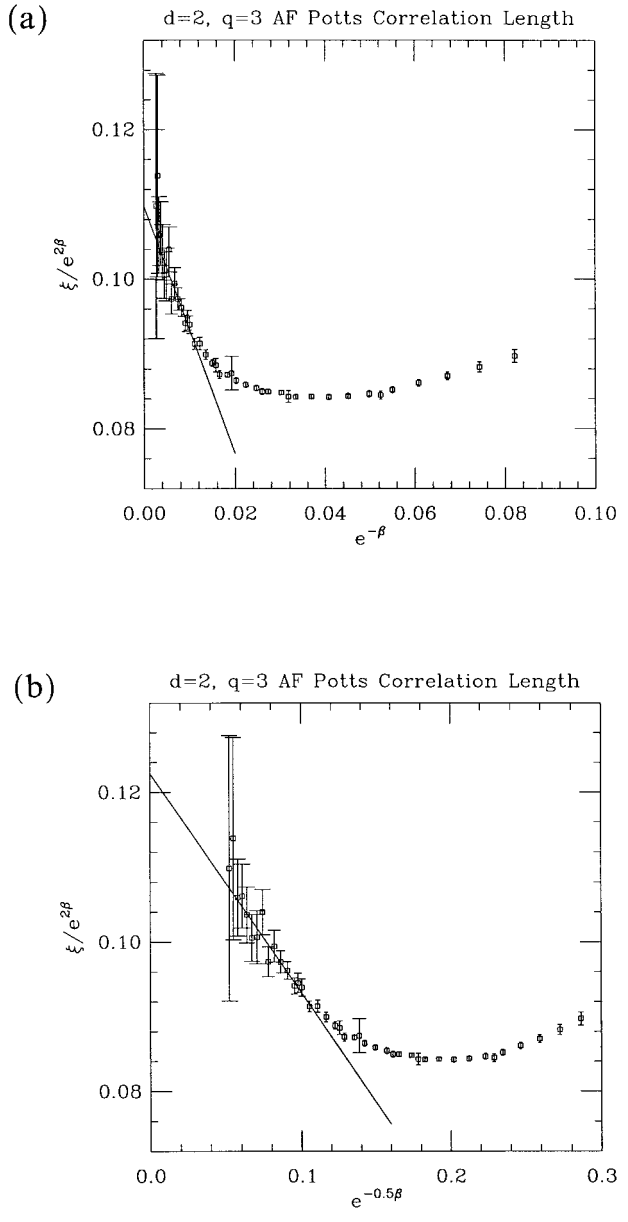

Fig. 7. $\xi_\infty/e^{2\beta}$ plotted versus $e^{-\lambda\beta}$. (a) $\lambda = 1$. Straight line is $\xi_\infty/e^{2\beta} = 0.1098 - 1.6574e^{-\beta}$, which is the least-squares fit to the data with $\beta \geqslant 4.50$ ($e^{-\beta} \lesssim 0.011$). (b) $\lambda = 0.5$. Straight line is $\xi_\infty/e^{2\beta} = 0.1225 - 0.2929e^{-0.5\beta}$, which is the least-squares fit to the data with $\beta \geqslant 4.50$ ($e^{-0.5\beta} \lesssim 0.105$).

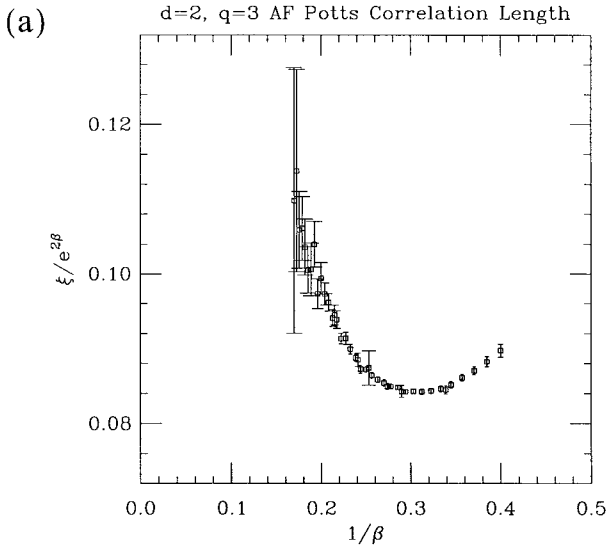

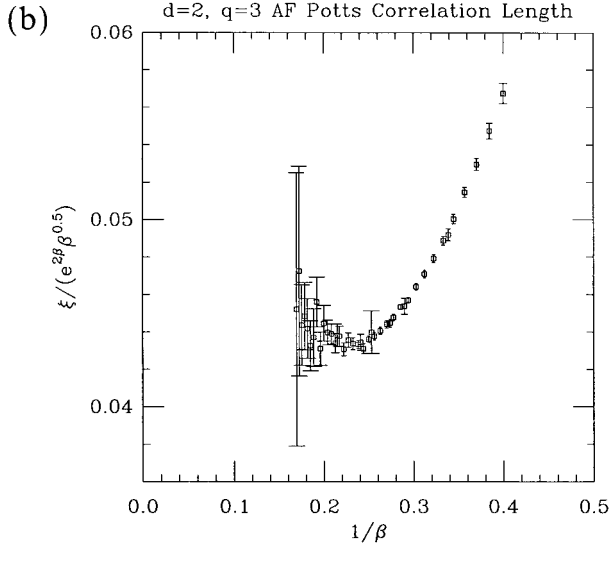

Fig. 8. $\xi_\infty/(e^{2\beta}\beta^p)$ plotted versus $1/\beta$ for (a) $p=0$, (b) $p=1/2$, (c) $p=1$.

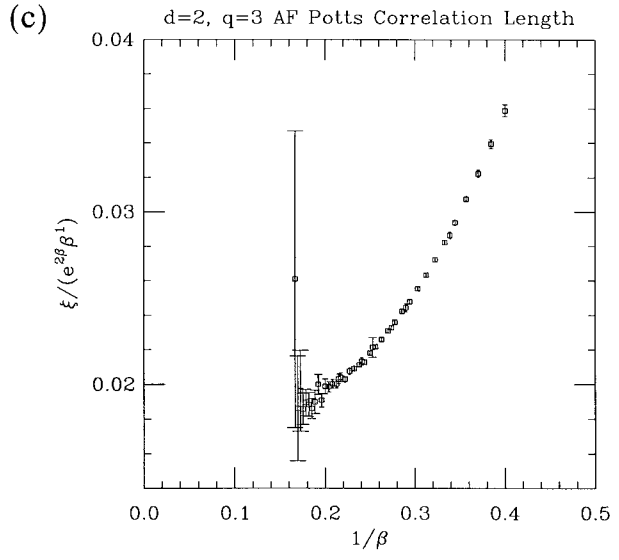

Fig. 8. (*Continued*)

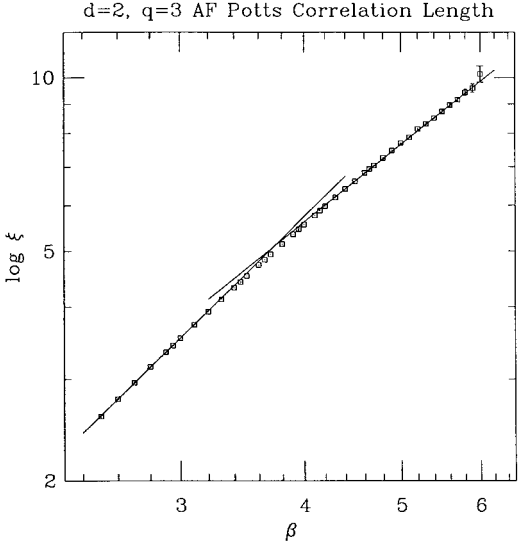

Fig. 9. Log–log plot of log ξ_∞ versus β. The indicated asymptotes are $\log \xi_\infty = 0.55300\beta^{1.68785}$ at small β, and $\log \xi_\infty = 0.82503\beta^{1.38387}$ at large β.

4.2.2. Staggered Susceptibility The staggered susceptibility is consistent with the believed exact behavior[32] $\chi_{\text{stagg},\infty} \sim \xi_\infty^{5/3}$, unmodified by any further powers of β. To test this behavior quantitatively, we need to set error bars on the ratio $\chi_{\text{stagg},\infty}/\xi_\infty^{5/3}$. Since unfortunately we do not know the covariance between our estimates of ξ_∞ and $\chi_{\text{stagg},\infty}$, the best we can do is to use the triangle inequality to set an *upper bound* on the error bar for the ratio; this upper bound is of course a gross overestimate of the true error, since the estimates of ξ_∞ and $\chi_{\text{stagg},\infty}$ are presumably strongly positively correlated. As a result, the error bars in all fits will be grossly overestimated, and the χ^2 will be grossly underestimated; only the *relative* values of χ^2/DF have any significance.

In Fig. 10 we plot $\chi_{\text{stagg},\infty}/\xi_\infty^{5/3}$ versus β (note the very narrow vertical scale); the error bars are those given by the triangle inequality, *reduced by a factor of 10 for visual clarity*. We see that $\chi_{\text{stagg},\infty}/\xi_\infty^{5/3}$ varies slightly with β, but appears to be tending to a constant ≈ 2.67 as $\beta \to \infty$.

If we fit $\chi_{\text{stagg},\infty}/\xi_\infty^{5/3}$ to the Ansatz $A\beta^p$, the estimates of the power p are extremely small, of order 0.02, and statistically consistent with zero. This confirms our belief that there are no additional powers of β in the ratio $\chi_{\text{stagg},\infty}/\xi_\infty^{5/3}$. If we impose $p = 0$ and fit $\chi_{\text{stagg},\infty}/\xi_\infty^{5/3}$ to a constant A, we obtain $A = 2.657 \pm 0.051$ ($\chi^2 = 0.007$, 13 DF, level $> 99.9\%$) using the

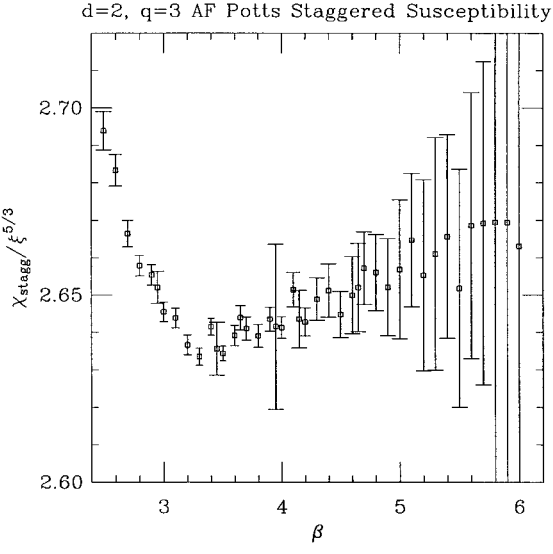

Fig. 10. $\chi_{\text{stagg},\infty}/\xi_\infty^{5/3}$ plotted versus β. Error bars are those given by the triangle inequality, *reduced by a factor of 10 for visual clarity*.

data from $\beta \geqslant 4.70$. Of course, the error bar on A here is a gross overestimate, and the χ^2 value is a gross underestimate.

We can, of course, investigate directly the behavior of $\chi_{\text{stagg},\infty}$ as a function of β, without reference to ξ. This approach has the advantage that the error bars on $\chi_{\text{stagg},\infty}$ are reliable. In Fig. 11 we plot $\chi_{\text{stagg},\infty}/(e^{(10/3)\beta}\beta^q)$ versus β for $q = 0, \frac{5}{6}, \frac{5}{3}$. The behavior is qualitatively similar to that observed in Fig. 5 for ξ, although the variation is somewhat sharper. If we try again the Ansatz

$$\chi_{\text{stagg},\infty}(\beta) = Be^{(10/3)\beta}\beta^q[1 + b_1 e^{-\beta} + b_2 e^{-2\beta} + \cdots] \tag{4.8}$$

a value $q \approx 5/3$ is favored (Fig. 12). The curvature is greater than in the corresponding plot for ξ, hut the linearity is still reasonable for $e^{-\beta} \lesssim 0.03$. A fit to (4.8) with $q = 5/3$, using the data points with $\beta \geqslant 3.60$ ($e^{-\beta} \leqslant 0.0273$), yields $B = 0.00329 \pm 0.00003$ and $Bb_1 = 0.06661 \pm 0.00124$ (hence $b_1 \approx 20$) with $\chi^2 = 17.55$ (27 DF, level = 92%). We omit the plots based on a fractional-power additive correction to scaling, which are similar to those shown for the correlation length (Fig. 7).

4.3. Behavior of the Energy

On theoretical grounds we expect that the infinite-volume energy per site has a low-temperature expansion of the form

$$E_\infty(\beta) = c_1 e^{-\beta} + c_2 e^{-2\beta} + \cdots \tag{4.9}$$

Unfortunately we do not have access to E_∞, as we have made no attempt to extrapolate the energies (which are *short*-distance quantities) to infinite volume. But examination of the finite-volume energies E_L indicates that for $L \geqslant 512$ (resp. 1024) the remaining L-dependence is less than $\approx 2 \times 10^{-4}$ (resp. 5×10^{-5}); so the energies appear to have *almost* reached their infinite-volume limits. In Fig. 13 we plot $E/e^{-\beta}$ versus $e^{-\beta}$, using different symbols to represent different lattice sizes. A fit to the $L = 1024$ points with $\beta \geqslant 5.00$ ($e^{-\beta} \leqslant 0.0067$) yields $c_1 = 0.21777 \pm 0.00003$ and $c_2 = 1.65303 \pm 0.00664$ ($\chi^2 = 5.09$, 8 DF, level = 75%). The $L = 1536$ points are also compatible with this fit, and the $L = 512$ points differ only slightly from it. This provides good support for the Ansatz (4.9).

We would like to make a warning concerning the use of reweighting methods[53–56][25] in which Monte Carlo runs at one temperature β are

[25] These methods are sometimes called "histogram" (or "multiple-histogram") methods, but in fact the reweighting is most conveniently carried out *without* forming histograms!

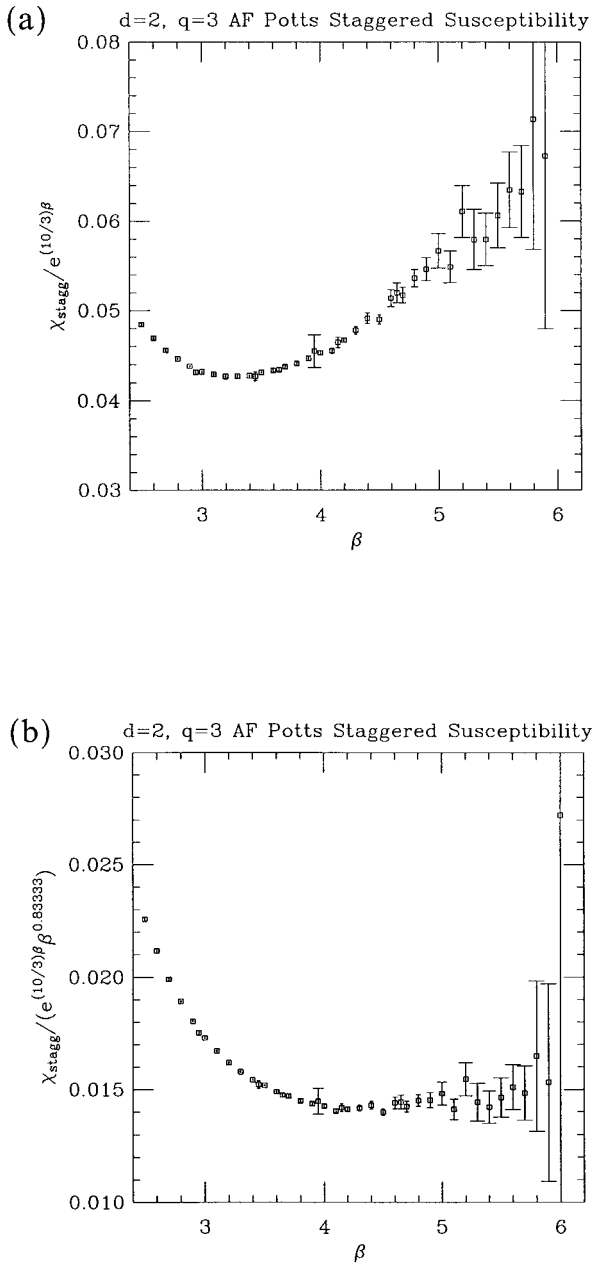

Fig. 11. Infinite-volume staggered susceptibility $\chi_{\text{stagg},\infty}$ divided by $e^{(10/3)\beta}\beta^q$ for (a) $q=0$, (b) $q=5/6$, (c) $q=5/3$. Error bars are one standard deviation.

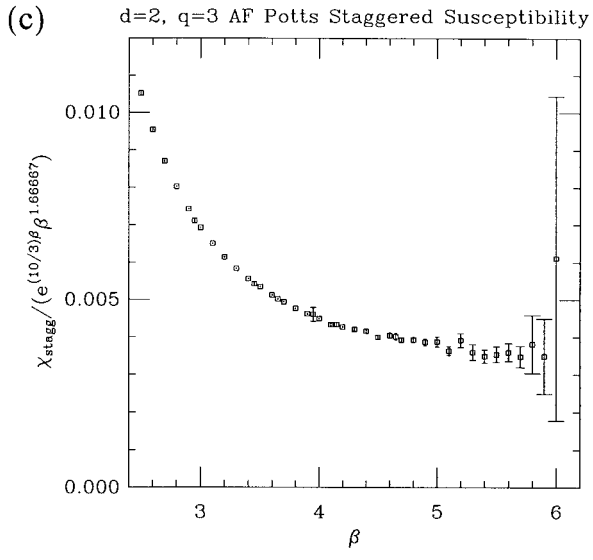

Fig. 11. (*Continued*)

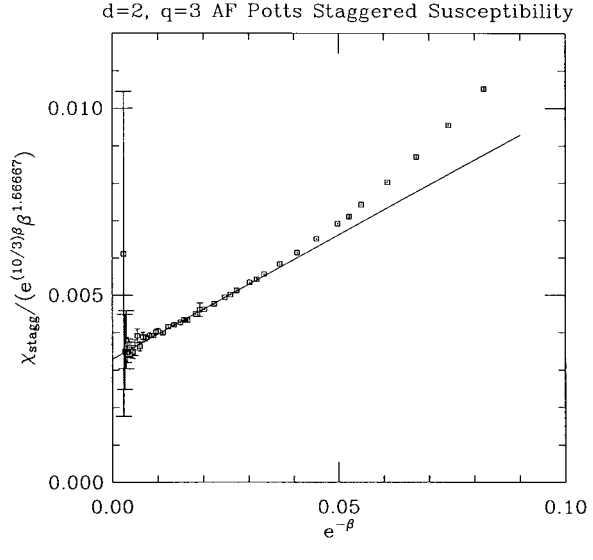

Fig. 12. $\chi_{\text{stagg},\infty}/(e^{(10/3)\beta}\beta^{q})$ with $q=5/3$, plotted versus $e^{-\beta}$. The behavior is reasonably linear for $e^{-\beta} \lesssim 0.03$, in good agreement with (4.8). Straight line is $\chi_{\text{stagg},\infty}/(e^{(10/3)\beta}\beta^{5/3}) = 0.00329 + 0.06661e^{-\beta}$, which is the least-squares fit to the data with $\beta \geqslant 3.60$.

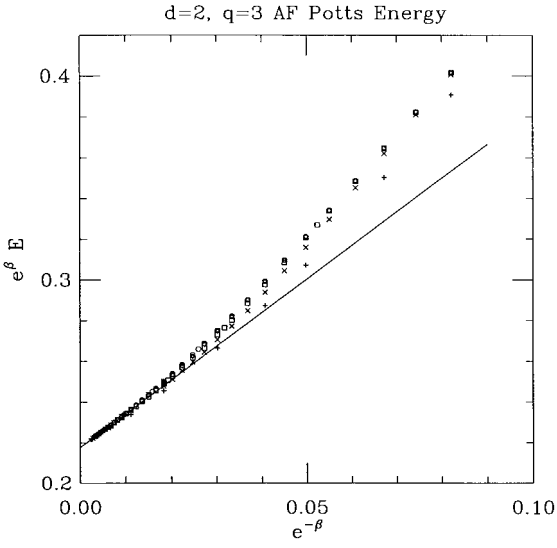

Fig. 13. Energy per site E divided by $e^{-\beta}$, plotted versus $e^{-\beta}$. Symbols indicate $L = 32$ (+), 64 (×), 128 (□), 256 (◇), 512 (○), 1024 (∗), 1536 (⊞). Error bars are invisibly small. The uppermost points at each β represent the infinite-volume limit. Note the nearly linear behavior for small $e^{-\beta}$, in good agreement with (4.9). Straight line is $E = 0.21777e^{-\beta} + 1.65303e^{-2\beta}$, which is the least-squares fit to the data with $L = 1024$ and $\beta \geqslant 5.00$.

employed to generate data at another temperature β' by reweighting with the factor $\exp[-(\Delta\beta)H]$, where $\Delta\beta \equiv \beta' - \beta$. This reweighting is of course always valid in principle; but one must be aware that the statistical error bars on the reweighted data grow rapidly as $|\Delta\beta|$ grows, and the maximum $|\Delta\beta|$ for which one can obtain a not-too-large error bar gets smaller for larger L:

$$|\Delta\beta| \lesssim \begin{cases} L^{-d/2} & \text{near a non-phase-transition point} \\ L^{-1/\nu} & \text{near a critical point} \\ L^{-d} & \text{near a first-order phase-transition point} \end{cases} \tag{4.10}$$

Our Monte Carlo data illustrate this point in a very striking way. In all of our runs with $L \geqslant 128$—totalling more than 60 million measurements—we did not observe even a single configuration (after the discard interval) with energy $E = 0$. In other words, none of our histograms for $L \geqslant 128$—even those at our largest β value, namely $\beta = 6.0$—have *any* overlap with the zero-temperature probability distribution. It follows that reweighting to zero temperature in these cases is *nonsense*. For $L = 64$, our runs at $\beta = 4.50$

and 5.00 (but not smaller β) do show *some* configurations with $E=0$, but the sample size of such configurations is very small: about 0.2% at $\beta=5.0$. Reweighting to zero temperature in these cases would thus produce *enormous error bars* (at least if the error bars are computed correctly!). Only for $L \leqslant 32$ do we have a significant number of zero-energy configurations: for example, for $L=32$ and $\beta=5.0$, we found that 21.6% of the configurations have $E=0$. Furthermore, even reweighting to nonzero temperatures is fraught with severe dangers. For example, although our run lengths are anywhere from 2×10^5 to 10^6 measurements, the energy histograms of a pair of runs typically show *no* overlap if $|\Delta\beta| \gtrsim 0.3$ (resp. 0.4, 0.5–0.6, 0.5–0.9, 1.2–1.4) for $L=1536$ (resp. 1024, 512, 256, 128).[26] It follows that reweighting beyond these limits is nonsense, and reweighting near these limits leads to huge statistical errors.

5. DATA ANALYSIS: $q=3$, DYNAMIC QUANTITIES

In this section we analyze the dynamic critical behavior of the WSK algorithm for the 3-state antiferromagnetic Potts model on the square lattice.

5.1. Integrated Autocorrelation Times

Examination of Table 1 indicates that the autocorrelation times $\tau_{\mathrm{int},\mathcal{M}^2_{\mathrm{stagg}}}$ and $\tau_{\mathrm{int},\mathcal{E}}$ are bounded uniformly in β and L. (Indeed, their values are very small: $\tau_{\mathrm{int},\mathcal{M}^2_{\mathrm{stagg}}} < 5$ and $\tau_{\mathrm{int},\mathcal{E}} < 4$.) We conclude that *critical slowing-down is completely eliminated.*

We can study the dynamic critical behavior in more detail by applying the standard dynamic finite-size-scaling Ansatz

$$\tau_{\mathrm{int},A}(\beta, L) \approx \xi(\beta, L)^{z_{\mathrm{int},A}}\, g_A(\xi(\beta, L)/L) \tag{5.1}$$

to the observables $A=\mathcal{M}^2_{\mathrm{stagg}}$ and $\mathcal{E}$. Here $z_{\mathrm{int},A}$ is a dynamic critical exponent, g_A is an unknown scaling function, and $g_A(0)=\lim_{x\downarrow 0} g_A(x)$ is supposed to be finite and nonzero.[27] Usually we would determine $z_{\mathrm{int},A}$ by plotting $\tau_{\mathrm{int},A}/\xi(L)^{z_{\mathrm{int},A}}$ versus $\xi(L)/L$ and adjusting $z_{\mathrm{int},A}$ until the points fall as closely as possible onto a single curve (with priority to the larger L

[26] The allowable $|\Delta\beta|$ depends slightly on β, getting smaller at smaller β. For example, at $L=512$ the $\beta=5.7$ run shows no overlap with the $\beta=5.1$ run, which in turn shows no overlap with the $\beta=4.65$ run, which in turn shows no overlap with the $\beta=4.2$ run.

[27] We emphasize that the dynamic critical exponent $z_{\mathrm{int},A}$ is in general *different* from the exponent z_{exp} associated with the exponential autocorrelation time τ_{exp}.[43, 57, 58]

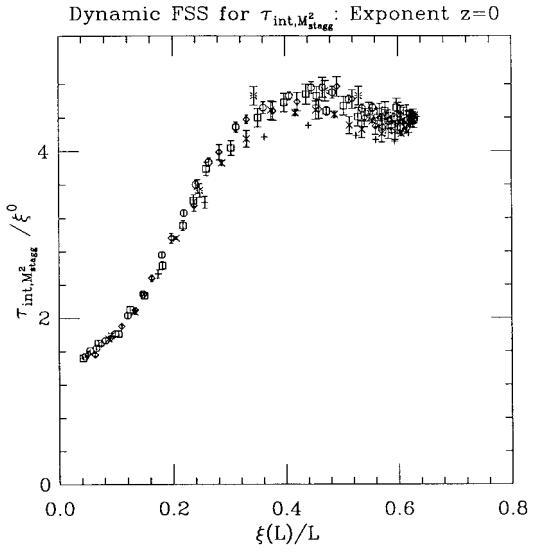

Fig. 14. Dynamic finite-size-scaling plot of $\tau_{\mathrm{int},\mathcal{M}^2_{\mathrm{stagg}}}$ versus $\xi(L)/L$, assuming dynamic critical exponent $z_{\mathrm{int},\mathcal{M}^2_{\mathrm{stagg}}} = 0$ Symbols indicate $L = 32$ (+), 64 (×), 128 (□), 256 (◇), 512 (○), 1024 (∗), 1536 (⊛). Error bars are one standard deviation.

values). But in our case the situation is much simpler: the dynamic critical exponents $z_{\mathrm{int},\mathcal{M}^2_{\mathrm{stagg}}}$ and $z_{\mathrm{int},\mathcal{E}}$ are *zero*.

In Fig. 14 we show the dynamic finite-size-scaling plot for $\tau_{\mathrm{int},\mathcal{M}^2_{\mathrm{stagg}}}$, assuming $z_{\mathrm{int},\mathcal{M}^2_{\mathrm{stagg}}} = 0$. The data collapse is amazingly good, especially for a plot with no free parameters. Indeed, in all our Monte Carlo work on dynamic critical phenomena we have never observed a data collapse this good, even when we had the freedom to adjust $z_{\mathrm{int},A}$.

For $\tau_{\mathrm{int},\mathcal{E}}$, by contrast, the data collapse is *not* so good: see Fig. 15, where we again assume $z_{\mathrm{int},\mathcal{E}} = 0$. Clearly there are *huge* corrections to dynamic finite-size-scaling for this observable. Even so, the points do appear to be converging as $L \to \infty$ to a limiting curve (which can be roughly traced using the $L = 512$ and $L = 1024$ points).

5.2. Autocorrelation Functions

Now we want to test the more detailed dynamic finite-size-scaling Ansatz

$$\rho_{AA}(t; \beta, L) \approx |t|^{-p_A} h_A(t/\tau_{\mathrm{exp},A}(\beta, L); \xi(\beta, L)/L) \tag{5.2}$$

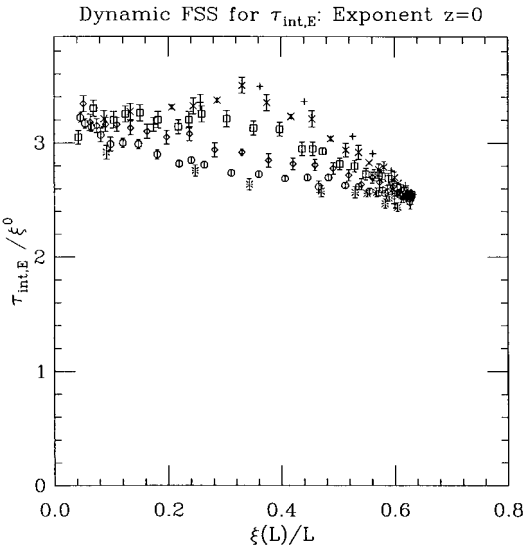

Fig. 15. Dynamic finite-size-scaling plot of $\tau_{\mathrm{int},\mathscr{E}}$ versus $\xi(L)/L$, assuming dynamic critical exponent $z_{\mathrm{int},\mathscr{E}}=0$. Symbols indicate $L=32$ (+), 64 (×), 128 (□), 256 (◇), 512 (○), 1024 (∗), 1536 (⊞). Error bars are one standard deviation.

where p_A is an unknown exponent and h_A is an unknown scaling function. If $p_A=0$, then (5.2) can equivalently be written as

$$\rho_{AA}(t;\beta,L)\approx\hat{h}_A(t/\tau_{\mathrm{int},A}(\beta,L);\xi(\beta,L)/L) \tag{5.3}$$

In this latter situation,[28] $\tau_{\mathrm{int},A}$ and $\tau_{\exp,A}$ have the *same* dynamic critical exponent $z_{\mathrm{int},A}=z_{\exp}$, and we furthermore have

$$\frac{\tau_{\mathrm{int},A}}{\tau_{\exp,A}}\approx F_A(\xi(\beta,L)/L) \tag{5.4}$$

where

$$F_A(x)\equiv\lim_{t\to+\infty}\frac{1}{t}\log\hat{h}_A(t;x) \tag{5.5}$$

Let us now test the Ansatz (5.3) for the observable $A=\mathscr{M}^2_{\mathrm{stagg}}$. (We restrict attention to this observable, since we already know that for $A=\mathscr{E}$ the dynamic finite-size-scaling behavior is poor.) In Fig. 16 we plot $\rho_{\mathscr{M}^2_{\mathrm{stagg}}\mathscr{M}^2_{\mathrm{stagg}}}(t)$ versus $t/\tau_{\mathrm{int},\mathscr{M}^2_{\mathrm{stagg}}}$, using *all* the data points. The points fall

[28] Contrary to much belief, $z_{\mathrm{int},A}$ *need not* equal $z_{\exp}$. Indeed, if $\rho_A>0$, we have $z_{\mathrm{int},A}=(1-p_A)\,z_{\exp}<z_{\exp}$. See refs. 43 and 58 for further discussion.

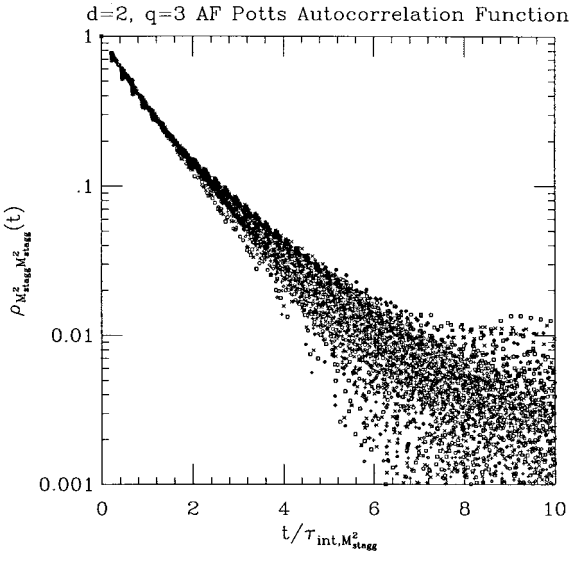

Fig. 16. Plot of $\rho_{\mathcal{M}^2_{\text{stagg}}\mathcal{M}^2_{\text{stagg}}}(t)$ versus $t/\tau_{\text{int},\mathcal{M}^2_{\text{stagg}}}$, using *all* data points. Symbols indicate $L = 32$ (+), 64 (×), 128 (□), 256 (◇), 512 (○), 1024 (∗), 1536 (⊞). Error bars are omitted.

roughly on a single curve before falling into the statistical noise (which we expect to be of order $(n/\tau_{\text{int},\mathcal{M}^2_{\text{stagg}}})^{-1/2}$ where n is the run length, hence of order ± 0.005). However, even at small $t/\tau_{\text{int},\mathcal{M}^2_{\text{stagg}}}$ there are clear deviations from a single curve, indicating that the scaling function $\hat{h}_{\mathcal{M}^2_{\text{stagg}}}$ depends in a nontrivial way on its second argument $\xi(L)/L$. Therefore, in Fig. 17a–f we show the same plot with the data subdivided into "slices" of $\xi(L)/L$; the slices are chosen empirically so that the data points within a slice fall reasonably well onto a single curve modulo statistical noise. On each plot we also draw, for reference, a line corresponding to a pure exponential decay $\tau_{\text{int},\mathcal{M}^2_{\text{stagg}}} = \tau_{\text{exp},\mathcal{M}^2_{\text{stagg}}}$. The data support the Ansatz (5.3) reasonably well, with each range of $\xi(L)/L$ defining roughly a single curve (until that curve falls into the statistical noise). The curves for small $\xi(L)/L$ are close to straight (i.e., close to a pure exponential), while the curves for larger $\xi(L)/L$ are increasingly convex.[29] (Note that the rescaled horizontal axis ensures that the total area under each curve is 1. Therefore, the more convex curves must be below the straight curve for small $\tau_{\text{int},\mathcal{M}^2_{\text{stagg}}}$ but above it for large $\tau_{\text{int},\mathcal{M}^2_{\text{stagg}}}$.) This means that the ratio $\tau_{\text{int},\mathcal{M}^2_{\text{stagg}}}/\tau_{\text{exp},\mathcal{M}^2_{\text{stagg}}}$

[29] It is amusing to note that a similar behavior was observed in our study of the multi-grid Monte Carlo algorithm for the two-dimensional $O(3)$ σ-model.[59] We wonder whether it is a general phenomenon.

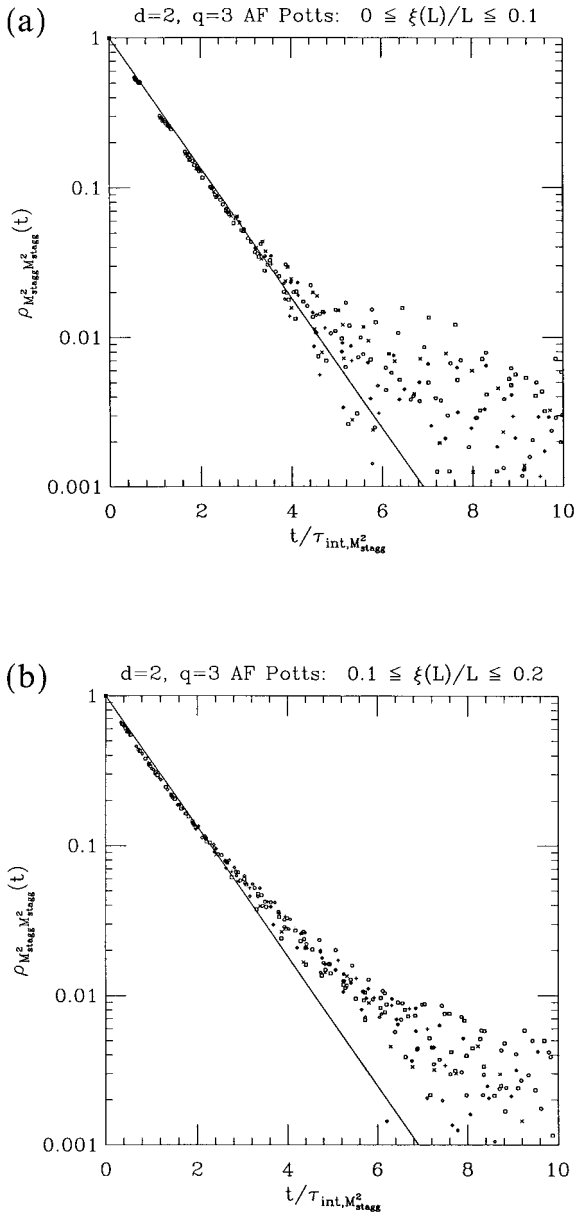

Fig. 17. Plot of $\rho_{\mathscr{M}^2_{\text{stagg}},\mathscr{M}^2_{\text{stagg}}}(t)$ versus $t/\tau_{\text{int},\mathscr{M}^2_{\text{stagg}}}$ subdivided by ranges of $\xi(L)/L$: (a) 0.0–0.1, (b) 0.1–0.2, (c) 0.2–0.5, (d) 0.50–0.54, (e) 0.54–0.58, (f) 0.58–0.63. Symbols indicate $L=32$ (+), 64 (×), 128 (□), 256 (◇), 512 (○), 1024 (∗), 1536 (⊞). Error bars are omitted. The straight lines correspond to a pure exponential decay $\tau_{\text{int},\mathscr{M}^2_{\text{stagg}}} = \tau_{\text{exp},\mathscr{M}^2_{\text{stagg}}}$.

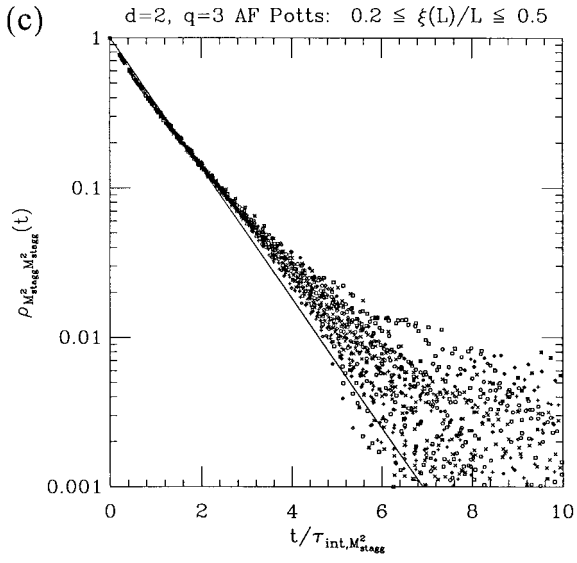

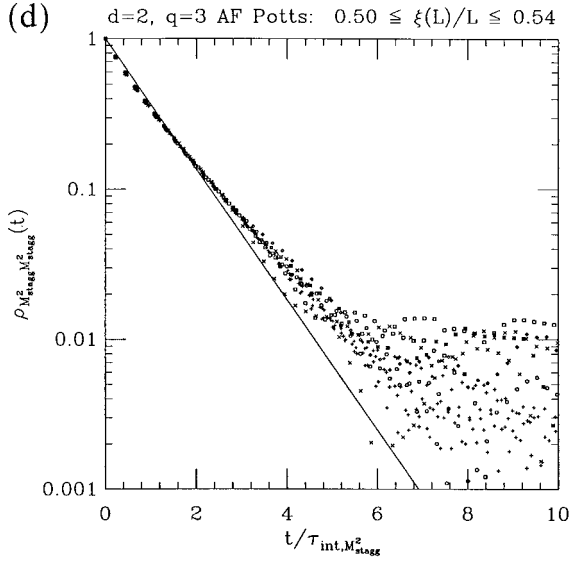

Fig. 17. (*Continued*)

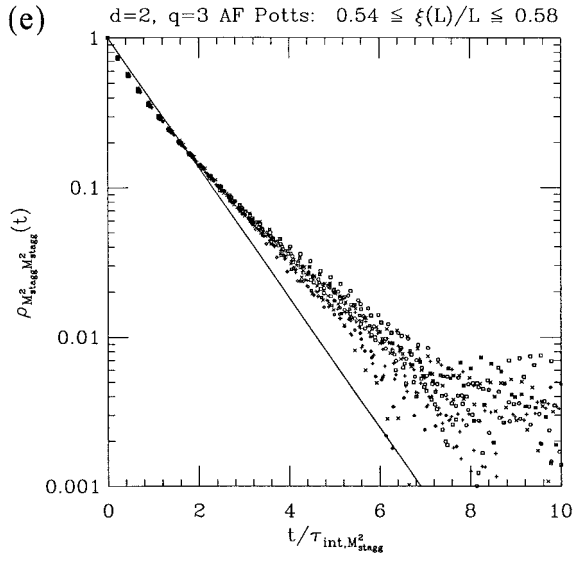

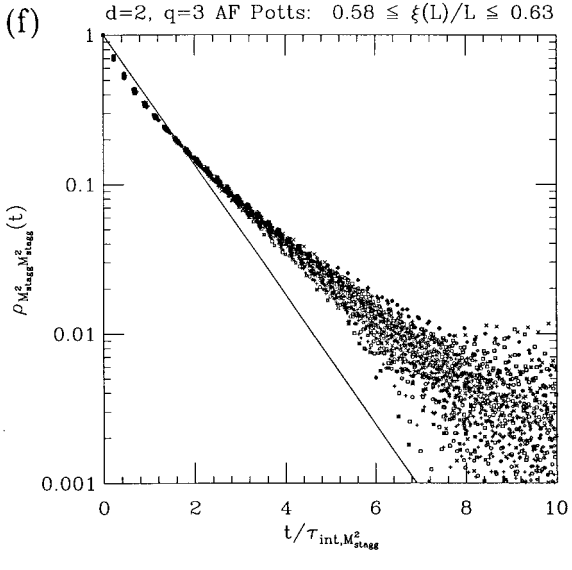

Fig. 17. (*Continued*)

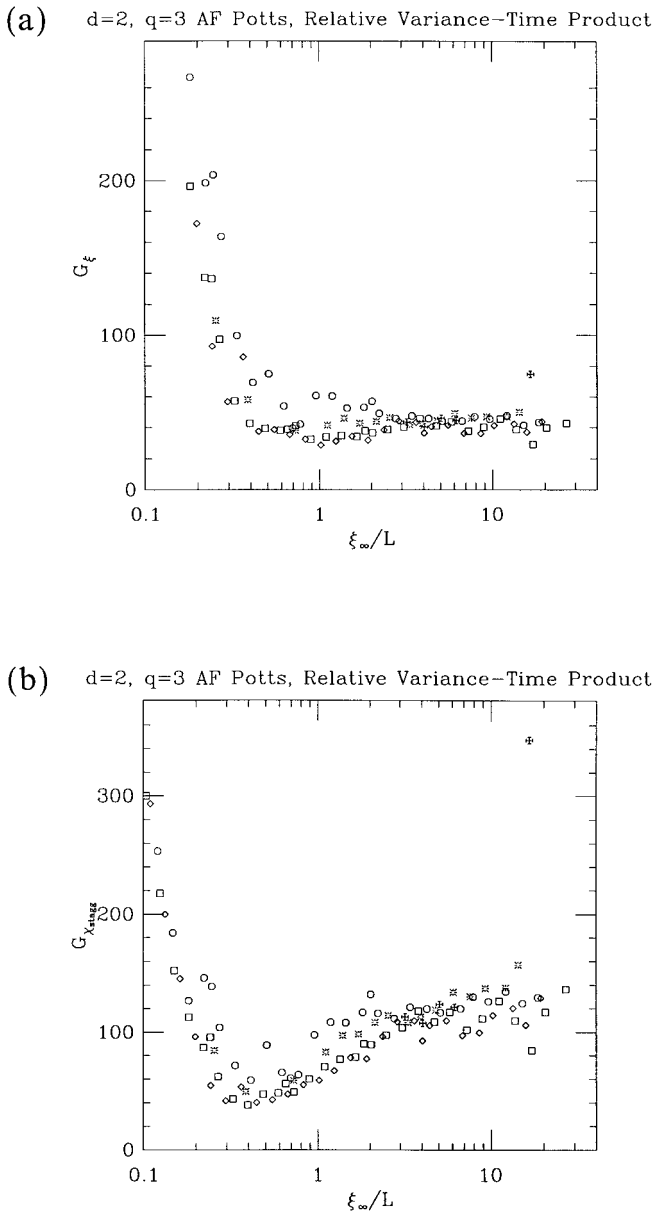

Fig. 18. Relative variance-time product [including errors of types (i) + (ii) + (iii)] divided by $\xi_\infty(\beta)^2$, plotted versus $\xi_\infty(\beta)/L$, for two-dimensional three-state Potts antiferromagnet. (a) is for $\mathcal{O} = \xi$, (b) is for $\mathcal{O} = \chi_{\text{stagg}}$. Symbols indicate $L = 128$ (□), 256 (◇), 512 (○), 1024 (∗), 1536 (⊞).

is close to 1 for small $\xi(L)/L$, and less than 1 for larger $\xi(L)/L$. It is *conceivable* that $\tau_{\text{int},\mathscr{M}^2_{\text{stagg}}}/\tau_{\text{exp},\mathscr{M}^2_{\text{stagg}}}$ tends to 1 as $\xi(L)/L \to 0$; if true, this would mean that $\mathscr{M}^2_{\text{stagg}}$ truly becomes the "slowest mode" in the limit $L \to \infty$, $\xi/L \to 0$.

5.3. Relative Variance-Time Product

Finally, let us look at the scaling (2.26) of the relative variance-time product. For each observable $\mathcal{O} = \xi, \chi_{\text{stagg}}$ we proceed as follows: For each run (β, L) we form the relative variance $(\Delta\mathcal{O}_\infty/\mathcal{O}_\infty)^2$ on the extrapolated infinite-volume value coming from that run; we then multiply by $L^2 \times (\#\text{iterations} - \#\text{discard})$, which is a normalized measure of the CPU time invested in that run (after the discard interval); the result is, by definition, RVTP(β, L). We then divide RVTP(β, L) by $\xi_\infty(\beta)^2$ [since $d=2$ and $z_{\text{int},\mathcal{O}} = 0$] and plot it versus $\xi_\infty(\beta)/L$.[30] The results are reported in Fig. 18a for ξ and Fig. 18b for χ_{stagg}. The scaling is reasonably good, though not perfect; this is not surprising, since our computed RVTP includes errors of types (i) + (ii) + (iii) while the scaling formula (2.26) refers only to errors of types (i) + (ii).[31, 32] Indeed, the fact that we see even modestly good scaling indicates that the errors of type (iii) are not dominant.

We see that for ξ the optimal value of ξ_∞/L is ≈ 1, but the minimum is very flat: any value in the range $0.5 \lesssim \xi_\infty/L \lesssim 10$ is almost equally good. It is only for $\xi_\infty/L \lesssim 0.3$ that the RVTP rises sharply, by a factor of 10 or more. In other words, the only region in which one should *not* run is the region in which one traditionally *always* ran, namely $\xi_\infty/L \lesssim 1/6$. For χ_{stagg} the story is similar, but the minimum is somewhat sharper: the optimum is at $\xi_\infty/L \approx 0.4$, and the RVTP rises by about a factor of 3 (resp. 10) as ξ_∞/L increases to ≈ 10 (resp. decreases to ≈ 0.1).

6. DATA ANALYSIS: $q = 4$

For $q=4$ the story is very brief: simulations on $L = 32, 64$ agree within statistical error and show that $\xi \lesssim 2$ uniformly as $\beta \to \infty$ (Table 2). Clearly

[30] In this latter computation, $\xi_\infty(\beta)$ is taken to be our best estimate (reported in Table 4), based on averaging *all* the runs at the given β.

[31] The much cleaner graph shown in [20, Fig. 2] was computed by using the theoretical formulae for the propagation of errors under extrapolation,[21, 22] and includes *only* errors of types (i) + (ii).

[32] The anomalous $L = 1536$ point at $\xi_\infty/L \approx 16.6$ corresponds to $\beta = 6.0$, where our statistics are poor and the extrapolation has almost broken down. Its relative error (33% for ξ and 71% for χ_{stagg}) is so large that both the extrapolated value and its error estimate are unreliable.

there is no critical point in the physical region. Physically, there is so much entropy that the correlations decay exponentially even at zero temperature. This can be proven rigorously to occur on the square lattice for $q \geqslant 7$,[9] and our simulations confirm Baxter's[23] prediction that it occurs in fact for $q > 3$.

The autocorrelation times $\tau_{\text{int},\mathcal{M}^2_{\text{stagg}}}$ and $\tau_{\text{int},\mathcal{E}}$ of the WSK algorithm are bounded uniformly in β and L, and indeed are almost constant: $\tau_{\text{int},\mathcal{M}^2_{\text{stagg}}} \approx 2.6$ and $\tau_{\text{int},\mathcal{E}} \approx 3.5$.

7. DISCUSSION AND CONCLUSIONS

In this section we summarize our conclusions and discuss their theoretical implications. We conclude by mentioning a few possible directions for future work.

7.1. Behavior of the Correlation Length

The numerical data presented in this paper (Section 4.2.1) show clearly that the correlation length diverges as $\beta \to \infty$ approximately like $\xi(\beta) \sim e^{2\beta}$. Since the fundamental variable in the Potts model is $t = e^J = e^{-\beta}$, an ordinary power-law critical point $\xi \sim (t - t_c)^{-\nu}$ with $t_c = 0$ would correspond to $\xi(\beta) \sim e^{\nu\beta}$. Therefore, our result can be interpreted as indicating a power-law critical point at zero temperature with critical exponent $\nu = 2$. The fact that ν is here a rational number reinforces our suspicion that this two-dimensional model can be solved exactly, at least in the sense of determining the exact asymptotic behavior as $\beta \to \infty$. The exponent $\nu = 2$ corresponds to an operator with scaling dimension $X = 2 - 1/\nu = 3/2$, which is one of the possibilities proposed by Saleur [36, p. 248]—albeit not the one he considered most likely!

On closer examination, however, the ratio $\xi(\beta)/e^{2\beta}$ appears *not* to be asymptotically constant as $\beta \to \infty$ (see Fig. 5a); rather, it begins to rise when $\beta \approx 3.4$ ($\xi \approx 75$), and this rise shows no sign of abating at least up to $\beta \approx 5.9$ ($\xi \approx 15000$). Indeed, our data are compatible with an asymptotic behavior

$$\xi(\beta) = Ae^{2\beta}\beta^p[1 + a_1 e^{-\beta} + a_2 e^{-2\beta} + \cdots] \tag{7.1}$$

with $p \approx 1$ (see Fig. 6). This corresponds to a power-law critical point with multiplicative logarithmic correction $\beta^p \sim |\log(t - t_c)|^p$. The problem is to make theoretical sense of such a behavior.

In the preliminary report of this work,[13] we asserted that a multiplicative logarithmic correction $\beta^p \sim (\log t)^p$ with p integer (particularly

$p=1$) can occur in the renormalization-group framework as a result of "resonance" between operators whose scaling dimensions are rationally related. This assertion is (we now realize) only half-true. For the susceptibility, specific heat, and similar observables, it is indeed true that multiplicative logarithmic corrections with positive integer powers p can occur as a result of resonance.[60–62] However, we have been unable to devise any renormalization-group scenario in which the *correlation length* acquires such a multiplicative logarithmic correction in the absence of marginal operators. For example:

(1) Suppose that we hypothesize a scenario with one relevant variable t (eigenvalue $\lambda > 0$) and one irrelevant variable u (eigenvalue $-\lambda$), satisfying the RG flow equations

$$\frac{dt}{dl} = \lambda t + t^2 u \tag{7.2a}$$

$$\frac{du}{dl} = -\lambda u \tag{7.2b}$$

where $t(0)$ and $u(0)$ are the couplings in the Hamiltonian, and $t(l)$ and $u(l)$ are the renormalized couplings after modes of momentum $\gtrsim e^{-l}$ have been integrated out. The solution is

$$t(l) = e^{\lambda l}\left(\frac{1}{t(0)} - Al\right)^{-1} \tag{7.3a}$$

$$u(l) = Ae^{-\lambda l} \tag{7.3b}$$

where $A = u(0)$. Let us now choose l so that $t(l) = 1$; this implies that $e^l = \xi/\xi_1$, where ξ_1 is the correlation length at $t = 1$ and $u = Ae^{-\lambda l} \approx 0$. Hence

$$\frac{\xi}{\xi_1} = \left[\frac{1}{t(0)} - A\log(\xi/\xi_1)\right]^{1/\lambda} = t^{-1/\lambda}[1 + O(t\log t)] \tag{7.4}$$

so that the presence of the irrelevant operator u (i.e., $A \neq 0$) induces only an *additive* correction to scaling $O(t\log t)$.

(2) Suppose, alternatively, that we hypothesize two relevant operators t, u with eigenvalues $n\lambda$ and λ, respectively, where n is an integer $\geqslant 1$ and $\lambda > 0$, satisfying the RG flow equations

$$\frac{dt}{dl} = n\lambda t + u^n \tag{7.5a}$$

$$\frac{du}{dl} = \lambda u \tag{7.5b}$$

The solution is

$$t(l) = [\, t(0) + u(0)^n \, l \,]\, e^{n\lambda l} \tag{7.6a}$$

$$u(l) = u(0)\, e^{\lambda l} \tag{7.6b}$$

Since there are two relevant operators, generically *two* couplings have to be adjusted in order to place the system at a critical point. But if some symmetry were to cause $t(0)$ to be exactly zero [or at least $\lesssim u(0)^n$], then a critical point can be reached by adjusting $u(0)$ alone. So assume this, and let us analyze the resulting critical behavior. Let us choose l so that $t(l) = 1$; this implies that $e^l = \xi/\xi_1$, where ξ_1 is the correlation length at $t = 1$ and $u = l^{-1/n} \approx 0$. Hence

$$\left(\frac{\xi}{\xi_1}\right)^{n\lambda} \log\left(\frac{\xi}{\xi_1}\right) = u(0)^{-n} \tag{7.7}$$

so that

$$\frac{\xi}{\xi_1} = u^{-1/\lambda}\, |\log u|^{-1/n\lambda} \left[\, 1 + O\left(\frac{\log\log u}{\log u}\right) \,\right] \tag{7.8}$$

(One expects a further correction-to-scaling term $O(|\log u|^{-1/n})$ arising from the fact that $u(l) = l^{-1/n} \neq 0$.) Hence there is a multiplicative logarithmic correction, but its power is *negative*; and there are very-slowly-decaying (logarithmic) additive corrections to scaling.

(3) In the presence of a *marginally irrelevant* operator u, multiplicative logarithmic corrections of either sign can be obtained.[33] Suppose, for example, that the flow equations are

$$\frac{dt}{dl} = \gamma(u)\, t \tag{7.9a}$$

$$\frac{du}{dl} = -\beta(u) \tag{7.9b}$$

[33] For a pedagogical discussion, see [63, Section 3.6]. Concrete manifestations of this phenomenon can be found in the four-dimensional N-vector model,[64, 65] the three-dimensional tricritical N-component model,[61] the three-dimensional N-component ferromagnet with strong dipolar interactions,[66, 67] and the two-dimensional 4-state Potts ferromagnet.[68–70]

Then the solution is given by the implicit equation

$$l = \int_{u(l)}^{u(0)} \frac{du'}{\beta(u')} \tag{7.10}$$

together with

$$t(l) = t(0) \exp\left(\int_{u(l)}^{u(0)} \frac{\gamma(u')}{\beta(u')}\, du' \right) \tag{7.11}$$

If we now assume that

$$\gamma(u) = \lambda + \gamma_1 u + \gamma_2 u^2 + \gamma_3 u^3 + \cdots \tag{7.12a}$$

$$\beta(u) = \qquad\qquad \beta_2 u^2 + \beta_3 u^3 + \cdots \tag{7.12b}$$

with $\lambda > 0$ and $\beta_2 > 0$, and assume further that $u(0) > 0$ is small enough so that $\beta(u) > 0$ for $0 < u < u(0)$, we then find that

$$t(l) = \text{const} \times t(0)\, e^{\lambda l} l^{\gamma_1/\beta_2} \left[1 + \frac{\beta_3 \gamma_1}{\beta_2^2} \frac{\log l}{l} + O\left(\frac{1}{l}\right) \right] \tag{7.13a}$$

$$u(l) = \frac{1}{\beta_2 l} \left[1 - \frac{\beta_3}{\beta_2^2} \frac{\log l}{l} + O\left(\frac{1}{l}\right) \right] \tag{7.13b}$$

Setting now $t(l) = 1$ and $e^l = \xi/\xi_1$ as before, we obtain

$$\frac{\xi}{\xi_1} = t^{-1/\lambda} |\log t|^{-\gamma_1/\beta_2\lambda} \left[1 + \frac{\beta_3 \gamma_1}{\beta_2^3 \lambda} \frac{\log |\log t|}{|\log t|} + O\left(\frac{1}{|\log t|}\right) \right] \tag{7.14}$$

The exponent of the multiplicative logarithmic correction, $-\gamma_1/\beta_2\lambda$, can thus be of either sign. Note, however, the presence of very-slowly-decaying additive corrections to scaling of the form $O(\log\log t/\log t)$ [with a universal coefficient] and $O(1/\log t)$ [with a nonuniversal coefficient].

Thus, we have been unable to devise any renormalization-group scenario in which the correlation length acquires a multiplicative logarithmic correction with exponent $p > 0$ in the absence of marginal operators; and we suspect that no such scenario exists. On the other hand, if marginal operators were present in our model (as in scenario #3), then one of their effects would be to induce $1/\log L$ corrections to scaling in the

finite-size scaling functions,[34] and we see no evidence of corrections decaying anywhere near so slowly. On the contrary, the corrections to scaling are here almost undetectable, and they appear to decay like $L^{-\Delta}$ with $\Delta \gtrsim 1$ (see Section 4.1.1).

Finally, an anonymous referee has pointed out to us the possibility that the important microscopic variable is not $t = e^{-\beta}$ but rather $t = 1/\beta$, and that this t is a *marginally relevant* operator:

$$\frac{dt}{dl} = B(t) = b_2 t^2 + b_3 t^3 + b_4 t^4 + \cdots \tag{7.15}$$

with $b_2 > 0$, i.e., a situation of asymptotic freedom. (This sounds implausible at first sight for a discrete-spin model, but is not impossible.) The solution to (7.15) is given by

$$l = \int_{t(0)}^{t(l)} \frac{dt'}{B(t')} \tag{7.16}$$

If we set $t(l) = 1$ and $t(0) = 1/\beta$ and use $e^l = \xi/\xi_1$ as before, we obtain

$$\xi = A e^{\beta/b_2} \beta^{-b_3/b_2^2} \left[1 + O\left(\frac{1}{\beta}\right) \right] \tag{7.17}$$

where A is a nonperturbative constant, and the corrections in inverse powers of β can be computed from the coefficients $b_4, b_5, \ldots$. On the other hand, the corrections to finite-size scaling are determined (as usual) by irrelevant operators, and so decay as inverse powers of L (provided there are no marginally irrelevant operators). So this scenario, unlike scenario #3, is not ruled out by our finite-size-scaling data (Section 4.1.1). However, if (7.17) is indeed the true behavior, then our data are so far from asymptotic that they give no useful information about A and $p \equiv -b_3/b_2^2$ (see Section 4.2.1 and in particular Fig. 8). So we cannot rule out this scenario, but neither can we obtain any evidence in its favor.

In summary, we really do not understand the theoretical basis for an asymptotic behavior of the form (7.1) with $p > 0$.

An alternative possibility is that the true asymptotic behavior is $\xi(\beta) \sim e^{2\beta}$ *without* multiplicative logarithmic corrections. This could happen in either of two ways:

[34] See [70, Section 3] for a detailed theoretical study of the $1/\log L$ corrections in the finite-size-scaling functions when a marginally irrelevant operator is present; and see [70, Fig. 6] for an illustration of their practical effect in the two-dimensional 4-state Potts ferromagnet.

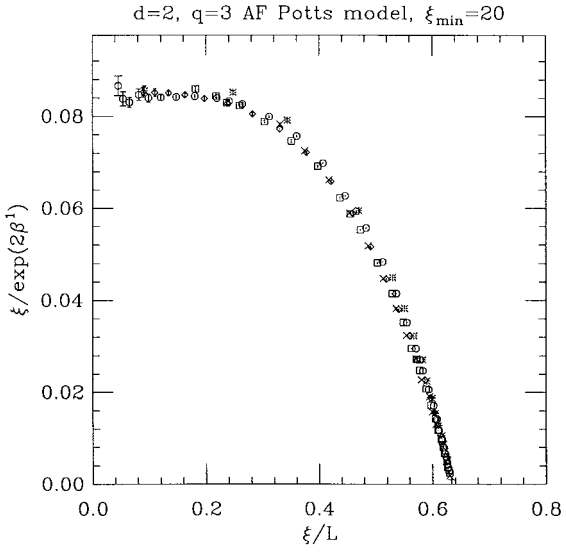

Fig. 19. Traditional finite-size-scaling plot of $\xi(L)/e^{2\beta}$ versus $\xi(L)/L$, using all data points with $\xi(L) \geqslant 20$. Symbols indicate $L = 32$ (+), 64 (×), 128 (□), 256 (◇), 512 (○), 1024 (∗), 1536 (⊕). Error bars (one standard deviation) are in almost all cases smaller than the symbol size.

(a) *The rise seen in Fig. 5a at* $\beta \gtrsim 3.4$ *might be spurious*, i.e., an artifact of some undetected systematic error in our extrapolation method. Indeed, it is suspicious that this rise begins at roughly the same correlation length ($\xi \approx 75$) where our extrapolation method begins to play a central role.[35] To test whether this rise is real, we produced a traditional finite-size-scaling plot in which $\xi/e^{2\beta}$ is plotted versus ξ/L (Fig. 19). One sees clearly that the points do *not* fall on a single curve, and that it is the *largest* lattices that deviate the most from the others (see particularly the range $0.25 \lesssim \xi/L \lesssim 0.4$); the data are most definitely *not* compatible with convergence to a limiting FSS curve. Rather, the deviations reflect precisely the rise of $\xi/e^{2\beta}$ when $\xi \gtrsim 100$. We therefore think that the rise observed in Fig. 5a is real.

(b) *The rise seen in Fig. 5a might level off at some* $\beta > 6$. This is perfectly possible, but it would mean that the corrections to the leading asymptotic behavior either have unusually strong amplitude or else decay

[35] From Fig. 1 we see that the finite-size corrections are negligible when $\xi/L < 1/6$. Inspection of Table 1 shows that we have raw data satisfying $\xi/L < 1/6$ up to $\beta = 3.50$ ($\xi \approx 94$), but not beyond that.

more slowly than the hypothesized $e^{-\beta}$. If the corrections behave as in (7.1), the coefficient a_1 would have to be approximately -15 in order to obtain a decent fit between $\beta = 4.5$ ($e^{-\beta} \approx 0.011$) and $\beta = 6.0$ ($e^{-\beta} \approx 0.002$), and the coefficients a_2 and a_3 would have to be large as well (see Fig. 7a). On the other hand, if we allow additive corrections to scaling that are *fractional* powers of $e^{-\beta}$,

$$\xi(\beta) = Ae^{2\beta}[1 + a_1 e^{-\lambda_1 \beta} + a_2 e^{-\lambda_2 \beta} + \cdots] \tag{7.18}$$

then the data for $\beta \geqslant 4.5$ can be fit reasonably well with $\lambda_1 \approx 0.5$ and $a_1 \approx -2.4$ (see Fig. 7b). Now such nonanalytic corrections to scaling can arise routinely from irrelevant operators: in the case at hand, an additive correction $e^{-\lambda_1 \beta} \sim \xi^{-\lambda_1/2}$ corresponds to a correction-to-scaling exponent $\Delta = \lambda_1/2 \approx 1/4$. Unfortunately, our study of the finite-size-scaling function (Section 4.1.1) gives no indication of any correction to scaling with $\Delta \lesssim 1$. So it is highly unlikely that a correction $e^{-\lambda_1 \beta}$ with $\lambda_1 \approx 0.5$ could arise from this mechanism. We do not know whether some other mechanism might lead to such behavior.

In conclusion, two distinct Ansätze on the large-β asymptotic behavior of the correlation length—(7.1) with $p \approx 1$, and (7.18) with $\lambda_1 \approx 0.5$—are compatible with our data, but both present difficulties of theoretical interpretation. We hope that someone will be able to sort this out, and that the numerical results presented here will serve as useful clues toward the exact solution of this model, possibly with the help of the methods of conformal field theory.[5, 6] Our estimate of the universal quantity $x^* \approx 0.633888$ (see also ref. 34) provides another constraint in determining the universality class of this model.

7.2. Prospects for Future Work

Here are some possible directions for future work on the 3-state square-lattice Potts antiferromagnet:

(1) Study small lattices (e.g., $L = 4, 8, 16, 32, 64$) with very high statistics in order to obtain quantitative information on the corrections to scaling. Salas and Sokal[34] have recently done this at $\beta = \infty$ (corresponding to $\xi(L)/L = \xi^* \approx 0.634$), but the corrections to scaling at this value of $\xi(L)/L$ are quite weak. As can be seen in Figs. 2(b) and 3(b), the corrections are much stronger in the interval $0.54 \lesssim \xi((L)/L \lesssim 0.62$, so it would be useful to get higher statistics in this region.

(2) Study large lattices (e.g., $L = 1024, 1536, 2048$) at $\xi/L < 1/6$ (where the finite-size effects are negligible, see Fig. 1) in order to verify that the observed rise of $\xi(\beta)/e^{2\beta}$ at $\beta \gtrsim 3.4$ ($\xi \gtrsim 75$) is real and not merely an artifact of our extrapolation method. Using $L = 2048$, we could hope to reach $\beta \approx 4.1$ ($\xi \approx 320$) with "essentially infinite-volume" simulations. By this time the rise of $\xi(\beta)/e^{2\beta}$ is about 4% (see Fig. 5a) and so should be clearly detectable.

Future studies of this model should also correct two defects in the present work:

(3) We measured here the susceptibility and correlation length associated to the *staggered* magnetization $\mathscr{M}_{\text{stagg}}$, which is the most relevant operator in this model ($\eta_{\text{stagg}} = 1/3$) and hence has the most strongly divergent susceptibility ($\gamma_{\text{stagg}}/\nu = 2 - \eta_{\text{stagg}} = 5/3$). What we failed to notice (until the runs had already been made and it was therefore too late!) is that the *uniform* magnetization $\mathscr{M}_u$ is also a relevant operator ($\eta_u = 4/3$)[30, 33, 34] with a divergent susceptibility ($\gamma_u/\nu = 2/3$). Future studies should measure it as well. Finally, the staggered polarization $\mathscr{P}_{\text{stagg}}$ (see refs. 33 and 34 for the definition) is also a relevant operator ($\eta_{\mathbf{P}_{\text{stagg}}} = 3$) albeit with a non-divergent susceptibility ($\gamma_{\mathbf{P}_{\text{stagg}}}/\nu = -1$). By measuring its correlation function at several different low momenta, it ought to be possible to check the prediction $\eta_{\mathbf{P}_{\text{stagg}}} = 3$ despite the non-divergence of the corresponding susceptibility.

(4) In the present paper we didn't bother to measure the cross-correlations between $\mathscr{M}^2_{\text{stagg}}$ and $\mathscr{T}_{\text{stagg}}$; as a result, we were unable to assign statistically valid error bars to ξ (instead we used the triangle inequality to obtain an overly conservative error bar). This was a serious mistake, as it prevented us from distinguishing clearly between statistical fluctuations and systematic errors (arising from corrections to scaling or other sources): see Section 4.1.1. Measuring the cross-correlations would allow one to determine the correct error bars not only on ξ but also on combinations such as $\chi/\xi^{5/3}$; this could lead to a very sensitive test of the conjecture that $\chi/\xi^{5/3} \to \text{const}$ as $\beta \to \infty$ (Section 4.2.2).

APPENDIX A. PROOF OF A CORRELATION INEQUALITY FOR ANTIFERROMAGNETIC POTTS MODELS ON A BIPARTITE GRAPH

Let V be a finite set of sites; we shall consider a q-state Potts model on V consisting of spins $\sigma_i \in \{1,..., q\}$ for $i \in V$, interacting via a Hamiltonian

$$\mathscr{H} = -\sum_{\langle ij \rangle} J_{ij}\, \delta_{\sigma_i, \sigma_j} \tag{A.1}$$

Here the sum runs over all pairs $i, j \in V$ (each pair counted once), and $\{J_{ij}\}_{i,j \in V}$ is some specified set of couplings.

In this appendix we shall prove some correlation inequalities for the Potts model (A.1). Our technique will be to embed a field of Ising spins into the given Potts model—using, in fact, precisely the Wang–Swendsen–Kotecký (WSK) embedding discussed in Section 2.3—and to exploit the well-known Griffiths inequalities[71, 72] for the induced Ising model. It is amusing that the WSK embedding can be used both as a Monte Carlo algorithm and as an analytical technique. Similar proofs of correlation inequalities based on the embedding of Ising or XY variables can be found in refs. 73–77.

We begin by introducing a redundant (but perfectly legitimate) parametrization of the q-state Potts spin σ_i in terms of a q-state Potts spin ω_i and an Ising spin τ_i. Let ω_i be uniformly distributed in $\{1,..., q\}$, and let τ_i be uniformly distributed in $\{-1, +1\}$; we then define

$$\sigma_i = \begin{cases} \dfrac{3+\tau_i}{2} & \text{if} \quad \omega_i = 1 \text{ or } 2 \\ \omega_i & \text{if} \quad \omega_i \geqslant 3 \end{cases} \tag{A.2}$$

It is easy to see that σ_i is uniformly distributed in $\{1,..., q\}$: indeed, each of the q possible values of σ_i arises from exactly two of the $2q$ possible values of (ω_i, τ_i). Performing this construction independently at each site $i \in V$, we construct the *a priori* measure for the spins $\{\omega_i, \tau_i\}_{i \in V}$, and thus also for the spins σ_i defined by (A.2) as functions of (ω_i, τ_i). The desired probability distribution is then obtained by multiplying this *a priori* measure by $Z^{-1} \exp[-\mathscr{H}(\{\sigma\})]$, where $\mathscr{H}$ is given by (A.1) and $\{\sigma\}$ is defined by (A.2).

Let us first compute the probability distribution of the set of spins $\{\tau\}$ *conditioned on the set of spins* $\{\sigma\}$. Here the Boltzmann weight factor $Z^{-1} \exp[-\mathscr{H}(\{\sigma\})]$ plays no role, since the $\{\sigma\}$ are being held fixed; the conditional distribution is the same as in the *a priori* measure. We thus have, independently for each site i,

$$\tau_i = \begin{cases} 2\sigma_i - 3 & \text{if} \quad \sigma_i = 1 \text{ or } 2 \\ \pm 1 \text{ with equal probability} & \text{if} \quad \sigma_i \geqslant 3 \end{cases} \tag{A.3}$$

It follows that the conditional expectation of $\tau_i \tau_j$ given $\{\sigma\}$ is

$$E(\tau_i \tau_j \mid \{\sigma\}) = I(\sigma_i \leqslant 2)\, I(\sigma_j \leqslant 2)(2\delta_{\sigma_i, \sigma_j} - 1) \tag{A.4a}$$

$$= \begin{cases} +1 & \text{if} \quad \sigma_i = \sigma_j = 1 \text{ or } \sigma_i = \sigma_j = 2 \\ -1 & \text{if} \quad \sigma_i = 1,\ \sigma_j = 2 \text{ or } \sigma_i = 2,\ \sigma_j = 1 \\ 0 & \text{in all other cases} \end{cases} \tag{A.4b}$$

where $I(\cdots)$ denotes the indicator function of the specified event. Next we want to take the unconditional expectation of (A.4). Since the probability distribution of the $\{\sigma\}$ is invariant under global permutations of $\{1,..., q\}$, we have in particular that the joint probability distribution of σ_i and σ_j is given by

$$\text{Prob}(\sigma_i, \sigma_j) = \frac{p}{q}\,\delta_{\sigma_i,\sigma_j} + \frac{1-p}{q(q-1)}\,(1-\delta_{\sigma_i,\sigma_j}) \tag{A.5}$$

where $p = \langle \delta_{\sigma_i,\sigma_j} \rangle$. Averaging (A.4) over the distribution (A.5), we find that

$$\langle \tau_i \tau_j \rangle = \frac{2(pq-1)}{q(q-1)} = \frac{2}{q}\left\langle \frac{q\delta_{\sigma_i,\sigma_j}-1}{q-1} \right\rangle \tag{A.6}$$

Note that on the right-hand side of this identity we have precisely the two-point correlation function of our Potts model [cf. (2.3)], multiplied by $2/q$.

On the other hand let us compute the probability distribution of the set of spins $\{\tau\}$ *conditioned on the set of spins* $\{\omega\}$. Note first that

$$\delta_{\sigma_i,\sigma_j} = I(\omega_i \geqslant 3)\, I(\omega_j \geqslant 3)\, \delta_{\omega_i,\omega_j} + I(\omega_i \leqslant 2)\, I(\omega_j \leqslant 2)\, \frac{1+\tau_i\tau_j}{2} \tag{A.7}$$

Inserting this into (A.1), we see that the model of spins $\{\tau\}$ conditioned on $\{\omega\}$ is an Ising model with interactions

$$J_{ij}^{\text{eff}} \equiv \tfrac{1}{2} J_{ij} I(\omega_i \leqslant 2)\, I(\omega_j \leqslant 2) \tag{A.8}$$

(The factor $\frac{1}{2}$ comes simply from the difference between the conventional Ising and Potts normalizations of couplings.) Below, we shall apply various correlation inequalities to this induced Ising model.

Let us consider some special cases:

Example 1 (ferromagnetic Potts model). Assume that $J_{ij} \geqslant 0$ for all $i, j \in V$. Then the couplings J_{ij}^{eff} are also $\geqslant 0$. So Griffiths' first inequality[71] applied to the induced Ising model (A.8) implies that

$$E(\tau_i \tau_j \mid \{\omega\}) \geqslant 0 \qquad \text{for all } \{\omega\} \tag{A.9}$$

In particular, averaging this over $\{\omega\}$ we deduce that $\langle \tau_i \tau_j \rangle \geqslant 0$; and hence by the identity (A.6) we have

$$\left\langle \frac{q\delta_{\sigma_i, \sigma_j} - 1}{q-1} \right\rangle \geqslant 0 \tag{A.10}$$

This is a "Griffiths' first inequality for ferromagnetic Potts models."

Of course, this inequality can be proven somewhat more simply using the Fortuin–Kasteleyn representation: the left-hand side of (A.10) is equal to a connection probability in the Fortuin–Kasteleyn bond variables, and thus is manifestly nonnegative. Indeed, this proof is valid for all real $q \geqslant 0$. So nothing much is gained by WSK embedding in this case; the real value of the method arises in the next case:

Example 2 (antiferromagnetic Potts model on a bipartite graph). Assume that the set of sites V can be partitioned as $V = A \cup B$ in such a way that

$$J_{ij} \begin{cases} \geqslant 0 & \text{if} \quad i, j \in A \\ \geqslant 0 & \text{if} \quad i, j \in B \\ \leqslant 0 & \text{if} \quad i \in A, \quad j \in B \end{cases} \tag{A.11}$$

(In particular, the pure antiferromagnet would have $J_{ij} = 0$ for $i, j \in A$ and for $i, j \in B$.) Now define

$$\tau'_i = \begin{cases} \tau_i & \text{if} \quad i \in A \\ -\tau_i & \text{if} \quad i \in B \end{cases} \tag{A.12}$$

It follows that the model of spins $\{\tau'\}$ conditioned on $\{\omega\}$ is an Ising model with interactions

$$J'^{\,\text{eff}}_{ij} \equiv \tfrac{1}{2} J_{ij} I(\omega_i \leqslant 2)\, I(\omega_j \leqslant 2) \times \left\{ \begin{array}{ll} +1 & \text{if} \quad i, j \in A \\ +1 & \text{if} \quad i, j \in B \\ -1 & \text{if} \quad i \in A,\ j \in B \end{array} \right\} \geqslant 0 \tag{A.13}$$

So Griffiths' first inequality[71] applied to this ferromagnetic Ising model implies that

$$E(\tau'_i \tau'_j \mid \{\omega\}) \geqslant 0 \qquad \text{for all } \{\omega\} \tag{A.14}$$

Averaging over $\{\omega\}$ we deduce that $\langle \tau'_i \tau'_j \rangle \geqslant 0$, and hence by the identity (A.6) that

$$\left\langle \frac{q\delta_{\sigma_i,\sigma_j}-1}{q-1} \right\rangle = \frac{q}{2} \langle \tau_i \tau_j \rangle \begin{cases} \geqslant 0 & \text{if} \quad i, j \in A \\ \geqslant 0 & \text{if} \quad i, j \in B \\ \leqslant 0 & \text{if} \quad i \in A, \quad j \in B \end{cases} \tag{A.15}$$

This is a kind of "Griffiths' first inequality for antiferromagnetic Potts models."

In particular, for antiferromagnetic Potts models on the square lattice, (A.15) implies that the two-point correlation function $G(x, y)$ has sign$(-1)^{|x-y|}$, where $|x-y|$ denotes the ℓ^1 norm. One consequence of this is that the Fourier-transformed two-point function $\tilde{G}(p)$ satisfies

$$|\tilde{G}(p)| \leqslant \tilde{G}((\pi, \pi)) \tag{A.16}$$

Example 3 (comparison-to-Ising inequality). Let us return to the general case of arbitrary $\{J_{ij}\}$. From (A.8) it follows immediately that

$$|J_{ij}^{\text{eff}}| \leqslant \tfrac{1}{2} |J_{ij}| \tag{A.17}$$

so by Griffiths' comparison inequality[72] we have

$$|E(\tau_i \tau_j \mid \{\omega\})| \leqslant \langle \varepsilon_i \varepsilon_j \rangle_{\text{Ising}, \{|J/2|\}} \qquad \text{for all } \{\omega\} \tag{A.18}$$

where $\langle \cdots \rangle_{\text{Ising}, \{|J/2|\}}$ denotes the expectation in an Ising model with couplings $\{\frac{1}{2}|J_{ij}|\}$. Averaging over $\{\omega\}$ and using (A.6), we conclude that

$$\left\langle \frac{q\delta_{\sigma_i,\sigma_j}-1}{q-1} \right\rangle \leqslant \frac{q}{2} \langle \varepsilon_i \varepsilon_j \rangle_{\text{Ising}, \{|J/2|\}} \tag{A.19}$$

Thus, the two-point function in an arbitrary Potts model can be bounded *above* by the corresponding two-point function in a *ferromagnetic Ising* model.[36]

[36] Of course, for a *ferromagnetic* Potts model a much stronger result is true, namely that each correlation function $G(x, y; q)$ is a *decreasing* function of q (for $q \geqslant 1$) at fixed $\{J_{ij}\}$. This follows from the Fortuin–Kasteleyn representation combined with the FKG inequality for the random-cluster model.[78, 79] So the real interest of (A.19) is for the *antiferromagnetic* or *mixed ferromagnetic/antiferromagnetic* Potts models.

For example, one consequence of (A.19) is that the transition temperature of the $q=3$ Potts antiferromagnet on the triangular lattice must satisfy

$$\beta_{\text{trans}}(\text{TRI } q=3 \text{ Potts AF}) \geqslant 2\beta_{\text{crit}}(\text{TRI Ising ferro}) = \tfrac{1}{2}\log 3 = 0.549306... \tag{A.20}$$

This bound is of course satisfied by the numerical estimate β_{trans} (TRI $q=3$ Potts AF) ≈ 1.594.[80] Likewise, for the $q=3, 4$ Potts antiferromagnets on the simple-cubic lattice, one must have

$$\beta_{\text{trans}}(\text{SC } q=3, 4 \text{ Potts AF}) \geqslant 2\beta_{\text{crit}}(\text{SC Ising ferro}) \tag{A.21}$$

which is satisfied by the numerical estimates $\beta_{\text{trans}}(\text{SC } q=3 \text{ Potts AF}) \approx 0.816$,[11, 81–84] $\beta_{\text{trans}}(\text{SC } q=4 \text{ Potts AF}) \approx 1.43$,[85] and $\beta_{\text{crit}}(\text{SC Ising ferro}) \approx 0.222$.[86]

APPENDIX B. PROOF OF ERGODICITY OF THE WSK ALGORITHM AT $T=0$ ON A BIPARTITE GRAPH

Let $G=(V, E)$ be a finite undirected graph with vertex set V and edge set E. Then G is said to he *bipartite* if the vertex set V can be partitioned as $V=A \cup B$ in such a way that every edge $e \in E$ has one endpoint in A and the other endpoint in B (i.e., there are no A–A or B–B edges).

Example 1. Any finite subset of the simple (hyper-)cubic lattice Z^d, with *free* boundary conditions, defines a bipartite graph.

Example 2. A box of size $L_1 \times L_2 \times \cdots \times L_d$ in Z^d, with *periodic* boundary conditions, defines a bipartite graph if and only if all the side lengths $L_1, L_2, ..., L_d$ are *even.*

The goal of this Appendix is to prove the following theorem:

Theorem B.1 Let G be a bipartite finite undirected graph, and let q be an integer $\geqslant 2$. Then the Wang–Swendsen–Kotecký algorithm for the q-state Potts antiferromagnet on G at zero temperature (i.e., for q-colorings of G) is ergodic.

Proof. We will prove, by induction on q, that the WSK algorithm for q-colorings (hereafter called WSK-q) is ergodic on G *and on all its subgraphs.*

Case $q=2$. Since G is bipartite, so are all its subgraphs H. The WSK algorithm acts independently on each connected component of H, so it suffices to prove the ergodicity for each connected component. But a connected bipartite graph has precisely two 2-colorings, which are related by a global interchange of the two colors; and this global interchange can trivially be realized by a WSK move.

Inductive step. Let $q \geqslant 3$, and suppose that WSK-$(q-1)$ is ergodic on G and all its subgraphs; we shall prove the same for WSK-q. So let $H=(V', E')$ be a subgraph of G, and define $A'=A \cap V'$, $B'=B \cap V'$. Define the *reference configuration* to be the q-coloring of H in which all sites in A' are colored 1 and all sites in B' are colored 2. Let $\{\sigma_x\}_{x \in V'}$ be an arbitrary q-coloring of H, which we call the *target configuration.* We shall show that the reference configuration can be transformed into the target configuration by a finite sequence of WSK-q moves. (This is sufficient to prove ergodicity, since the inverse of a WSK move is also a WSK move.)

(a) *Step 1.* Choose $1, q$ as the pair of colors to be used in the WSK move, and focus attention on all sites $x \in A'$ such that the target configuration has $\sigma_x = q$. All these sites are of course currently colored 1, and all their neighbors (which are in B') are currently colored 2. So each of these sites is a singleton (i.e., a one-site connected component) in the subgraph of H formed by those sites currently colored 1 or q. Therefore, each of these sites can be recolored q by a WSK move, while leaving all other sites unchanged.

(b) *Step 2.* Choose $2, q$ as the pair of colors to be used in the WSK move, and focus attention on all sites $x \in B'$ such that the target configuration has $\sigma_x = q$. All these sites are of course currently colored 2; and all their neighbors (which are in A' *and have target color* $\neq q$) are currently colored 1. So each of these sites is a singleton in the subgraph of H formed by those sites currently colored 2 or q. Therefore, each of these sites can be recolored q by a WSK move, while leaving all other sites unchanged.

(c) *Step 3.* All sites with target color q are now colored q, while the remaining sites are now colored 1 or 2. The latter sites (along with their corresponding edges) define a subgraph $K \subset H$; and by the inductive hypothesis they can be given their target colors (which lie in $\{1, 2, \ldots, q-1\}$) by a sequence of WSK-$(q-1)$ moves (which are of course also WSK-q moves). ▮

Note. After completion of this work, we learned that the same theorem (as well as some generalizations of it) was obtained independently by Burton and Henley.[33] Their proof is essentially the same as ours.

ACKNOWLEDGMENTS

We wish to thank John Cardy, Chris Henley, Gustavo Mana, Paul Pearce, Andrea Pelissetto, Jesús Salas and Hubert Saleur for helpful conversations and/or correspondence. The authors' research was supported in part by the Conselho Nacional de Desenvolvimento Cientifico e Tecnológico-CNPq, the Financiadora de Estudos e Projetos (FINEP-MCT), the Fundação de Amparo à Pesquisa do Estado de Minas Gerais (FAPEMIG), and U.S. National Science Foundation Grants DMS-9200719 and PHY-9520978.

REFERENCES

1. R. B. Potts, *Proc. Camb. Philos. Soc.* **48**, 106 (1952).
2. F. Y. Wu, *Rev. Mod. Phys.* **54**, 235 (1982); **55**, 315 (E) (1983).
3. F. Y. Wu, *J. Appl. Phys.* **55**, 2421 (1984).
4. R. J. Baxter, *Exactly Solved Models in Statistical Mechanics* (Academic Press, London/New York, 1982).
5. C. Itzykson, H. Saleur, and J.-B. Zuber, eds., *Conformal Invariance and Applications to Statistical Mechanics* (World Scientific, Singapore, 1988).
6. P. Di Francesco, P. Mathieu, and D. Sénéchal, *Conformal Field Theory* (Springer-Verlag, New York, 1997).
7. B. Nienhuis, *J. Stat. Phys.* **34**, 731 (1984).
8. R. Kotecký, unpublished, cited in H.-O. Georgii, *Gibbs Measures and Phase Transitions* (de Gruyter, Berlin/New York, 1988), pp. 148–149, 457.
9. J. Salas and A. D. Sokal, *J. Stat. Phys.* **86**, 551 (1997), cond-mat/9603068.
10. J.-S. Wang, R. H. Swendsen, and R. Kotecký, *Phys. Rev. Lett.* **63**, 109 (1989).
11. J.-S. Wang, R. H. Swendsen, and R. Kotecký, *Phys. Rev. B* **42**, 2465 (1990).
12. M. Lubin and A. D. Sokal, *Phys. Rev. Lett.* **71**, 1778 (1993), hep-lat/9304002.
13. S. J. Ferreira and A. D. Sokal, *Phys. Rev. B* **51**, 6727 (1995), hep-lat/9405015.
14. M. Lüscher, P. Weisz, and U. Wolff, *Nucl. Phys. B* **359**, 221 (1991).
15. J.-K. Kim, *Phys. Rev. Lett.* **70**, 1735 (1993).
16. J.-K. Kim, *Nucl. Phys. B (Proc. Suppl.)* **34**, 702 (1994).
17. J.-K. Kim, *Phys. Rev. D* **50**, 4663 (1994).
18. J.-K. Kim, *Europhys. Lett.* **28**, 211 (1994).
19. J.-K. Kim, *Phys. Lett. B* **345**, 469 (1995), hep-lat/9502005.
20. S. Caracciolo, R. G. Edwards, S. J. Ferreira, A. Pelissetto, and A. D. Sokal, *Phys. Rev. Lett.* **74**, 2969 (1995), hep-lat/9409004.
21. G. Mana, A. Pelissetto and A. D. Sokal, *Phys. Rev. D* **55**, 3674 (1997), hep-lat/9610021.
22. S. Caracciolo, A. Pelissetto, and A. D. Sokal, in preparation.
23. R. J. Baxter, *Proc. Roy. Soc. London A* **383**, 43 (1982).
24. L. Onsager, *Phys. Rev.* **65**, 117 (1944).
25. A. Lenard, cited in E. H. Lieb, *Phys. Rev.* **162**, 162 (1967) at pp. 169–170.
26. R. J. Baxter, *J. Math. Phys.* **11**, 3116 (1970).
27. T. T. Truong and K. D. Schotte, *J. Phys. A* **19**, 1477 (1986).
28. P. A. Pearce and K. A. Seaton, *Ann. Phys.* **193**, 326 (1989).
29. D. Kim and P. A. Pearce, *J. Phys. A* **22**, 1439 (1989).

30. M. den Nijs, M. P. Nightingale, and M. Schick, *Phys. Rev. B* **26**, 2490 (1982).
31. J. Kolafa, *J. Phys. A* **17**, L777 (1984).
32. H. Park and M. Widom, *Phys. Rev. Lett.* **63**, 1193 (1989).
33. J. K. Burton, Jr. and C. L. Henley, *J. Phys. A* **30**, 8385 (1997), cond-mat/9708171.
34. J. Salas and A. D. Sokal, *J. Stat. Phys.* **92**, 729 (1998), cond-mat/9801079.
35. M. P. Nightingale and M. Schick, *J. Phys. A* **15**, L39 (1982).
36. H. Saleur, *Nucl. Phys. B* **360**, 219 (1991).
37. H. Saleur, *Commun. Math. Phys.* **132**, 657 (1990).
38. C. L. Henley, in preparation.
39. S. Caracciolo, R. G. Edwards, A. Pelissetto, and A. D. Sokal, *Nucl. Phys. B* **403**, 475 (1993), hep-lat/9205005.
40. M. B. Priestley, *Spectral Analysis and Time Series*, Vols. 1 and 2 (Academic, London, 1981).
41. T. W. Anderson, *The Statistical Analysis of Time Series* (Wiley, New York, 1971).
42. N. Madras and A. D. Sokal, *J. Stat. Phys.* **50**, 109 (1988).
43. A. D. Sokal, in *Functional Integration: Basics and Applications* (1996 Cargèse summer school), C. DeWitt-Morette, P. Cartier, and A. Folacci, eds. (Plenum, New York, 1997).
44. M. N. Barber, in *Phase Transitions and Critical Phenomena*, Vol. 8, C. Domb and J. L. Lebowitz, eds. (Academic Press, London, 1983).
45. J. L. Cardy (ed.), *Finite-Size Scaling* (North-Holland, Amsterdam, 1988).
46. V. Privman, ed., *Finite Size Scaling and Numerical Simulation of Statistical Systems* (World Scientific, Singapore, 1990).
47. H. Flyvbjerg and F. Larsen, *Phys. Lett. B* **266**, 92 (1991).
48. H. Flyvbjerg and F. Larsen, *Phys. Lett. B* **266**, 99 (1991).
49. P. Nightingale, *Proc. Konink. Ned. Akad. B* **82**, 235, 245, 269 (1978).
50. S. Hassani, *Foundations of Mathematical Physics* (Allyn & Bacon, Boston, 1991).
51. R. H. Swendsen and J.-S. Wang, *Phys. Rev. Lett.* **58**, 86 (1987).
52. U. Wolff, *Phys. Rev. Lett.* **62**, 361 (1989).
53. A. M. Ferrenberg and R. H. Swendsen, *Phys. Rev. Lett.* **61**, 2635 (1988).
54. A. M. Ferrenberg and R. H. Swendsen, *Phys. Rev. Lett.* **63**, 1195 (1989).
55. R. H. Swendsen, *Physica A* **194**, 53 (1993).
56. A. M. Ferrenberg, D. P. Landau, and R. H. Swendsen, *Phys. Rev. E* **51**, 5092 (1995).
57. S. Caraccioio, A. Pelissetto, and A. D. Sokal, *J. Stat. Phys.* **60**, 1 (1990).
58. A. D. Sokal, *Nucl. Phys. B (Proc. Suppl.)* **20**, 55 (1991).
59. T. Mendes, A. Pelissetto, and A. D. Sokal, *Nucl. Phys. B* **477**, 203 (1996), hep-lat/9604015.
60. F. J. Wegner, *Phys. Rev. B* **5**, 4529 (1972).
61. F. J. Wegner and E. K. Riedel, *Phys. Rev. B* **7**, 248 (1973).
62. F. J. Wegner, in *Phase Transitions and Critical Phenomena*, Vol. 6, C. Domb and M. S. Green, eds. (Academic Press, London, 1976), Section V.E.
63. M. Le Bellac, *Quantum and Statistical Field Theory* (Oxford University Press, Oxford, 1991).
64. E. Brézin, J.-C. LeGuillou, and J. Zinn-Justin, *Phys. Rev. D* **8**, 2418 (1973).
65. H. S. Kogon, *J. Phys. A* **14**, 3253 (1981).
66. A. I. Larkin and D. E. Khmel'nitskii, *Zh. Eksp. Teor. Fiz.* **56**, 2087 (1969) [*Sov. Phys.-JETP* **29**, 1123 (1969)].
67. E. Brézin and J. Zinn-Justin, *Phys. Rev. B* **13**, 251 (1976).
68. M. Nauenberg and D. J. Scalapino, *Phys. Rev. Lett.* **44**, 837 (1980).
69. J. L. Cardy, M. Nauenberg, and D. J. Scalapino, *Phys. Rev. B* **22**, 2560 (1980).
70. J. Salas and A. D. Sokal, *J. Stat. Phys.* **88**, 567 (1997), hep-lat/9607030.

71. G. S. Sylvester, *J. Stat. Phys.* **15**, 327 (1976).
72. D. Szàsz, *J. Stat. Phys.* **19**, 453 (1978).
73. G. Mack and V. B. Petkova, *Ann. Phys.* **123**, 442 (1979).
74. J. Fröhlich, *Phys. Lett. B* **83**, 195 (1979).
75. A. Patrascioiu and E. Seiler, *J. Stat. Phys.* **69**, 573 (1992).
76. M. Aizenman, *J. Stat. Phys.* **77**, 351 (1994).
77. S. Caracciolo, R. G. Edwards, A. Pelissetto, and A. D. Sokal, Phase diagram and universality classes of RP^{N-1} and mixed isovector/isotensor σ-models in two dimensions, in preparation.
78. M. Aizenman, J. T. Chayes, L. Chayes, and C. M. Newman, *J. Stat. Phys.* **50**, 1 (1988).
79. C. M. Fortuin, *Physica* **59**, 545 (1972).
80. J. Adler, A. Brandt, W. Janke, and S. Shmulyan, *J. Phys. A* **28**, 5117 (1995).
81. A. P. Gottlob and M. Hasenbusch, *Physica A* **210**, 217 (1994), cond-mat/9404087.
82. A. P. Gottlob and M. Hasenbusch, *J. Stat. Phys.* **77**, 919 (1994), cond-mat/9406092.
83. M. Kolesik and M. Suzuki, *J. Phys. A* **28**, 6543 (1995), cond-mat/9504091.
84. R. K. Heilmann, J.-S. Wang, and R. H. Swendsen, *Phys. Rev. B* **53**, 2210 (1996), cond-mat/9509140.
85. Y. Ueno, G. Sun, and I. Ono, *J. Phys. Soc. Japan* **58**, 1162 (1989).
86. A. L. Talapov and H. W. J. Blöte, *J. Phys. A* **29**, 5727 (1996), cond-mat/9603013.